Identification and Analysis of Germination-Active Proteins in *Bacillus* Spores

Cameron Vincent Sayer

Dissertation submitted to the faculty of Virginia Polytechnic Institute and State University in partial fulfillment of the requirements for the degree of

Doctor of Philosophy
In
Biological Sciences

David L. Popham, Chair
Clayton C. Caswell
Florian D. Schubot
Ann M. Stevens

14 May 2019
Blacksburg, Virginia

Keywords: *Bacillus anthracis*, *Bacillus subtilis,* anthrax, spore germination

Identification and Analysis of Germination-Active Proteins in *Bacillus* Spores

Cameron Vincent Sayer

ABSTRACT

Many spore forming bacteria are the causative agents of severe disease, such as *Bacillus anthracis* and anthrax. In these cases, the spore often acts as the infectious agent. Spores boast extreme resistance to chemical and UV damage among other bactericidal conditions. This is problematic due to the difficulty and economic costs of decontaminating exposure sites. The present work focuses on identifying and characterizing proteins active within spore germination, with a focus towards understanding the triggering of the major stages of germination. Understanding how each stage is initiated could allow for development of methods that induce these processes to efficiently germinate spores, thus facilitating cheap and effective decontamination.

Sequencing of a spore transposon insertion library after exposure to germinants led to the identification of 42 genes with previously uncharacterized roles in spore germination. Fourteen of the genes, encoding proteins associated with the inner spore membrane, were further characterized. Mutants lacking these genes portrayed phenotypes consistent with failure of a GerA receptor-mediated germination response, and these genes affect the earliest stages of germination.

Chemical cross-linking was used to characterize protein interactions important for stage II of spore germination. Site-directed *in vivo* crosslinking indicated that YpeB may exist as a multimer within the dormant spore. Further investigation of individual protein domains using bacterial two-hybrid analysis suggested that both N- and C-terminal domains of YpeB contribute

to the formation of a multimer. In addition, the uncharacterized YpeB N-terminal domain was demonstrated to have strong self-association and may mediate self-association within the dormant spore.

Additional genes that contribute to efficient initiation of spore germination in a GerA-dependent manner were identified via TnSeq. Chemical cross-linking of dormant spores was implemented to characterize protein interactions leading to stabilization and activation of an important enzyme that contributes to cortex degradation in stage II of germination. The presented studies employed a variety of techniques to provide additional insight into both stages of spore germination with a goal of furthering understanding of specific events that contribute to a loss of spore dormancy.

Identification and Analysis of Germination-Active Proteins in *Bacillus* Spores

Cameron Vincent Sayer

GENERAL AUDIENCE ABSTRACT

Few bacterial species can undergo a specialized division process leading to the generation of a bacterial endospore. Endospores are dormant cells that boast resistance to a variety of environmental conditions that would otherwise cause bacterial cell death. These resistance traits make endospores immune to traditional bactericidal methods, making decontamination a nontrivial task. Further complicating the matter, spores are often the infectious particle of the associated disease, including hospital acquired diarrhea, infant botulism, anthrax, and many others. Presented work focuses on furthering understanding the process by which a dormant spore returns to a typical growing bacteria cell. Comprehension of major steps in this process may lead to novel methods for spore cleanup in which mechanisms within the spore are subverted to force a return to a typical bacterial cell state.

DEDICATION

This work is dedicated to my enormously supportive family. I always seem to be drawn to an uncommon path, but my parents Brice and Traci have encouraged me all the same. Jennifer, my friend and wife, I can never thank you enough for supporting me through everything, this would not have been possible without you.

ACKNOWLEDGEMENTS

Firstly, I would like to thank my advisor, David Popham, for allowing me to join your lab and learn from you. I cannot thank you enough for mentoring me over the years. Your depth of knowledge, patience and time management is unmatched. You encouraged my development as a scientist by pushing me to present my own solutions and experiments. You managed multiple projects and students seemingly effortlessly while maintaining record turnaround times on edits and keeping an open door policy. You worked with me through numerous posters, meetings, and prelims. Perhaps most importantly, you allowed me time to troubleshoot and work through issues while offering support and suggestions when they were required most. It is from these experiences I feel that I learned the most. I have immense respect for you not only as a scientist but as a person, thank you for everything.

I would like to thank my committee members, Clay Caswell, Florian Schubot, and Ann Stevens. Your expectations and critical reviews pushed me to do better. I always felt that I could discuss my work with you at any time. Thank you for your support and encouragement.

This experience would have been vastly different without each member of the Popham Lab. Casey Bernhards, Yan Chen, and Sean Mury, thank you for being so welcoming and creating an environment I looked forward to working in each day. Casey, I always felt as though you were the leader of the lab when I first joined and we couldn't have had a better one. Your positivity, professionalism and work ethic served as a stellar example as to what I should strive towards. Yan, thank you for imparting your protein and mass spectrometry knowledge on to me. I very clearly remember watching you masterfully operate the MALDI while I scrambled to write everything you said, only to later realize that you had already given me printed protocols. Sean,

thank you for being such a great friend and providing so much training during my early years in the lab. You all made me feel as though this goal was obtainable and provided the pattern to emulate. To current members of the Popham Lab, Bidisha Barat and Matt Flores. Bidisha, thank you for being so outgoing and easy to talk to, these past years would not have been nearly as interesting without you. I knew that I could always count on you to get people conversing and bring up everyone's mood. Matt you fit into the lab perfectly. You are already off to a strong start and I look forward to following your progress in the upcoming years.

I would also like to thank members of all the Micro labs for fostering an atmosphere of respect and collaboration. Jordan Mancl and Kylie Ryan, thank you for being such good friends and entertaining my protein structure questions. Keane Dye, for helping me generate mutants over a summer, only to later join the program and be one of the driving forces encouraging people to gather outside of lab. I also want to thank everyone in the teaching labs Katrina Lasley and Kevin Laoh, for making things run smoothly and providing a fun welcoming environment in which to work.

TABLE OF CONTENTS

LIST OF FIGURES

CHAPTER 1

CHAPTER 2

CHAPTER 3

LIST OF TABLES

CHAPTER 2

CHAPTER 3

CHAPTER 1

Introduction and Literature Review

Bacillus anthracis:

Bacillus anthracis is a Gram-positive, rod-shaped, nonmotile, spore-forming bacterium that can be naturally isolated from soil (1). *B. anthracis* can infect all mammals including humans although it is most commonly identified as a disease of herbivores (1). Human disease is primarily classified according to the route of infection: cutaneous, gastrointestinal, inhalational or injectional anthrax (1-4). In all cases, the spore of *B. anthracis* is the causative agent. Most common cases arise from contact with an infected animal or animal products, most frequently resulting in cutaneous anthrax infections (1-3). Cutaneous infection is characterized by the appearance of a painless black eschar accompanied by edema, several days post infection (1). This infection is easily diagnosed and treated with a variety of antibiotics (1). More rare and harder to diagnose are the gastrointestinal and inhalational forms of disease. Both clinically present as mild flu-like symptoms, but suddenly develop into a systemic infection that may become resistant to treatment and is rapidly fatal in many instances, causing sepsis and respiratory failure (5). All infections follow a similar pattern regardless of the route of entry. Spores are identified by host macrophages and translocated to nearby lymph nodes (6). It has been suggested that spores may germinate within alveolar macrophages during inhalational infections, which has been associated with early expression of toxins (7, 8). Eventually regional lymph node phagocytic capacity is overwhelmed, allowing infection of further lymph nodes leading to septicemia in many instances. (1).

Disease occurs upon germination of spores within the host and a return to vegetative growth, at which point virulence factors are produced (1, 9). The two primary virulence factors of *B. anthracis* are the tri-part toxin and the γ-D-glutamic acid polymer capsule expressed from the virulence plasmids pXO1 and pXO2 respectively. pXO1 encodes the three primary structural

toxin genes *pagA, lef,* and *cya* in addition to other features including the *gerX* operon and the regulatory gene *atxA* (10). *B. anthracis* toxins fill a substantial role in overall pathogenesis. Each is formed through the combination of three proteins, protective antigen (PA), lethal factor (LF) and edema factor (EF)(1). Separately, the subunit proteins do not exhibit toxic effect, however when either lethal factor or edema factor is combined with protective antigen, toxigenic effects are visualized (11, 12). The PA protein is 753 amino acids and folds into four functional domains (13). The first step in toxin assembly and function is the binding of PA to specific cell surface receptors. Once bound, PA is cleaved by a furin-like protease exposing the binding sites for both LF and EF (14). PA heptamers bind either LF or EF, followed by receptor-mediated endocytosis of the toxin complex (15). Once inside the host cell, toxins pass through acidic vesicles leading to eventual insertion into the membrane and translocation of LF or EF into the cytosol (16). EF is an adenylate cyclase converting host intracellular ATP into cAMP in association with host calmodulin protein (17). Edema toxin causes substantial increases to cAMP levels, facilitating the characteristic edema, in addition to inhibiting host phagocytic and oxidative burst capacity (18). LF is a zinc metalloprotease which has been demonstrated to cleave mitogen-activated protein kinases (MAPKKs), causing breakdown of signaling pathways from environmental signals to gene regulation within the host (19). Signaling involving MAPKKs are crucial in host activation of macrophages and cytokines and thus LF may facilitate bacterial proliferation within the host (1).

The *B. anthracis* capsule is the second of the two major virulence factors and is expressed from the pXO2 virulence plasmid. The pXO2 plasmid encodes *capB, capC, capA* and *dep*, all genes known to be necessary for capsule synthesis and degradation (20). The three *cap* genes are sufficient to create capsule in *E. coli*, while *dep* has been associated with depolymerization and is thought to control size of the capsule (20, 21). The *B. anthracis* capsule was first described in

1903, but direct association of capsule production within the host and virulence was established later. Generally, capsules primarily aid bacteria in avoiding the host immune response and thus contribute to further pathogenicity. The γ-D-glutamic acid polymer capsule produced by *B. anthracis* has been demonstrated to inhibit phagocytosis (21, 22) and is only slightly immunogenic, thus limiting host immune responses (23). Early attempts to attenuate *B. anthracis* for vaccine purposes led to plasmid curing and as such it has been noted that pXO2 is lost more readily than pXO1 (24). The Sterne strain first isolated in 1937 is $pXO2^-$ and this live vaccine strain is still used in veterinary settings (5).

B. anthracis infections can be treated upon prompt administration of antibiotics, although if left untreated, septicemia and death can result from any form of anthrax infection. Even though cutaneous anthrax infection is the most common, inhalational anthrax poses the greatest threat to the general public given its severity and its propensity for use as a biological weapon. The devastating effects of anthrax spore exposure was realized in an epidemic that occurred in Sverdlovsk, Russia, in 1979, resulting in the death of many unsuspecting civilians due to accidental dissemination of spores from a facility responsible for weaponizing anthrax (25). The threat of an anthrax attack became a reality in the United States in 2001 when letters containing *B. anthracis* spores were sent to various locations, infecting a total of 22 people (26).

Although difficult, especially in inhalational infections, early diagnosis and initiation of early treatment is critical for patient survival. Following treatment, cutaneous anthrax infections have a mortality rate of ≤2% (27). However, inhalational, gastrointestinal and injection anthrax feature mortality rates of 45%, 40%, and 28%, respectively, even with modern treatment methods (28, 29). Anthrax infections are treated with a combination of antimicrobial drugs, typically both bactericidal agents as well as protein synthesis inhibitors to combat *B. anthracis*

toxin production (30, 31). Naturally occurring multidrug resistance has been reported in *B. anthracis* and similar results could be created *in vitro*, further encouraging a multidrug approach (32, 33). Further complicating the matter, patients exposed to aerosolized spores are at risk of developing inhalational anthrax for up to 60 days post exposure and as such it is necessary to continue drug therapy to clear remaining germinating spores (34). Ciprofloxacin, levofloxacin and doxycycline are FDA approved for treatment in instances of exposure to aerosolized spores and are recommended as the first line of defense. In the event of widespread spore dissemination, effective post exposure prophylaxis is critical and can potentially save thousands of lives (27). Treatment should begin immediately following exposure as effectiveness wanes with delays (27). The US Advisory Committee on Immunization Practices recommends 60 days of drug prophylaxis and administration of 3 doses of anthrax vaccine for long-term treatment post exposure (35). It should not need mentioning that the potential ramifications of widespread spore dissemination would be devastating, inciting the seemingly impossible task of providing a 60-day antibiotic course for potentially thousands of people exposed in combination with additional treatments. It is because of this that *B. anthracis* remains a potential bioterrorism threat.

Bacterial vaccination was famously demonstrated by Pasteur using an attenuated *B. anthracis* strain; the first live vaccine to be implemented successfully. While live attenuated *B. anthracis* strains are still used for vaccination of livestock, these vaccines have not been approved for widespread human use due to residual virulence (5). Cell free vaccines for human use were developed in the 1950s based on toxin subunit PA from supernatants of the Sterne strain (36, 37). Now recombinant PA is produced from related organisms included *B. subtilis,* for use in anthrax vaccines (37). However, PA vaccines have been demonstrated to provide less protection

to lethal challenge than live spore vaccines, indicating that some combination of additional antigens is necessary for cellular immunity and full protection (24, 38).

Bacillus subtilis:

Bacillus subtilis is an important species in the study of Gram-positive and spore-forming organisms. *B. subtilis* is naturally competent, taking up genetic material from the extracellular environment, facilitating genetic manipulation (39). Natural competency and application of extensive molecular techniques over the years have made *B. subtilis* the best studied Gram positive bacterium (40). This extensive knowledge makes *B. subtilis* an ideal model system for further studies and adaptation to industrial settings. *B. subtilis* strains are nonpathogenic and free of toxins; therefore strains are regarded as safe for industrial and pharmaceutical applications (41, 42). Currently *B. subtilis* is used in many industries as a factory for overproduction of proteins and other chemicals including surfactants, riboflavin and various antimicrobial substances (43-45). The reasons as to why *B. subtilis* is such an important organism for industry hold true for the experimental community as well. The extensive research that has already characterized this organism provides context for future work into more specialized processes such as sporulation and germination.

Bacterial Sporulation:

Bacillus cells faced with unfavorable environmental conditions, such as an absence of nutrients, undergo an asymmetric division process ultimately leading to the formation of the bacterial spore. Spores are resistant to a variety of unfavorable environment conditions including UV radiation, heat, pressure, chemicals, starvation, desiccation and traditional decontamination

techniques (46, 47). The preservation of a dehydrated dormant core is the single biggest factor in spore resistance to environmental factors. This dormancy is maintained largely by a thick layer of peptidoglycan, termed the cortex, and high concentrations of small molecules within the core, such as calcium dipicolinic acid (DPA) (47, 48). Although the mature spore is fully dormant, it retains the ability to return to a vegetative state through a process called germination.

Vegetative *Bacillus* cells, when faced with a lack of carbon and or nitrogen, undergo the process of sporulation, whereby the vegetative cell is transformed into the dormant spore (49, 50). The decision to sporulate is made by integrating a range of signals both environmental and physiological, including nutrient depletion, cell density, and DNA damage (51). These signals are fed into a phosphorelay system that is responsible for the phosphorylation of key transcriptional regulator Spo0A (51). Accumulation of phosphorylated Spo0A activates transcription of genes that control commencement of sporulation and transition into the two-compartment sporangium (51). Following formation of the septum, sporulation follows a highly regulated pattern of gene expression in which sporulation-specific σ factors cause a cascade of gene activation across and between the mother cell and developing forespore (51, 52). The entire sporulation event takes approximately 6-8 hours and is characterized by several stages (50, 53, 54). The first stage of sporulation is characterized by the development of the axial filament. The axial filament is the aligning of the two chromosome copies, immediately following DNA replication, along the long axis of the cell (51). The formation of the septum at an extreme polar position signifies the second stage of sporulation. The septum splits the cell into a larger mother and smaller forespore component, each of which receives a copy of the chromosome (49, 51). Following the formation of the septum, the forespore is engulfed by the larger mother cell (49, 51). Cortex peptidoglycan is then deposited between the inner and outer membranes of the

engulfed forespore. DPA synthesized within the mother cell is then transported and accumulates within the forespore (47). DPA chelates calcium ions, leading to high concentrations of Ca^{2+} DPA within the spore core (47). Once engulfed, the forespore will pinch off as a free protoplast within the mother cell (47, 51). The forespore will then undergo a series of biochemical changes that include the addition of external coat layers. The final stage of sporulation is the period in which the spore matures, gaining its full resistance capabilities. Eventually the mother cell is lysed, releasing the free spore into the environment, thereby completing the process.

Spore Structure:

The structure of the spore differs significantly from that of a vegetative cell. The spore features several novel envelope layers, some of which confer additional resistance properties. These layers from inside out are the spore core, inner membrane, germ cell wall, cortex, outer membrane, coats and exosporium (Figure 1). The spore core is the dehydrated cytoplasm of the protoplast formed during sporulation. This core includes the spore's DNA, ribosomes and the majority of its enzymes (47). The DNA of the spore is tightly complexed with proteins called small acid-soluble proteins (SASPs) (55). SASP-DNA complexing, as well as the high levels of calcium dipicolinic acid and other ions, confer protection against heat and UV radiation (55). The inner membrane is very similar to that of the plasma membrane of vegetative cells except for the membrane lipids in the dormant spore are in a non-fluid state (56). This membrane serves as a permeability barrier conferring resistance to many chemicals which would otherwise mutate or destroy the spore DNA (47). The inner membrane is also the site of the germinant receptors (46, 57). Outside of the inner membrane is the germ cell wall. This cell wall is composed of peptidoglycan whose structure is much like that of a vegetative cell. The germ cell wall provides

little resistance for the spore, but it does become the cell wall of an outgrowing spore (46). The cortex is a thick layer composed of modified peptidoglycan. Peptidoglycan structure of the typical bacterial cell wall is comprised of repeating *N*-acetylglucosamine and *N*-acetylmuramic acid residues that are cross-linked though peptide side chains. However, in the spore cortex peptidoglycan, *N*-acetylmuramic acid may be modified to muramic-δ-lactam, or have its side chains converted to a single L-alanine (58-62). Cortex peptidoglycan, in addition to containing the modified muramic-δ-lactam, shows less extensive cross-links between glycan strands (58-60). The modified structure of cortex peptidoglycan is conserved among Gram-positive sporulating bacteria, including *Bacillus* and *Clostridium* species (57). The cortex is required for maintenance of proper spore core dehydration and its degradation is essential for spores to complete outgrowth. Although the outer membrane is present during spore formation, it has been found that this membrane plays little role in resistance to heat, radiation or chemicals, and its integrity in the dormant spore is questionable (63, 64). The spore coat is a multilayered structure composed of many different proteins. The coat has a role in resistance to some enzymes that would otherwise degrade the cortex and chemicals that would disrupt the inner membrane of the spore, but no role in heat or radiation resistance (47, 65). The exosporium is a large loose fitting structure composed of proteins and glycoproteins specific to this layer (65). The exosporium is not a conserved structure and is absent from many Bacilli, including *B. subtilis*. The specific function of the exosporium is unknown, but it is hypothesized that it plays a role in spore interactions with host cells given the pathogenic nature of some spores possessing an exosporium (1). The outermost layers of the spore may contain enzymes, such as alanine racemase that may play a role in regulating germination by modifying specific germinants (66-68). Maintenance of a dehydrated state of the core is the most important factor in upkeep of

spore resistance properties (47). The protective functions of these structures in combination allow bacterial spores to remain dormant for many years and potentially significantly longer periods of time (69).

Germination:

Germination is the process through which a dormant spore returns to a vegetative growth state (Figure 2). This occurs rapidly, taking only a few minutes to transform the dormant spore into an outgrowing vegetative cell. Most resistance properties of spores are rapidly lost during germination and as such this process has been a focus of methods to possibly simplify spore eradication. Germination occurs in response to the presence of key molecules called germinants. These include nutrients such as L-alanine, sugars (glucose and fructose), purine nucleosides or a combination of nutrient classes. In addition, spores will also germinate in response to non-nutrients such as Ca^{+}DPA, lysozyme, high pressure and salts, although it is likely that steps of the germination pathway utilized in response to germinants may be bypassed if germination is triggered in this manner (46, 48, 70). In order for germination to occur, the germinant must travel across the coat and cortex of the spore to contact germinant receptors (Ger) located on the inner membrane (46). The expression of specific genes such as *gerP* encode for proteins that make the spore more permeable to germinants (71). Once germinants have contacted the Ger receptors, a poorly understood commitment step occurs, where spores will continue through germination even with the removal of germinant (72). The release of monovalent cations including Na^{+} and K^{+}, begins to occur around the same time as commitment (46). Following commitment, germination proceeds into Stage 1. Water begins to partially rehydrate the spore core as large stores of Ca^{+}DPA are released. The release of Ca^{+}DPA is facilitated via channels composed of

SpoVA proteins (73). The events of Stage I ultimately trigger the second stage of germination. Stage II is characterized by the degradation of the spore cortex by GSLEs that recognize cortex peptidoglycan by its muramic-δ-lactam content, thus leaving the germ cell wall intact (46, 74-76). Degradation of the cortex allows the spore core to continue to expand and return to a fully hydrated state. Enzymes within the core become active and initiate metabolism and other cellular processes. At the end of Stage II, the spore is no longer dormant and has lost the majority of its resistance characteristics. Stage II is followed by outgrowth, a period in which normal cell metabolism and protein synthesis resume (46).

Germination Receptors:

Germination is initiated through environmental sensing achieved by Ger receptors, which are expressed late in sporulation. *B. subtilis* encodes three functional Ger receptors: GerA, GerB, and GerK (77). The GerA receptor responds to amino acids such as L-alanine and L-valine, while the GerB and GerK receptors collaborate to respond to a mixture of L-asparagine, D-glucose, D-fructose and K^+ ions (AGFK) (70). GerA alone has been shown to trigger germination while neither GerB nor GerK alone initiate germination efficiently (78). Recent work has suggested that GerA is poised for activation within the spore and in instances of morphological defects during sporulation such as defects in assembly of spore protective layers, can trigger premature germination (79). Signal transduction from Ger receptors to initiate germination is not well understood, however both cations and Ca^+DPA are released shortly after sensing by the receptor. GerD is required for a rapid response to germinants as Δ*gerD* strains exhibit reduced germination rates (80). Recent work suggests that GerD is required for the colocalization of Ger receptors in the inner membrane, organized in a cluster termed the germinosome (73, 81). It is thought that

GerD may have a role in the signal transduction pathway from germinant receptor complex to downstream germination effectors (73, 81). Ger receptors are composed of three subunits: A, B, and C; commonly expressed within operons. The A subunits are transmembrane proteins featuring a large N-terminal hydrophobic domain and a small hydrophilic C-terminal domain (46, 77). The B subunit proteins are thought to be integral membrane proteins that may be involved in germinant recognition (82). The C subunits are lipoproteins attached to the outer surface of the inner membrane. The structure of the C subunit of the GerB receptor has been solved, but the protein is a novel structure, thus not providing specific insights (83). The levels of Ger receptors in spores can vary tremendously, in rich media levels of individual receptors in *B. subtilis* range from 600-1100 molecules per spore but can be up to 8-fold lower in minimal media (84). Ger receptor levels vary between individual spores within populations as well, thought to be due to complicated regulation of expression of the receptors during sporulation (85-87). Levels of Ger receptors within spores is thought to be directly related to response and rate of germination for both populations and individual spores (88, 89).

Germination Specific Lytic Enzymes:

The degradation of the spore cortex during Stage II of germination is accomplished through the activity of the Germination Specific Lytic Enzymes (GLSEs) which are classified into two groups: the spore cortex-lytic enzymes (SCLE) and cortical fragment-lytic enzyme (CFLE) (57, 76). SCLEs preferentially hydrolyze intact spore cortex peptidoglycan while CFLEs are thought to further degrade partially hydrolyzed peptidoglycan (57, 76). Both SCLEs and CFLEs recognize and require the presence of δ-lactam for their activity and are therefore only able to act on cortex peptidoglycan and not germ cell wall peptidoglycan (57).

GSLEs have been identified in many spore forming bacteria including some Clostridia and several *Bacillus* species including *B. megaterium, B. subtilis, B. cereus,* and *B. anthracis* (57, 90-92). However, in contrast to *Bacillus* species, most *Clostridium* species appear to only contain a single essential GLSE, SleC (78). The GSLEs in *B. anthracis* are SleB and CwlJ1, which are SCLEs, and SleL, a CFLE (76, 92, 93). The function of these enzymes is critical to completing spore germination. Spores whose cortex is not broken down are unable to complete germination and return to the vegetative state (75, 76).

SleL, an *N* –acetylglucosaminidase, is formed by three conserved domains: two N-terminal LysM domains and a C-terminal glycosyl hydrolase family 18 domain (93). Mutants lacking both SleL LysM domains have decreased peptidoglycan binding and hydrolysis, but it appears that these domains play no role in recognition of muramic-δ-lactam (93). These LysM-lacking proteins were also unable to properly localize within the spore during sporulation and instead were degraded within the mother cell (93). SleL with both LysM domains intact is localized in the dormant spore between the outer cortex and coat layers (93). During sporulation, *sleL* is expressed in the mother cell under the control of sigma E. Homologs of SleL are found in both *B. subtilis* and *B. cereus.* In *sleL* mutant spores, cortex hydrolysis has been shown to occur more slowly but germination and outgrowth are still completed (93).

In *B. anthracis, cwlJ1* is expressed from a bicistronic operon with its partner *gerQ,* unlike in *B. subtilis* where *cwlJ* is separated from *gerQ* (75). The gene *cwlJ* is expressed under the control of sigma E in the mother cell of sporulating *Bacillus* cells, and CwlJ is subsequently localized to the spore coat layer (94). The presence of CwlJ in the coat layers is required for spore germination induced by exogenous Ca^{2+}-DPA (46, 95-97). GerQ has been shown to be required for localization of CwlJ to the spore coats; in *B. subtilis gerQ* mutant strains, CwlJ appears to be nonfunctional

(96). The lytic domain of CwlJ1 shares significant sequence homology with that of SleB, and CwlJ1 alone has been shown to carry out sufficient cortex hydrolysis to allow completion of spore germination although at a slightly reduced rate (76). In *B. anthracis,* another SCLE, CwlJ2 has been identified but has been shown to play only a very minor role in cortex degradation (76).

SleB and CwlJ have been shown to fulfill partially redundant roles in the germination process in *B. subtilis, B. megaterium,* and *B. anthracis* (74, 76). Unlike *sleL* and *cwlJ*, *sleB* is expressed under the control of σ^G within the developing forespore (98). SleB is widely conserved among the *Bacillus* species including *B. subtilis, B. cereus, B. halodurans,* and *B. megaterium* (99). The *sleB* gene is organized in a tricistronic operon containing both *ypeB* and open reading frame BAS2560 in *B. anthracis* while only in bicistronic operon with *ypeB* in *B. subtilis* (92). The organization of *sleB* and *ypeB* in an operon is conserved across *Bacillus* species and a few *Clostridia* (92). BAS2560 shows homology to lipoproteins YlaJ and YhcN from *B. subtilis.* YlaJ is an uncharacterized spore protein, and YhcN has been demonstrated to be present within dormant spores although it fulfills an unknown role (92, 100).

SleB is a lytic transglycosylase whose specific target, like other GSLEs, is peptidoglycan containing muramic-δ-lactam, which is present in as much as 50% of cortex peptidoglycan (61) (92). The full length *B. anthracis* SleB protein is 253 amino acids long including an N-terminal signal sequence, a peptidoglycan binding domain, and a C-terminal catalytic domain (101). Although SleB functions during germination, the protein is present in its mature form, lacking its signal sequence, within the dormant spore (96). The mechanism by which SleB is stabilized and held inactivate within the dormant spore is unknown but YpeB has be implicated in fulfilling this role (98).

YpeB:

B. anthracis YpeB is 446 amino acids long in its mature form within the dormant spore. Its N-terminal region includes a hydrophobic region, which is predicted to anchor the protein to the inner membrane, and three PepSY domains are near the C-terminus (98). PepSY domains are predicted to play a role in the inhibition of enzymatic activities of other protein domains, but the mechanism of this inhibition is currently unknown in most instances (102). One study has shown that a PepSY domain is involved in protease inhibition prior to autoprocessing and subsequent activation of the thermolysin M4 family of zinc metalloproteases (103). In this instance the C-terminus of the PepSY domain is physically disruptive of the active site, this domain is later cleaved to facilitate enzyme activation (103). Several factors implicate YpeB in the stabilization and inhibition of SleB in dormant spores. As previously mentioned, YpeB and SleB are organized in the same operon in *Bacillus* species. The two proteins are co-dependent, meaning that in strains in which either *sleB* or *ypeB* has been inactivated or deleted, the germination defects are the same and both proteins are unable to be detected by western blot (99, 104). The time of expression of both *sleB* and *ypeB* aligns with that of genes regulated by sporulation factor σ^G, which is active in the forespore upon completion of engulfment (105). This suggests that both proteins would be transported outside of the cytoplasm at that time; YpeB remaining anchored in the inner forespore membrane. Thus SleB and YpeB are believed to be co-localized at the inner spore membrane of the dormant spore. One study has suggested that SleB and YpeB also localize to a second location outside the cortex, close to the spore coats, but this is in disagreement with previous data and current models (99).

Previous studies in *B. subtilis* indicate that YpeB is required for both SleB activity and stable incorporation into the spore (70, 98). Recently, this relationship has been demonstrated

within *B. anthracis* spores as well (104). Studies investigating the role of the individual domains of YpeB in the stabilization of SleB have implicated both N and C terminal domains of YpeB. It has been shown that that the C-terminal domain of YpeB, fused to its signal sequence, is unable to complement a germination defect when co-expressed with full length SleB, demonstrating that the N-terminal region of YpeB is required (106). A study from our lab indicated that not only is this N-terminal region required, but the C-terminal PepSY domains are also required for stable incorporation of SleB (104). Further studies demonstrated that the N-terminal region of YpeB including residues 67-203, although itself stable within the spore, was insufficient to properly stabilize SleB (104). In addition, a truncation mutant containing residues 1-283 of YpeB, corresponding to the entire N-terminal region and the first PepSY domain, was unable to stabilize SleB as demonstrated by western blot analysis (104). These results taken together indicate that both the N-terminal and the C-terminal (containing the PepSY domains) regions of YpeB are required for stable incorporation and subsequent function of SleB within the dormant spore.

The simplest explanation for this relationship is that the two proteins physically interact within the dormant spore. Both YpeB and SleB are present at the inner spore membrane of a dormant spore. During germination, YpeB is rapidly cleaved into distinguishable degradation products (96, 107). If YpeB were stabilizing SleB, perhaps this cleavage of YpeB is the event that releases SleB to degrade the spore cortex. Several attempts have been made to isolate or provide evidence of a SleB-YpeB complex. Thus far, efforts have proven to be unsuccessful.

HtrC:

HtrC is a serine protease expressed in the forespore under the control of σ^G (108). HtrC features a transmembrane helix and was determined to be localized to the inner spore

membrane via proteomic studies (109, 110). Recent work demonstrated that HtrC is required for specific degradation of YpeB during spore germination in both *B. anthracis* and *B. subtilis* (107). Although HtrC degrades YpeB specifically, YpeB is still degraded into nonspecific fragments during germination of a Δ*htrC* strain (107). The validity of a model in which YpeB degradation is necessary for spore germination mediated through SleB activity remains to be determined.

Chemical Cross-linking:

Most commonly, protein-protein interactions have been identified *in vivo* through affinity purification methods including co-immunoprecipitation or affinity pull-down assays. These assays are effective, although problems can arise leading to false positives or more likely missing weaker interactions through the rigorous washing steps. The detection of protein interactions *in vivo* is complicated by the fact that proteins themselves are chemically distinct with different charges and folding patterns and many of these interactions are transient or have small interfaces through which the interaction occurs. Chemical cross-linking can be used to rapidly form stable covalent bonds between interacting proteins *in vivo* and thus allow isolation of a complex which can be further studied using various techniques including mass spectrometry (111).

Several peptide cross-linking reagents exist and are commercially available. These reagents are classified based on specificity, spacer length, permeability and reactivity. Specificity refers to which functional groups are targeted by each arm of the cross-linker. Spacer length is the allowable distance between the ends of the cross-linker. Permeability refers to the ability of the cross-linker to penetrate intact cells, and reactivity is how quickly covalent bonds may be formed. In addition to commercial cross-linking reagents, others including formaldehyde have proven useful in the detection of protein interactions within intact cells (111-114).

Formaldehyde cross-linking in conjunction with mass spectrometry has been demonstrated as an effective technique for identifying protein-protein interactions *in vivo* (112) (111, 113, 114). Several features of formaldehyde make it ideal for cross-linking studies. Cross-links formed by formaldehyde represent interactions over a short distance (2 Å) thus, proteins cross-linked by formaldehyde must be closely interacting (112). Formaldehyde's small size allows it to penetrate cell membranes easily and form cross-links within intact cells (112). The product of formaldehyde cross-linking is stable and will retain its structure even in nonphysiological conditions (112). Possibly most important, the cross-links formed as a result of formaldehyde are reversible, which allows for analysis of the individual components within a complex (112).

Photo-affinity cross-linking is a relatively recently developed tool within chemical cross-linking. These cross-linkers are heterobifunctional featuring a primary amine or sulfhydryl targeted motif and a photoactivatable group. The advantage of the photoactivatable group is that upon irradiation with UV light, this group can form non-specific covalent bonds with any molecule within spacer arm distance, including DNA, RNA, or peptides (115, 116). These reagents have become powerful tools for not only determining protein complexes but also investigating protein-DNA interactions as well as intramolecular interactions between various domains of a protein of interest (117).

Transposon Sequencing (TnSeq):

Transposon sequencing (TnSeq) is a high throughput genetic screen in which a saturated transposon library is submitted to specific experimental conditions to determine genes required for the tested condition. After submission of the transposon insertion library to desired testing conditions, DNA is extracted and digested with restriction enzymes generating transposons

flanked by genomic DNA sequences (118). Adapters are ligated to facilitate next generation sequencing workflows, and sequences are PCR amplified (118). Insertions are then sequenced and mapped to the genome of interest using the Tn-flanking genomic DNA segments (118). Insertion profiles can then be compared between experimental conditions and controls. Genes with an altered number of insertions following selection are those likely to be necessary in the conditions tested. TnSeq has proven to be a powerful tool and has been used to investigate genes required for numerous cellular processes, including sporulation (118-121).

Previously, the process of spore germination and specifically the interaction of proteins within this process, has been studied on a relatively small scale, focusing on individual interactions one at a time. In order to identify possible genes that may play a role in a putative YpeB – SleB interaction and the germination process as a whole we needed to expand the scope of our experiments. TnSeq gives the potential for genetic interaction analysis on the genome scale. A generated transposon insertion library can be submitted to germination conditions and separated into dormant and germinated populations. High throughput sequencing can be performed and comparisons can be made between populations elucidating candidate genes for further study.

Study Objectives:

The focus of this research was to identify and characterize proteins active in spore germination including further characterization of potential YpeB interactions within the dormant spore. Previous work has demonstrated that both the N-terminal and C-terminal domains of YpeB are required for stable incorporation of SleB and subsequent function in Stage II of germination. The roles these domains play in maintaining SleB and spore dormancy is not well characterized.

Additionally, there are many key events within spore germination that remain poorly understood, including signal transduction from germinant receptor to initiate spore germination.

Chapter 2 describes the implementation of a TnSeq workflow to identify additional germination active proteins. A transposon library featuring 5.5 x 10^4 insertions over 3,114 genes with ≥ 10 unique insertions per gene was generated in *B. subtilis* and submitted to germination conditions via L-valine. In total, 61 genes were determined to be underrepresented in germinated spores compared to those unable to complete germination. Of those genes not previously implicated in spore germination, 14 were found to express proteins present in the spore membrane proteome by previous studies (109, 110). These genes were ultimately determined to be affecting initiation of germination rather than a specific slowing of germination. It was determined that deletions of these genes often altered levels of the GerA receptor within dormant spores thus slowing germination initiation. How or why these proteins effect GerA abundance within the spore remains to be determined.

Chapter 3 investigates the role of the YpeB domains in stabilization of SleB. Through *in-vivo* chemical cross-linking of dormant spores, it was determined that YpeB likely exists as an multimer within the dormant spore. Cross-linking mediated through targeted sites in the YpeB C-terminal PepSY domains indicate that YpeB readily cross-links to produce a complex twice the mass of the YpeB monomer. Studies of YpeB internal truncations further indicate YpeB dimerization occurs mediated through C-terminal PePSY residues. Bacterial two-hybrid assays demonstrate the N-terminal domain of YpeB to have a strong self-association, thus suggesting this domain to have a role in oligomerization. In addition, both N and C terminal domains were determined to interact with full length YpeB, a possible further indication that both domains are required for an YpeB oligomerization. Determination of the role of YpeB oligomerization in

stabilizing SleB remains difficult due to the co-dependent nature of the two proteins. If YpeB oligomerization is required for SleB stability and is disrupted, SleB would likely be degraded, but if YpeB structure is unstable this too would lead to SleB degradation and thus it becomes difficult to attribute cause to either individual structural stability or oligomerization.

Furthering our understanding of spore germination, especially early initiation and commitment steps, could potentially lead to novel and more effective spore decontamination methods. Better understanding of the proteins acting within germination may identify targets for triggering germination, such as SleB, or provide additional insight into how signals are transduced within the spore to induce germination, so that these pathways may be subverted or bypassed to cause spores to germinate, facilitating easier spore killing and decontamination efforts.

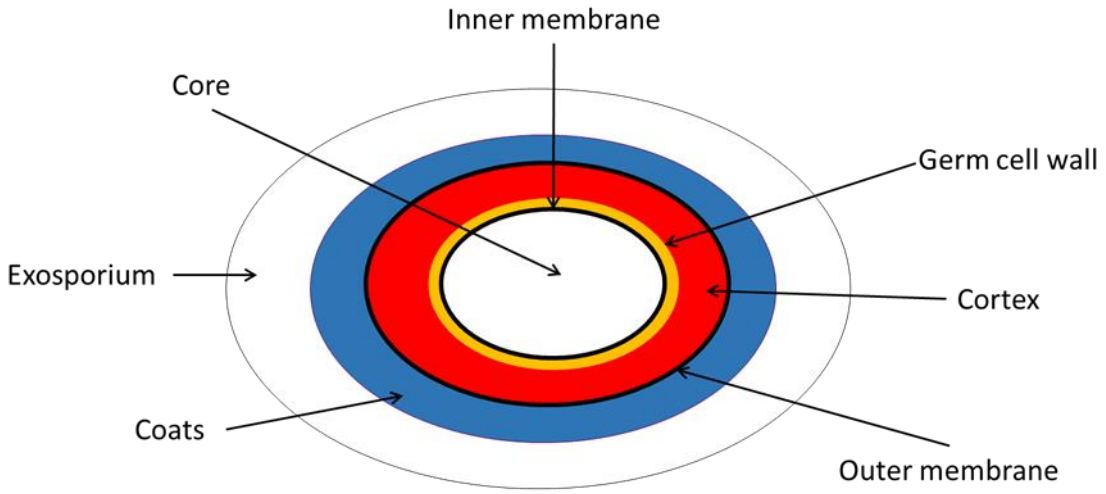

Figure 1.1. Spore structure. Simplified schematic depicting individual layers of the dormant spore. The core, which stores all of the spore's DNA and cellular machinery is surrounded by multiple layers contributing to spore resistance capacities and dormancy. The spore includes an inner membrane, a germ cell wall, the cortex, an outer membrane, and proteinaceous coats. *B. anthracis* includes an additional exosporium layer, but this is not present in all species.

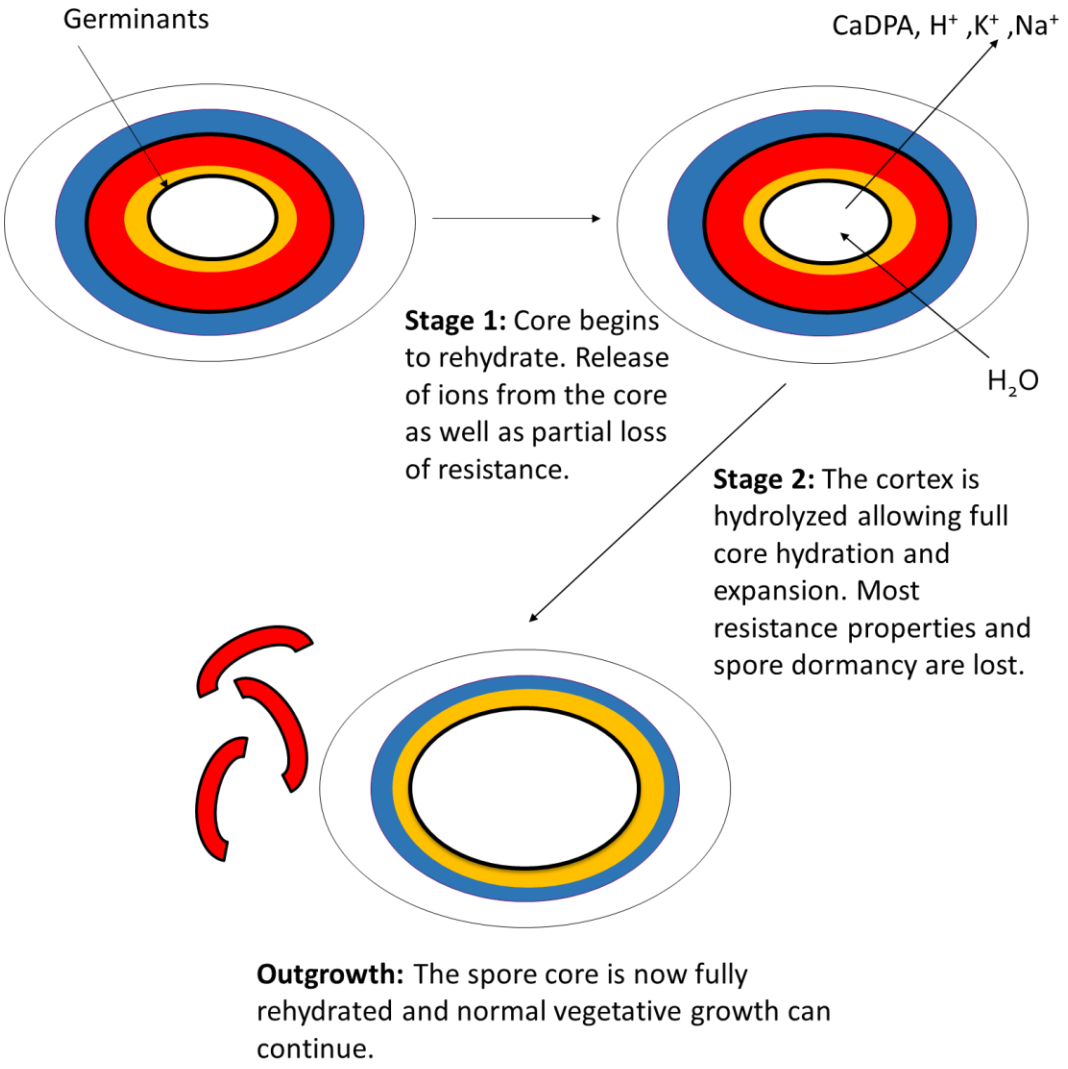

Figure 1.2. Spore germination. Germination is initated when germinants contact germinant receptors embedded in the inner spore membrane. Following initiation and commitment, the spore proceeds into Stage I. Stage I features partial rehydration of the core coinciding with a release of Ca^{2+}-DPA and other ions. Hydration of the core activates Stage II, in which GSLEs are activated, degrading the cortex. Following cortex degradation, the spore continues through an outgrowth period in which the core swells as it becomes fully hydrated and normal metabolism resumes.

CHAPTER 2

Identification of Germination-Active Genes in *Bacillus subtilis* using TnSeq

Cameron V. Sayer, Bidisha Barat, and David L. Popham. Submitted April 2019.

ATTRIBUTIONS

Cameron V. Sayer and Bidisha Barat contributed equally in performing the research, experimentation, and data analysis of the material presented. David L. Popham was the principle investigator. Cameron and David created the Transposon library in PS832 and designed the TnSeq germination experiment. Cameron analyzed the TnSeq sequencing read data and is responsible for the work presented in Figures 2.1 and 2.4 in addition to Tables 2.1, 2.2, 2.3, and 2.4. Bidisha is responsible for work presented in Figures 2.2, 2.3, and 2.4 in addition to Tables 2.3, 2.4, and 2.5. Cameron, Bidisha, and David contributed to the writing of the manuscript.

ABSTRACT

Bacterial endospores can survive harsh environmental conditions and long-term dormancy in the absence of nutrients, but can rapidly germinate under favorable conditions. In the present study, we employed transposon sequencing (TnSeq) to identify genes with previously uncharacterized roles in spore germination. Identified genes that encoded spore inner membrane proteins were chosen for study of defined mutants, which exhibited delayed germination in several assays in response to varying germinants. Significantly slowed release of DPA indicated that mutants were affected in Stage I of germination. Several mutants exhibited phenotypic traits consistent with failure of a GerA germinant receptor-mediated response, while others appeared to have a more general loss of response to varied germinants. Use of a *gerA-lacZ* transcriptional fusion and quantitative western blotting of GerAC allowed mutants to be classified based upon normal or decreased *gerA* transcription and normal or reduced GerA accumulation. Fourteen genes were identified to have newly described roles within *Bacillus* spore germination. A more complete understanding of this process can contribute to the development of better spore decontamination procedures.

INTRODUCTION

Bacterial endospores are capable of extended periods of dormancy while remaining resistant to a variety of chemical and physical decontamination measures (47). Dormant spores can rapidly germinate when in a suitable environment, returning to a vegetative state (122, 123). These factors allow endospores produced by certain species of *Bacillus* and *Clostridium* to excel as human pathogens, act as potential bioterrorism agents, and contribute to significant food contamination events (124, 125). Preservation of dehydration of the metabolically inactive spore core is the greatest factor in spore resistance properties and maintenance of spore dormancy (47). This dormant state is maintained by the inner spore membrane, which exists in a largely non-fluid state (126), and a thick layer of peptidoglycan termed the cortex (127). Additionally, the accumulation of small molecule solutes within the core, such as calcium dipicolinic acid (DPA), contribute to spore dehydration and resistance properties (47).

When dormant spores sense an environment conducive to vegetative growth, they will rapidly germinate. Environmental sensing is achieved through the action of proteins expressed late in sporulation, termed germinant receptors. *Bacillus subtilis* encodes three functional Ger receptors: GerA, GerB, and GerK (77). The GerA receptor responds to amino acids such as L-alanine and L-valine, while the GerB and GerK receptors work together to respond to a mixture of L-asparagine, D-glucose, D-fructose and K^+ ions (AGFK) (122). The mechanism of signal transduction from Ger receptors to other spore components to initiate germination is not well understood, but a major event is the opening of a channel involving SpoVA proteins to release Ca^{2+} - DPA from the spore core (73). The GerD protein of *Bacillus* species is required for a rapid response to germinants. Recent work suggests that GerD is essential for the colocalization of Ger

receptors in the spore's inner membrane in a cluster termed the germinosome and probably plays an intermediate role in the signal transduction pathway from germinant-receptor complex to downstream germination effectors (73, 81).

Each Ger receptor is composed of three subunits: A, B, and C. The A subunits are transmembrane proteins featuring sizable domains on each side of the membrane (77, 123). The B subunit proteins are thought to be integral membrane proteins that may be involved in germinant recognition (82). The C subunits are lipoproteins attached to the other surface of the membrane (128). Following triggering of the Ger receptors, water begins to partially rehydrate the spore core, and Ca^{2+} DPA is released along with other ions contained within the spore core. The spore cortex is then degraded through the action of germination-specific lytic enzymes (GSLEs) which allow the spore core to continue to expand and return to a fully hydrated state (129). The spore will then resume metabolism and continue through outgrowth, eventually returning to a fully vegetative state.

The goals of the current study were to identify additional genes with potential roles in spore germination. Whereas previous studies have characterized genes whose loss resulted in a near complete block of germination, we sought to find genes with more subtle phenotypes that were potentially missed by previous procedures. Creation of a transposon-insertion mutant library and submission of spores produced by that library to germination conditions, in combination with Transposon Sequencing (TnSeq)(118), facilitated identification of 61 genes that exerted significant effects on germination efficiency or rate. Among these, 14 genes had not been previously associated with spore germination and had been shown to produce proteins within the spore membrane proteome, and these were selected for further characterization. Defined

gene knockout strains demonstrated reduced germination. Further studies implicated certain genes in affecting the overall GerA receptor abundance within the dormant spores.

MATERIALS AND METHODS

Strain construction. DNA extracted from a previously constructed Tn-insertion library (119) was transformed into PS832 with selection for spectinomycin resistance (100 µg/mL). Roughly 150,000 independent transformants were pooled from plates to produce a new library.

Mutants lacking single genes were obtained from the *Bacillus* Genetic Stock Center. Each mutation was a deletion/insertion, with the gene of interest replaced by an erythromycin resistance gene flanked by two *loxP* sites (130). The mutations were introduced into *B. subtilis* strain PS832 by natural transformation with selection for erythromycin (2.5 µg/ml) and lincomycin (12.5 µg/ml) (MLS) resistance.

Chromosomal DNA from *B. subtilis* strain DPVB724 with a *gerB* deletion and insertion of a chloramphenicol (3.0 µg/ml) resistance gene was used to transform strains to $GerB^-$. This was done to reduce background detection of GerBC during western blot quantification of GerAC.

B. subtilis strain DPVB761 with a *gerA-lacZ* fusion marked with an MLS resistance gene was obtained from the Setlow lab (131, 132). Since all the putative Ger mutant strains had the same resistance gene marker, it was essential to delete the MLS resistance gene in order to transform the mutant strains with chromosomal DNA carrying the *gerA-lacZ* fusion. The Cre recombinase was expressed from plasmid pDR244 (130) to stimulate deletion of the resistance gene, leaving an unmarked in-frame deletion mutation. The *gerA-lacZ* fusion was then introduced

by natural transformation into mutant strains carrying an unmarked deletion, with selection for MLS resistance.

Chromosomal DNA from *B. subtilis* strain DPVB833, in which *gerA* expression is under the control of spore-specific promoter *PsspD (133),* was introduced by natural transformation into strains with an unmarked deletions, with selection for MLS resistance. All mutations were verified by PCR and agarose gel electrophoresis.

Spore preparation. *B. subtilis* spores, both single strains and the Tn-insertion strain library, were prepared in 2xSG broth (134). Spores were harvested after 3-4 days incubation at 37°C and washed in water for several days.

To prepare germinated spores from the Tn-insertion library, a 10-ml suspension of dormant spores at an optical density at 600 nm (OD_{600}) of 100 in water was heat-activated at 70°C for 30 min and cooled on ice for 10 min. The spores were then submitted to germination conditions in 50 mM $NaPO_4$ with 10 mM L-valine at 37°C for 45 minutes. OD_{600} was monitored to ensure progression through germination. Germinated spores were collected by centrifugation at 12,000 *g* for 5 min at 4°C. After germination, subpopulations of dormant and partially germinated spores (d≥1.25 g/ml) and fully germinated spores (d~1.19 g/ml) were collected following centrifugation through a layer of 43% sodium diatrizoate.

Sequencing of Tn insertion sites. All spore samples were decoated using urea, sodium dodecyl sulfate, and dithiothreitol as described previously (84). DNA was extracted from decoated spores using the Gram-Positive protocol from the Qiagen Blood and Tissue kit. DNA was digested with *Mme*I and quantified using Qubit (ThermoFisher). Samples were sent to the High-Throughput Sequencing and Genotyping Center at the University of Illinois for library preparation and sequencing. Adaptor ligations were performed including index bar codes as well

as flow cell sequences. Following adaptor ligation, samples were PCR amplified for 18 cycles. After amplification, samples were purified and sequenced using an Illumina Hi Seq 2500, yielding reads with 5' transposon sequence followed by a 16-bp region of genomic DNA. Sequencing read data files were uploaded an analyzed using Geneious (version 10.0) (http://www.geneious.com, (135)). Reads were filtered and trimmed leaving only genomic sequences and mapped to the JH642 *B. subtilis* genome (136). Tables were exported from Geneious listing number of reads contained within each annotated gene. Reads within each individual data set were expressed as a function of the total number of reads per million from that sample. Once normalized, both experimental data sets, dormant and germinated, were compared against one another allowing reporting of fold change between samples. DESeq2 was used to determine p-values comparing dormant and germinated samples (137). Genes with 2-fold higher number of reads in the dormant versus the germinated sample and significant p-values (≤0.05) were selected for further study.

Germination assays. Purified spores were heat activated at 70°C for 30 min, quenched on ice for 5 min, and diluted to an OD_{600} of 0.2 in 50 mM $NaPO_4$ buffer (pH 7.4) containing L-valine (10 mM) or AGFK (10 mM L-asparagine, 1 mM D-glucose, 1 mM D-fructose, 10 mM KCl). Purified spores were heat activated at 70°C for 30 min, quenched on ice for 5 min, and stimulated to germinate by dilution to an OD_{600} of 0.2 in 2xYT (Final concentrations: 8 mg/ml Yeast Extract, 12.8 mg/ml Tryptone, 4 mg/ml NaCl). Changes in optical density were monitored using a Spectronic Genesys 5 spectrophotometer (Spectronic).

Purified spores of strains with and without overexpressed *gerA* were heat activated at 70°C for 30 min, quenched on ice for 5 min, and diluted to OD_{600} of 0.1 in 25 mM HEPES buffer

(pH 7.4). Nutrient germinants were added as described above, and changes in optical density were monitored using a Tecan M200 plate reader (Tecan).

Purified spores at an OD_{600} of 1.0 were germinated with 1 mM dodecylamine in 20 mM KPO_4 (pH 7·4) at 37°C. At indicated times, 1 ml of germinating spore suspensions were centrifuged 15,800 x g for 2 min. The A_{270} of the supernatant was measured to quantify DPA release, which was expressed as a fraction of the total spore DPA content. Total spore DPA was determined by boiling spores for 30 min and measuring the A_{270} of the resulting supernatant.

Spores from each mutant strain were heat activated at 70°C, suspended in 25 mM HEPES buffer (pH 7.4) and submitted to germination conditions with 10 mM L-valine at 37°C. Aliquots were taken from the germinating spores at indicated times and centrifuged at 10,000 g for 45 secs. The spore exudate was analyzed to determine the amount of DPA released (138).

To measure Dpm and NAM release, mutant spores were heat activated at 70°C, suspended in 25 mM HEPES buffer (pH 7.4) and incubated with 10 mM L-valine at 37°C. OD_{600} was recorded and aliquots were taken from the germinating spores at indicated times. Samples were centrifuged, and the spore exudate was subjected to amino acid/amino sugar analysis as previously described (139). Sample peaks were identified based on elution times and quantified by integration of peak areas in comparison to known standards.

Dormant spores were observed using phase-contrast microscopy prior to germination, such that there were 70-100 spores per field of view and images were collected for 10 fields per sample. Spores were then heat activated at 70°C for 30 min, quenched on ice for 5 min, resuspended in 50 mM $NaPO_4$ buffer and stimulated to germinate by addition of 10 mM L-valine for 60 min, and observed by microscopy again. The image processing toolkit Fiji was combined with segmentation machine learning algorithms (140), in the open-source software project

Trainable Weka (Waikato Environment for Knowledge Analysis) Segmentation (TWS)(141). Images in which spores had been manually classified as phase-bright and phase-dark were used to train the classifier. Once the classifier was trained, this segmentation algorithm was used to classify phase-bright and phase-dark spores in further images. Data was analyzed for images from 3 fields per sample.

Assay of *gerA* transcription. *B. subtilis* strains with a *gerA-lacZ* transcriptional fusion were grown and sporulated at 37°C in 2xSG medium. Purified spores were chemically decoated, washed, and extracted, and β-galactosidase activity was assayed using methyl-umbelliferyl-D-galactoside (MUG) as previously described (87, 142, 143). MUG fluorescence was measured in a microplate reader (Tecan) using excitation and emission wavelengths of 365 nm and 450 nm, respectively. Standard solutions of methylumbelliferone were prepared in the same mix of buffers in order to calibrate the fluorescence readings. The average activity of PS832 (wildtype without *gerA-lacZ* fusion) samples was subtracted from the values for all samples containing the *gerA-lacZ* fusion, and all readings were normalized to decoated spore OD_{600} values.

Western blotting. Quantitative western blots were performed on strains carrying a *gerB* deletion to avoid cross-reactivity with the GerAC antibody. Purified dormant *B. subtilis* spores (~100 OD_{600} units) were decoated and proteins were extracted as previously described for western blot analysis (84). Samples were then serially diluted with 2x SDS-PAGE sample loading buffer and *gerA gerB* or *gerD* spore protein extract. TGX Stain-Free Fast Cast premixed acrylamide solution (Bio-Rad) was used, which enabled rapid fluorescent detection of tryptophan residues in proteins directly within gels and blots. The proteins were Trp-modified after separation by a trihalo compound included in the electrophoresis gel, allowing fluorescent visualization and quantitation of proteins on gels and blots immediately after the completion of

electrophoresis and transfer. The total protein load and recovery for each lane was measured as the total fluorescence intensity for each lane of the blot. This was followed by probing with anti-GerAC (87) or anti-GerD (87) antibodies via chemiluminescent western blot. Band intensity was normalized to the protein present in each lane. Biorad Image Lab 6.0 was used to perform data analysis of quantitative blots. Dilutions of 1.0, 0.5, 0.25, and 0.125 concentration were blotted. Only the 1.0 and 0.5 concentrations were found to be within the linear range of detection, and these were used for quantification. Quantitative GerAC and GerD western blots were performed in triplicate for the strains featuring deletions of genes included in Table 2.

RESULTS

Identification of mutant strains with slowed or reduced germination. Seeking to identify additional genes that contribute to spore germination, TnSeq was used to reveal genes functioning in the early stages of germination. A library of *magellan6x* transposon insertions (119) was transformed into a *B. subtilis* wild type strain, PS832, that is highly efficient at spore formation and germination. An estimated 150,000 independent transformants were pooled into a library from which dormant spores were produced. A sample of this spore library was collected for Tn insertion site sequencing.

Dormant spores were heat-activated and were submitted to germination-inducing conditions with 10 mM L-Valine at 37°C for 45 min. A 45% drop of the starting OD_{600} was observed as an indication of germination. Following germination, a density gradient was used to separate dormant (and possibly partially germinated) spores (≥1.25 g/ml) from fully germinated spores (~1.19 g/ml)(144). This procedure was performed using two independent dormant spore preparations (NCBI BioSamples accessions: SAMN11823435, SAMN11823436, SAMN11823437).

DNA was extracted from the starting spore population and the dormant and germinated spores, and the Tn insertion sites were sequenced as described (119) and mapped to the *B. subtilis* genome. The total library was found to have 5.5 x 10^4 unique insertions spread over 3,114 genes featuring ≥10 unique insertions per gene. The number of reads within each gene were normalized as a fraction of the total reads obtained for that sample. Normalized data sets from germinated and dormant spores were then compared against one another to determine fold change. Genes with a higher proportion of reads in the dormant population indicating a possible role in germination. DESeq2 was implemented to determine p-values to further differentiate mutant abundance between sample sets (137, 145).

In total, Tn insertions in 61 genes were found to be ≥2-fold underrepresented in the germinated spores compared to those unable to complete germination (Table 2.1). These included all three genes of the *gerA* operon, *gerE,* coat proteins *cotH and cotE*, and genes from the *gerP* operon, all of which have known strong effects on germination. Slightly less than half of the genes identified were known previously to have either sporulation or germination defects.

The identified genes that were not previously implicated in spore germination were cross-referenced against proteins found in the inner spore membrane proteome (109, 110), identifying a group of 14 genes that were studied further (Table 2.2). The majority of these genes were largely uncharacterized and were annotated with a wide range of putative functions. Many of the genes are not known to be expressed via sporulation-specific regulatory factors but rather are regulated by vegetative cell transcriptional controls.

Characterization of germination of mutant strains. Strains carrying insertion mutations (130) in each of the genes listed in Table 2.2 were obtained from the *Bacillus* Genetic Stock Center, and these mutations were transformed into PS832. Mutant strains were characterized

with regard to growth rate and sporulation efficiency (Table 2.3). They were then analyzed using several germination assays to verify the defect indicated by the TnSeq data in addition to providing insight into potential function of these genes in germination. Strains were germinated with the addition of 10 mM L-valine, and OD_{600} was monitored; an example assay is shown in Fig 2.1 (Additional data in Fig S1). Each mutant strain exhibited a significant germination rate defect in response to L-valine in comparison to the wild type (Table 2.4). The most severe delays in germination rate were observed for the *ylbC, dnaJ, sipT,* and *hfq* mutants.

The slowed germination phenotype was further characterized by examining the individual stages of germination using assays for release of dipicolinic acid (DPA) (Stage I) and N-acetylmuramic acid (Stage II)(123). Spores from each mutant strain were heat-activated, suspended in 25 mM HEPES buffer, and submitted to germination conditions with 10 mM L-valine at 37°C. The amount of DPA released from many of the mutant strains was vastly reduced compared to that of PS832 (Table 2.3). The only strains that were not significantly different from PS832 were the *yybT, ytxG*, *pcrB*, and *phoR* mutants. Mutant strains lacking *sipT, ylbC, or ytpA* demonstrated NAM release significantly less ($p<0.05$) than that of PS832 (Table 3, Fig S2). The rest of the mutants exhibited reduction compared to PS832 but due to high variation among replicates were not found to be significantly different (Table 2.3, Fig S2).

When mutant spore populations exhibit a decreased OD change during germination, it could result from a large percentage of the spore population germinating incompletely or from a smaller percentage of the population germinating at a normal rate with the remainder remaining fully dormant. Spores of the various strains were imaged using phase-contrast microscopy, both prior to and one-hour post-germination with 10 mM L-valine (Fig 2.2), and spores were classified as phase-bright or phase-dark based on pixel intensities (Fig S3). All spore samples had ≥95%

phase-bright spores prior to germination. Post-germination, the wildtype spores had 95% phase-dark spores while most of the mutant strains had significantly decreased percentages of phase-dark spores (Table 2.4), indicating that much of the mutant strain spore populations did not initiate germination.

Additional assays were performed using the germinants AGFK and 2xYT (Table 2.4), which began to differentiate the mutants into distinct phenotypic groups. The first group features a reduction in germination rate to all nutrient germinants tested: L-valine, AGFK, and 2xYT, and includes strains with mutations in *skfE, ylbC, hfq* and *dnaJ*. The second phenotype includes strains with a significantly delayed L-valine germination response, via a GerA receptor, but otherwise germinate normally in response to rich medium and AGFK, via the GerB and GerK receptors. The following strains featured this phenotype: *yybT, ygaC, yqhL, yqeF* and *sipT.* The final group included strains with significantly slower germination rates in response to L-valine but have a delay in response to either AGFK or 2xYT, but not both. Mutants lacking *ytpA, phoP, phoR, pcrB* and *ytxG* feature these phenotypes. In addition, all mutant strains were capable of normal non-nutrient, non-Ger-receptor-mediated germination, in response to dodecylamine (Table 2.4).

To determine if spores from mutant strains were blocked in germination or if they were simply severely delayed, spores were plated and colonies that appeared over a 48-hour period were counted. After 24 hours, all strains produced cfu/OD_{600} values similar to that of the wild type strain, and none of the strains produced a >4% increase in colonies after the first 24 hours (Table S3), indicating that the defects were a significantly slowed germination process and not complete death of the spores.

Expression of the GerA receptor in mutant strains. Decreased germination in response to L-valine can result from a low abundance of the GerA receptor (87, 143). A *gerA-lacZ* transcriptional fusion was used to determine if germination defects were correlated to reduced *gerA* transcription. Mutant strains lacking *sipT, ytpA, ylbC*, or *ygaC* showed a significant decrease in *gerA* transcription following sporulation in comparison to the wildtype (Fig 2.3). To determine if this was a general effect on σ^G-dependent transcription, the effects of these mutation on the expression of *pbpF* and *sspB* were examined using *lacZ* fusions. The expression of these two genes was unaffected by these mutations (Fig S4).

Quantitative GerAC western blots were performed to determine the amount of GerA receptor in spores of all strains (An example western blot is in Fig 2.4A; additional blots are in Fig S5). Many of the mutant strains exhibited significant decreases in GerAC abundance; the most significant being a 75% decrease in a *dnaJ* mutant (Fig 2.4B). The abundance of GerD was also determined using quantitative western blots for spores of all mutant strains, as a GerD deficiency could result in reduced germination efficiency. All the strains contained amounts of GerD similar to that of the wild type, suggesting that GerD remains unaffected in these mutant strains (Fig S6).

Overexpression of the GerA receptor in spores has previously been shown to increase the response to GerA-specific germinants (133). A fusion of the *gerA* operon to the forespore-specific *sspD* promoter (133) was introduced into strains in order to determine if GerA overexpression could reverse the germination defects associated with the mutations under study. In almost all cases, GerA overexpression reversed the germination deficiency with L-valine (Table 2.5), suggesting that decreased GerA abundance made a significant contribution to the reduced germination efficiency in these mutant strains. Strikingly, in the *ytxG* mutant, overexpression of GerA increased the germination deficiency. As previously observed (133),

overexpression of GerA resulted in significant decreases in the germination response to AGFK in all strains (Table S2). In mutant strains that exhibited reduced germination in response to 2xYT, GerA overexpression reversed this deficiency (Table S2).

DISCUSSION

The germination and return to growth of bacterial spores is an essential step in the initiation of several diseases and of some causes of food spoilage. This TnSeq analysis identified 42 *B. subtilis* genes that had not previously been associated with germination, but are required for a highly efficient germination response to L-valine. As the majority of proteins previously found to play major roles in germination are membrane-associated, fourteen of these genes, whose products had also been identified in a study of the spore membrane proteome, were further characterized. Well-defined mutations in these genes caused significantly reduced responses to L-valine, and in some cases a decreased response to other nutrient germinants. For all these mutants, the germination defect appears to largely be a slow initiation of germination rather than a specific slowing of a subsequent step in the germination process. The reduced percentage of spores within the population that do initiate germination progress through Stages I and II of germination at a normal pace. This suggests that the genes under study play a role in the earliest steps of triggering the germination process.

Consistent with this idea, many of the mutant strains had a reduced abundance of the GerA receptor, indicating effects on receptor expression and stability or membrane incorporation. A GerA deficiency is not surprising, given that the primary screen for identification of these genes was for a reduced response to L-valine, which is recognized via GerA (122). Based

on responses to additional germinant classes, the mutant strains could be separated into distinct phenotypic groups. The first group features a reduction in germination rate to all nutrient germinants tested (L-valine, AGFK, and 2xYT), demonstrating reduced germination efficiency mediated through all receptors: GerA, GerB, and GerK. Mutant strains lacking *skfE, ylbC, hfq*, or *dnaJ* fall in this group, and also includes the strains with the greatest decreases in GerA abundance. These genes may play roles in expression or assembly of all Ger receptors or in facilitating signal transduction from germinant receptors to other parts of the germination apparatus. The well-studied function of DnaJ as a protein chaperone (146) might explain its effect on GerAC abundance in spores, and this effect suggests that DnaJ is active in the forespore late into sporulation. While the role of Hfq in Gram-positive species is not as well studied as in some Gram-negative species, its known role as an RNA chaperone (147) might exert post-transcriptional effects on the production of proteins important in the germination process. Interestingly, several other genes found in this study to affect germination (*dnaJ*, *ylbBC*, *yqeF*, *yqhL*, *yybT*) have sizable 5' untranslated regions in their mRNAs, which might be sites for post-transcriptional regulation, or for which antisense RNAs have been identified (*yqeF, yqhL,* and *yybT)* (148). A mechanism by which SkfE, which is involved in export of a sibling-killing antimicrobial, might affect germination is harder to imagine, but the fact that Tn insertions in two other genes in the *skf* operon also reduced germination supports the importance of this effect. Interestingly, expression of the *skf* operon is regulated by PhoPR, genes also implicated by this study in altering germination response.

One of the more interesting genes identified for future study may be *ylbC*, which is likely expressed as the downstream gene in the σ^F-regulated *ylbB-ylbC* operon (149). YlbC contains two conserved domains: an N-terminal cysteine rich secretory "CAP" domain, and a YkwD domain of

unknown function that is found only in proteins of spore-forming bacteria (150). YlbB contains two conserved CBS domains (150), which in at least one case has a role in ATP-binding (151). Tn insertions in *ylbB* were significantly underrepresented in the germination screen (p=0.014) but did not achieve the cutoff of a 2-fold change. Thus, *ylbB* may function with *ylbC*, but might be partially redundant with the paralogous *yhcV*, which is σ^G-dependent (149, 152) and encodes one of the most abundant transcripts in the dormant spore (153). The mechanism by which YlbC affects *gerA* transcription and GerA abundance is a topic for ongoing study.

A second phenotypic group is composed of mutant strains with significantly delayed germination via a GerA-mediated response but germinate normally through GerB and GerK sensing. Strains lacking *yybT, ygaC, yqhL, yqeF,* or *sipT* exhibit this phenotype, and all except the *yybT* mutant have significantly reduced spore GerA content. The roles of these genes in germination are unclear, as most are relatively uncharacterized. YybT (GdpP) acts as a c-di-AMP phosphodiesterase and exerts pleotropic effects on physiology and gene expression (154-157). SipT, acting as a signal peptidase (158), could certainly exert effects on assembly of membrane proteins important for germination, including GerA.

The third phenotypic group includes strains with significantly slower germination rates in response to L-valine but either have a decreased response to AGFK or 2xYT but not both. Mutants lacking *ytpA, phoP, phoR, pcrB* or *ytxG* feature these phenotypes. It is not clear how or why a mutant would be deficient in GerA-mediated response, have a normal GerB and GerK response, but still be deficient for germination in rich media. The PhoPR mutants have poor vegetative growth and pleotropic effects on gene expression, which might exert quite variable effects into the sporulation process. These mutants seemed to exhibit significant variability between multiple spore preparations. Three mutants in this group may exert effects on membrane structure. YtpA

is a phospholipase (159, 160), PcrB is a heptaprenylglyceryl phosphate synthase (161), and a *ytxG* mutant exhibits defects in membrane morphology (120). Alterations in the spore inner membrane might affect assembly or function of the germination initiation apparatus. None of these three genes are specifically expressed in sporulating cells, and thus their activity levels and effects on germination might be more varied among spore preparations and possibly with regard to different germinants. Interestingly, the *ytxG* mutant was the only strain in which overexpression of *gerA* did not correct the L-valine germination defect. This overexpression in the *ytxG* mutant did decrease AGFK germination, as in other strains, suggesting that the *gerA* overexpression was successful. Perhaps a membrane defect in this mutant renders Ger protein complexes nonfunctional regardless of their expression level.

Four of the mutants identified here exhibit decreased *gerA* transcription. The predicted functions of these gene's products provide no simple explanation for how such an effect on transcription could come about, and the mechanisms may therefore be indirect. The expression of two other σ^G-dependent genes, *pbpF* and *sspB*, was not decreased in the mutant strains, indicating that this was not an effect on the entire regulon. Altered activity of a transcription factor involved in *gerA* transcription, SpoVT or YlyA (86, 131, 149, 152, 162), could be an expected pathway for such an effect. Future work should examine the effects of these mutations on other genes within forespore-specific regulons to resolve this.

Among the germination mutants identified in our TnSeq screen, strains that could complete Stage I of germination but were blocked in Stage II were not present. This may be due to the mutant screening process utilized. Mutants with Tn insertions in *cwlD*, which should exhibit this phenotype (163, 164), were slightly enriched in our non-germinating spore population, but not above the significance cutoff value used. Spores blocked at stage II were

expected to pellet with dormant spores in the density gradient utilized (144). One possibility is that spores blocked at Stage II were unstable through the time of incubation with germinant, density gradient separation, and subsequent washing, and thus were not efficiently recovered. Utilization of an alternative isolation method might allow identification of mutants with this phenotype.

ACKNOWLEDGEMENTS

We thank Alan Grossman for providing the Tn insertion library, Peter Setlow and George Korza for strains and antibodies, and Jennifer Meador-Parton and Isabelle Wal for technical assistance.

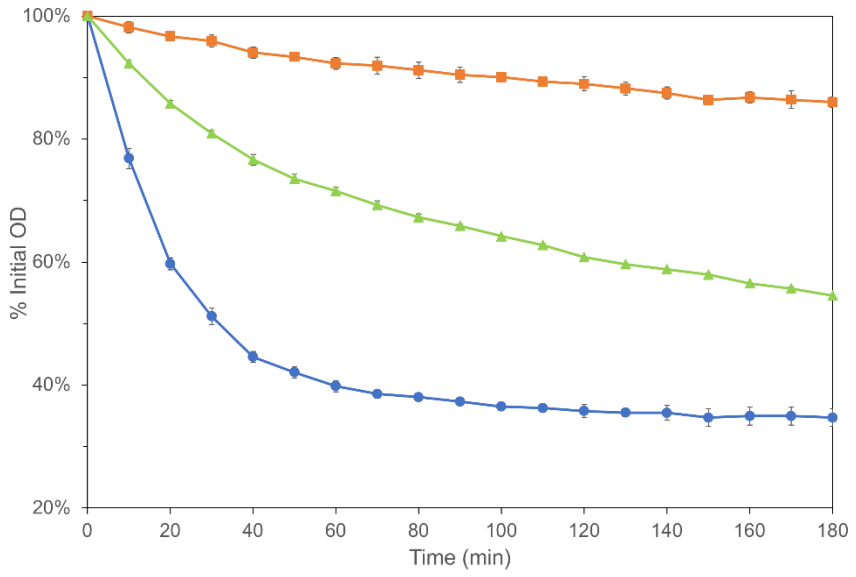

Fig 2.1. Germination rates of *B. subtilis* strains. Purified spores were heat activated, stimulated to germinate by addition of 10 mM L-valine, and shaken at 37°C, during which the OD_{600} was monitored. Values are averages of three assays and error bars are standard deviations. Each assay was performed on three replicate spore preparations. For the *ylbC* (■) and *phoP* (▲) mutants, all points after 10 min are significantly different from those of the wild type(●); P≤0.05.

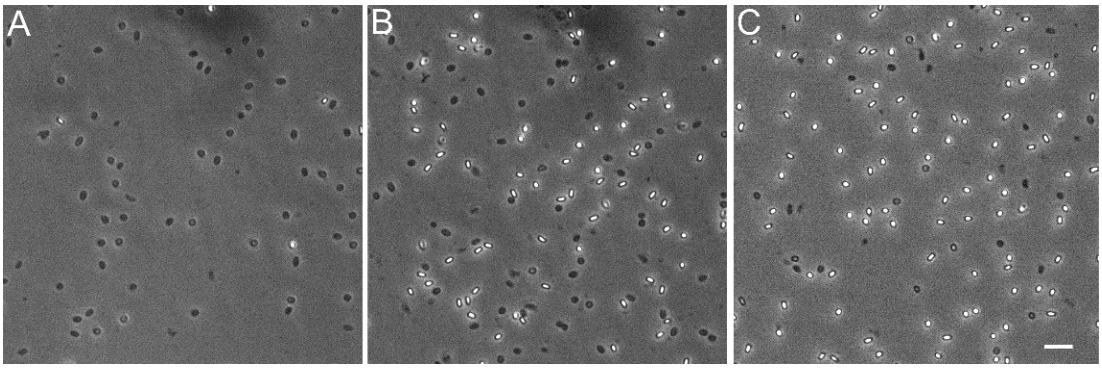

Fig 2.2. Phase-contrast microscopy of germinating *B. subtilis* spore populations. Purified spores of *B. subtilis* wild type and mutant strains were heat-activated and stimulated to germinate by addition of 10 mM L-valine followed by incubation at 37°C for 60 min. A) PS832 B) *ytpA* mutant strain C) *ylbC* mutant strain All panels are the same magnification; the bar in panel C is 5 µm. Images are representative of three biological replicates.

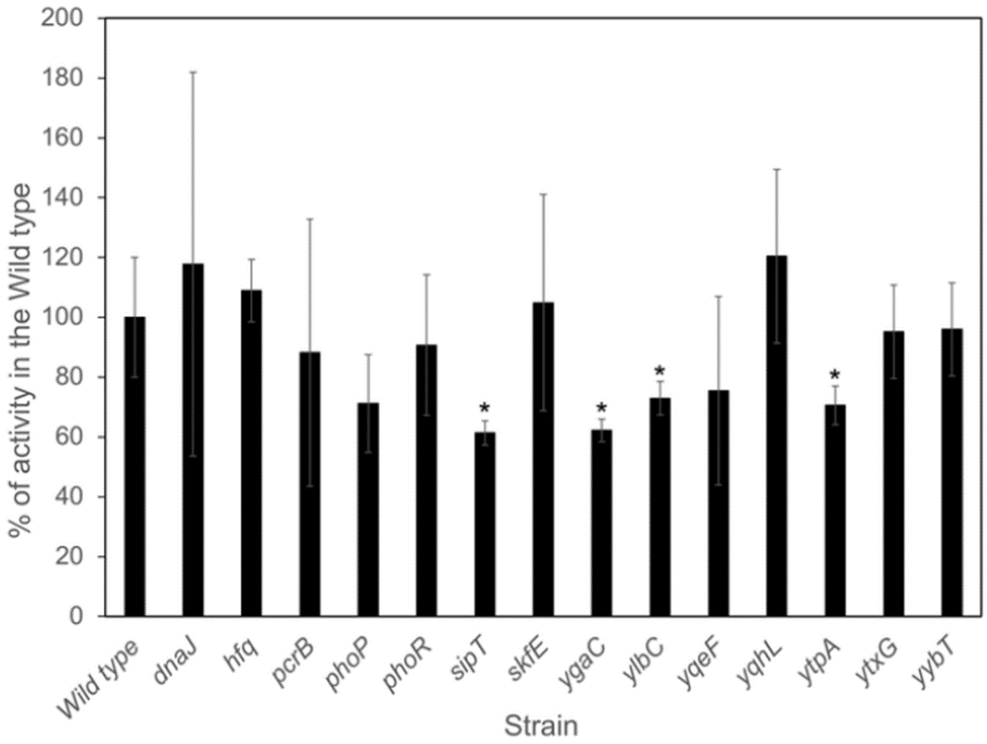

Fig 2.3. **Expression of a *gerA-lacZ* transcriptional fusion**. Purified spores carrying a *gerA-lacZ* transcriptional fusion were decoated and lysed, and extracts were assayed for β-galactosidase. Values are expressed as a percentage of that detected in DPVB761, the wild type strain containing the *gerA-lacZ* fusion. Values are averages of assays on three replicate spore preparations and error bars are standard deviations. * indicates a significant difference from the wild type ($p \leq 0.05$).

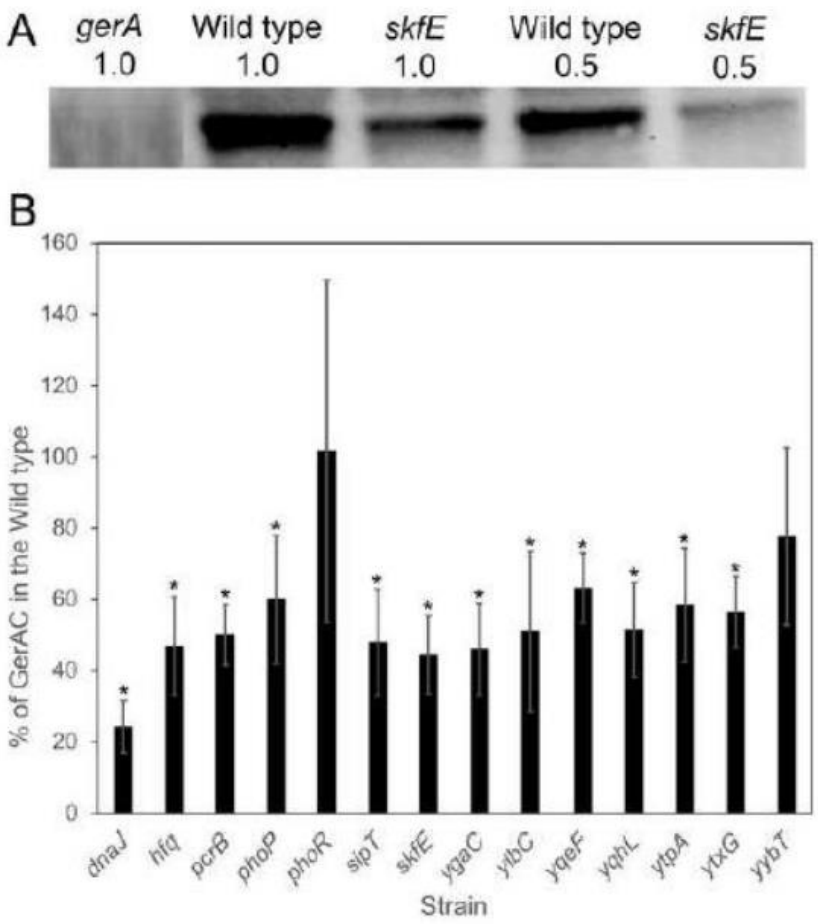

Fig 2.4. GerAC is reduced in the spores of several *B. subtilis* mutant strains. Equal quantities of spore suspensions were decoated and broken, and proteins were extracted, serially diluted, separated on SDS-PAGE, and transferred to PVDF membrane as described previously (84). The membrane was probed with anti-GerAC antibodies (87) (Panel A and Fig S5). Strain genotype (All strains were also Δ*gerB*.) and sample dilution is indicated above each lane. Protein load and transfer to membrane in each lane was normalized as described in Materials and Methods, and the amount of GerAC detected in each strain was compared to that found in the wild type (Panel B). Values are averages of three biological replicates and error bars indicate standard deviations. * indicates a significant difference from the wild type ($p \leq 0.05$).

Table 2.1: Genes in which Tn insertions altered germination

Gene	p-value[a]	Fold-change Sample 1[b]	Fold-change Sample 2[b]
cotH	2.2E-35	15.0	10.9
gerAA	4.4E-31	150.1	43.7
gerAC	2.0E-29	279.9	73.9
cotE	3.8E-24	17.0	12.0
ygaC	2.3E-18	4.6	4.2
yqfT	3.0E-16	15.4	8.8
ypzK	6.3E-16	10.1	9.7
yqeF	2.0E-15	3.3	5.5
ymzD-ymcC[c]	5.7E-13	2.5	2.7
gerPF	5.8E-13	7.4	4.1
safA	1.1E-11	7.3	4.1
pcrB	2.3E-11	3.0	2.6
ylbC	3.9E-11	4.1	2.9
gidA	1.3E-10	4.2	2.8
gerPB	1.0E-09	5.9	3.6
gerPC	3.1E-09	11.7	3.9
nocA	4.2E-09	2.0	2.2
veg	1.1E-08	4.8	3.2
gerE	1.8E-08	Infinite	32.0
ytoA	2.2E-08	5.1	4.1
ytpA	1.0E-07	5.3	4.6
ytpB	1.1E-07	3.9	3.5
rsbW	1.2E-07	2.2	2.5
yfhD	2.8E-07	4.2	4.6
cotZ	7.7E-07	2.1	3.1
yqhL	1.1E-06	4.3	2.5
kinB	1.8E-06	1.6	1.9
skfC	1.9E-06	7.9	3.7
skfE	3.8E-06	8.4	3.7
gerAB	5.8E-06	181.7	73.6
ymaB	6.6E-06	1.9	2.9
sipT	7.5E-06	2.5	2.8
skfG	9.7E-06	3.5	2.3
phoR	1.0E-05	2.5	3.0
cotN	1.5E-05	2.1	2.2
yhbJ	2.8E-05	1.8	1.7
yhaM	3.3E-05	4.6	2.5
ymaF	3.7E-05	8.1	2.8

yabG	1.7E-04	2.5	2.3
spoVID	1.8E-04	2.7	2.1
yqhR	3.6E-04	2.3	2.0
yonF	4.7E-04	1.8	3.0
spoVAF	4.8E-04	2.2	1.8
hfq	6.7E-04	3.2	2.5
yosK	9.2E-04	4.4	6.4
yozE	9.4E-04	3.0	4.8
yopI	1.1E-03	2.3	2.8
flgN	1.2E-03	14.2	3.6
gerD	1.2E-03	2.6	1.9
fliW	2.0E-03	1.9	3.4
yfbJ	2.0E-03	3.1	2.3
ytmO	2.1E-03	4.0	3.5
gerPE	2.1E-03	6.5	1.7
phoP	2.3E-03	3.2	3.4
gerPD	4.7E-03	8.2	3.2
tufA	5.2E-03	5.7	3.1
ispA	5.7E-03	2.9	2.8
yoqL	1.7E-02	6.1	3.7
dnaJ	4.7E-02	2.5	2.9
yaaB	5.0E-02	7.4	2.3
ytxG	2.1E-01	2.7	2.9
yybT (gdpP)	2.4E-01	7.5	2.1

[a] p-value determined using DESeq2 (137) comparing Dormant and Germinated sample read counts.
[b] Fold change in read counts of Dormant/Germinated samples
[c] Intergenic region

Table 2.2: Genes without previously known germination role identified by TnSeq and in spore membrane proteome.

Gene	Function	Locus structure	Regulation of expression
dnaJ	Protein quality control	*hrcA-grpE-dnaK-dnaJ-yqeTUV*	σ^A, HrcA (165)
hfq	RNA chaperone	*hfq*	Increased protein during transition to stationary phase (166)
pcrB	Heptaprenylglyceryl phosphate synthase	*pcrB-pcrA-ligA-yerH*	LexA regulon (167)
phoP	Response regulator, phosphate metabolism	*phoPR*	σ^A, σ^B, σ^E, CcpA, ScoC (168, 169)
phoR	Sensor kinase, phosphate metabolism	*phoPR*	σ^A, σ^B, σ^E, CcpA, ScoC (168, 169)
sipT	Signal peptidase I	*sipT*	DegU (170)
skfE	Export of spore killing factor (SkfA)	*skfABCEFGH*	Spo0A, AbrB, PhoP (171-173)
ygaC	Unknown	*ygaCD*	
ylbC	Unknown	*ylbBC*	σ^F (149)
yqeF	Unknown	*yqeF*	
yqhL	Unknown	*yqhL*	mRNA processed by RNase Y (174)
ytpA	Phospholipase, Bacilysocin synthesis	*ytpAB*	σ^M (159)
ytxG	General stress	*ytxGHJ*	σ^B, σ^H (175)
yybT (gdpP)	c-di-AMP phosphodiesterase. Functions in DNA damage and acid resistance (176)	*yybS-gdpP-rplI*	σ^A, σ^D-induced antisense RNA (177)

Table 2.3: Phenotypic properties of *B. subtilis* strains

Genotype	Doubling time[a] (min)	Sporulation efficiency[b] (%)	DPA release[c] (µg/ml/OD)	NAM release[c] (nmole/ml/OD)	% phase-dark spores[d]
Wild type	20	66	5.3 ± 0.1	61.0 ± 14.2	95
dnaJ	31	89	1.1 ± 0.4*	25.9 ± 12.7	14
hfq	40	63	2.2 ± .03*	30.1 ± 6.2	48
pcrB	31	68	3.0 ± 0	30.3 ± 8.0	41
phoP	44	83	2.7 ± 0.4*	46.6 ± 5.8	63
phoR	35	54	3.9 ± 0.5	39.2 ± 9.5	86
sipT	34	54	2.3 ± 1.0*	23.5 ± 10.2*	22
skfE	27	59	1.8 ± 0*	40.6 ± 10.7	38
ygaC	21	71	3.1 ± 0.4*	36.6 ± 9.9	60
ylbC	29	48	1.1 ± 0.3*	14.3 ± 3.4*	19
yqeF	23	84	1.9 ± 0*	37.2 ± 9.4	50
yqhL	20	53	2.6 ± 0.4*	36.1 ± 8.1	69
ytpA	22	95	1.63 ± 0*	17.7 ± 2.7*	55
ytxG	31	18	4.8 ± 0.3	50.9 ± 4.8	90
yybT	21	69	4.7 ± 0.4	56.6 ± 14.1	92

[a] Growth in 2xSG medium at 37°C

[b] Heat-resistant count/total viable count after 24 hr incubation on 2xSG medium at 37°C.

[c] Release of DPA and NAM 30 or 45 min, respectively, after exposure to 10 mM L-valine at 37°C.
* indicates a significant difference from the wild type (T-test, $p<0.05$). Values are averages and standard deviations of three biological replicates.

[d] Spores pixel intensities quantified and classified as described in Materials and Methods after 60 min exposure to 10 mM L-valine at 37°C.

Table 2.4: Response of *B. subtilis* strains to varied germinants.

Genotype	% OD_{600} loss[a]			% DPA released by dodecylamine[b]
	L-Val (60 min)	AGFK (60 min)	2xYT (40 min)	
Wild type	60 ± 1	41 ± 2	60 ± 2	75 ± 1
dnaJ	6 ± 0**	28 ± 10*	40 ± 3*	68 ± 4
hfq	26 ± 5*	30 ± 1*	52 ± 2*	75 ± 1
pcrB	47 ± 10*	27 ± 3*	58 ± 4	87 ± 2
phoP	28 ± 1*	36 ± 10	53 ± 1*	59 ± 6
phoR	44 ± 2*	22 ± 10*	56 ± 1	52 ± 6
sipT	7 ± 0**	33 ± 10	57 ± 7	69 ± 5
skfE	35 ± 10*	28 ± 6*	50 ± 3*	82 ± 5
ygaC	22 ± 3*	37 ± 10	55 ± 2	67 ± 5
ylbC	8 ± 1**	13 ± 2**	23 ± 8**	66 ± 3
yqeF	38 ± 3*	33 ± 7	58 ± 1	84 ± 1
yqhL	33 ± 6*	37 ± 10	54 ± 3	71 ± 2
ytpA	32 ± 3*	41 ± 3	47 ± 3*	73 ± 4
ytxG	35 ± 0*	28 ± 8	53 ± 1*	72 ± 4
yybT	47 ± 2*	44 ± 7	60 ± 0	76 ± 4

[a] Values are averages and standard deviations of assays on three replicate spore preparations. OD_{600} of purified spore suspension monitored at the indicated time after addition of 10 mM L-valine, 1X AGFK, or 2xYT while shaking at 37°. * indicates a significant difference (T-test, $p<0.05$) or ** indicates a significant difference (T-test, $p<0.01$) from the wild type.

[b] Values are averages and standard deviations of assays on three replicate spore preparations. DPA release by purified spore suspension monitored 100 min after addition of 1 mM dodecylamine while shaking at 37°.

Table 2.5. Overexpression of *gerA* suppresses germination defect of multiple mutants.

Genotype	% OD Loss	
	without *sspDp-gerA*	with *sspDp-gerA*
Wild type	35 ± 4	38 ± 2
skfE	23 ± 5*	38 ± 3
pcrB	34 ± 7	37 ± 1
ygaC	26 ± 1*	36 ± 1
sipT	9 ± 5*	41 ± 1
ylbC	7 ± 0*	37 ± 0
hfq	27 ± 3*	38 ± 3
yqhL	29 ± 3*	37 ± 0
dnaJ	12 ± 2*	36 ± 2
yqeF	28 ± 2*	31 ± 2
phoR	37 ± 1	42 ± 9
phoP	32 ± 1	36 ± 0
ytxG	25 ± 6*	15 ± 4*
ytpA	25 ± 0*	38 ± 2
yybT	37 ± 2	37 ± 2

[a] Values are averages and standard deviations of assays on three replicate spore preparations. OD_{600} of purified spore suspension monitored 45 min after addition of 10 mM L-valine while shaking at 37°. * indicates a significant difference from the wild type (T-test, $p<0.05$)

CHAPTER 3

YpeB Dimerization may be required for SleB Stabilization and Effective Germination of *Bacillus anthracis* Spores

Cameron V. Sayer and David L. Popham

ATTRIBUTIONS

Cameron Sayer performed the research, experimentation, and data analysis. David Popham is the principal investigator.

ABSTRACT

Bacillus cells faced with unfavorable environmental conditions undergo an asymmetric division process ultimately leading to the formation of the bacterial spore. In many instances the spore acts as the infectious agent; such is the case with the spore of *Bacillus anthracis* and the disease anthrax. Cellular structures formed during sporulation confer resistance to a variety of conditions including traditional bacterial decontamination methods. The spore cortex, a thick layer of modified peptidoglycan, contributes to maintaining the dehydrated state of the spore core and overall spore dormancy. A major event of spore germination is the degradation of the cortex. Hydrolysis of the cortex is accomplished through germination-specific lytic enzymes. The removal of the cortex is required for full hydration of the core and subsequent outgrowth. One such enzyme, SleB, has been demonstrated to require the presence of YpeB for its stable incorporation and subsequent function in spores of *B. anthracis.* The focus of the present study is to identify protein interactions within the dormant spore through *in vivo* chemical cross-linking. Conserved residues within YpeB PepSY domains were altered to facilitate implementation of a site-specific chemical cross-linker, 4-azidophenacyl bromide. Analyses of crosslinked spore extracts suggests that YpeB exists as a dimer within the spore potentially mediated through interactions of the C-terminus. Spores expressing stable truncated forms of YpeB were crosslinked and corresponding truncated dimers were visualized via western blot. Further characterization of individual YpeB domains using bacterial two hybrid indicate a possible role for both N and C terminal domains in YpeB oligomerization.

INTRODUCTION

Bacillus anthracis has the potential to cause widespread illness and severe disease through multiple routes of infection. As with many other disease-causing endospore-producing bacterial species, the bacterial endospore serves as the infectious agent of the disease anthrax (1). This is especially problematic because the inherent resistance characteristics of bacterial spores render many standard decontamination methods ineffective (1, 46, 47). The greatest factor in maintenance of spore resistance properties is preservation of the metabolically dormant and dehydrated state of the spore core (55). Dormancy is maintained by specialized spore structures including the inner spore membrane and cortex peptidoglycan, and high spore core concentrations of Ca^{2+}-dipicolinic acid (DPA). (46, 47, 76). These factors contribute to the overall threat that *B. anthracis* poses, especially as a bioterrorism agent.

When the dormant spore senses an environment with favorable nutrient availability, such as within a host, it will rapidly germinate, returning to a vegetative growth state. Germination is initiated following sensing of germinants by receptors at the inner spore membrane, after which large stores of Ca^{2+}-DPA are released from the spore core and partial rehydration of the core begins (46). The spore cortex is then depolymerized, facilitating complete hydration of the core and a return to a vegetative growth state (46). Completion of germination of *B. anthracis* within the host is required for production of the anthrax toxins and ultimately progression of the disease (1).

The cortex is degraded by germination specific lytic enzymes (GSLEs). *B. anthracis* encodes four of these enzymes, but the majority of the cortex degradation has been demonstrated to be completed through the action of partially redundant enzymes SleB and CwlJ1 (75, 92). These

enzymes specifically recognize modified muramic-δ-lactam (58, 101, 178-181), which is found uniquely in spore cortex peptidoglycan (182, 183). CwlJ1 is localized to the spore coat layer and has been shown to be activated by the release of Ca^{2+}-DPA (46, 95, 96).

In *Bacillus* species, both SleB and YpeB are expressed from a conserved operon and this is also true of several *Clostridium* strains (184). Previous studies have determined that SleB and YpeB co-localize to the inner spore membrane as well as potentially to a second location near the outside of the cortex (96, 99). Further studies have determined that SleB and YpeB are co-dependent, requiring one another for stable incorporation within the dormant spore in both *B. subtilis* and *B. anthracis* (96, 104, 106, 185). SleB and YpeB are expressed under the control of σ^G and are translocated across the inner spore membrane via N-terminal signal sequences (99, 178, 185, 186). The signal sequence of YpeB is not predicted to be cleaved, leaving YpeB anchored to the inner spore membrane, while SleB is expressed in its active form, with signal sequence removed, within the dormant spore (99, 186-188). Given the co-localization, co-dependency, and that SleB is present but held inactive in the dormant spore, it has been theorized that YpeB and SleB interact in some manner to stabilize one another within the dormant spore (104). Previous studies have implicated a role for both N-terminal (residues 21-202) and C-terminal (residues 203-446) regions of YpeB in interactions with SleB (104, 106). It has been demonstrated that the N-terminal domain of YpeB was most effective in inhibiting SleB activity *in vitro* (106), while a region of YpeB beyond the first PepSY domain is required for SleB incorporation within the dormant spore (104).

The goal of the current study was to further characterize the relationship between YpeB and SleB within the dormant spore. *In vivo* peptide cross-linking was used to study potential interactions of YpeB, identifying interactions that may form only within the unique environment

of the dormant spore. Bacterial two-hybrid analysis was used to detect domain-specific interactions. Both methods indicate YpeB oligomer formation, which may be required for stable incorporation of SleB and subsequent germination of the *Bacillus* spore.

MATERIALS AND METHODS

Strain construction. Site-directed mutagenesis by overlap extension PCR (189) was performed to create cysteine point mutants within *ypeB*. PCR products were then cloned into the *ypeB* complementation plasmid (pDPV424(104)) via restriction-free cloning (190). Plasmids were sequenced to verify cysteine codon substitutions and introduced into *B. anthracis* through conjugation as described previously (104, 191). Plasmid integration was obtained by shifting the temperature to 42°C and verified via PCR as described previously (104).

Construction of strains for two hybrid assays was performed as follows. Desired *ypeB* and *sleB* domains were PCR amplified using primers with flanking restriction sites. PCR products were then digested with restriction enzymes along with selected vectors pUT18C and pKT25 (Euromedex). Ligations were carried out to insert *ypeB* or *sleB* domain sequences in frame with N-terminally fused p18 or p25 domains of adenylate cyclase. Plasmids were then co-transformed into BTH101 (Euromedex) to test potential interactions.

Spore preparation. *B. anthracis* spores were prepared in liquid Modified G medium (192) with antibiotics where necessary. Spores were harvested after 3-4 days incubation at 37°C and washed in water for several days until >95% free of vegetative cells and cell debris. Decoated spores were prepared as described previously (104). Briefly, spores were suspended in decoating solution (50 mM Tris-HCl pH 8, 8 M Urea, 1% SDS, 50 mM dithiothreitol) and incubated for 60

min at 37°C. Spores were centrifuged at 8,000 x g for 2 min, and the decoating solution was removed. This procedure was repeated, followed by 5 washes with deionized water.

Cross-linking. 10 OD units of decoated spores were suspended in PBS pH 7.5 and p-azidophencyl bromide (APB) crosslinker (Sigma) was added to a final concentration of 5 mM. Decoated spores were incubated with APB at 37°C for 30 min in the dark. Samples were then exposed to UV light for an additional 15 min at room temperature. Following UV exposure, cross-linked spores were centrifuged at 10,000 x g for 1 min and the supernatant was removed. Cross-linked spore pellets were stored at -80°C until later use.

YpeB-His6 purification. Following cross-linking of 200 OD units of decoated spores, frozen pellets were lypholized. Dried spores were broken mechanically with 100 mg 0.1 mm glass beads using Wig-L-Bug bead beaters for 20 pulses of 30 sec each at 4,200 rpm. Samples were stored on ice between cycles. Broken spores were suspended in Urea Binding Buffer (8 M Urea, 500 mM NaCl, 50 mM Tris-HCl, 30 mM imidazole, pH 7.5) and incubated at 4°C for 2 hours. The samples were centrifuged at 6,800 x g for 10 min, and the soluble fraction was collected, filtered, and loaded onto a 1 mL Ni Sepharose HisTrap HP (GE Healthcare) column equilibrated in Urea Binding Buffer. Bound YpeB-His6 was eluted with Urea Elution Buffer (8 M Urea, 500 mM NaCl, 50 mM Tris-HCl, 1 M imidazole, pH 7.5). Fractions were stored at -80°C for western blot analysis.

Western blotting. YpeB and SleB were detected via western blot as described previously (104, 107). Briefly, proteins were transferred to Amersham Hybond-P PVDF membranes (GE Healthcare). Anti-YpeB and anti-SleB antibodies were used at 1:3,000 and 1:1,000 dilutions, respectively, and horseradish peroxidase (HRP) conjugated secondary goat anti-rabbit antibodies (Bio-Rad) were used at 1:200,000 dilution. Antibody detection utilized chemiluminescence (Clarity Max Western ECL substrate; Bio-Rad).

Bacterial Adenylate Cyclase Two-Hybrid Assay. Protein interactions were screened via spotting 2 µl of co-transformed overnight culture on MacConkey agar (ampicillin 100 µg/ml, kanamycin 50 µg/ml, 1% maltose, 0.5 mM IPTG). Spotted plates were incubated for 48 hours at 30°C. Positive interactions were visualized by acidification of the media resulting in production of red coloration.

RESULTS

***In vivo* site-directed cross-linking of YpeB in *B. anthracis* dormant spores**. Previous work has highlighted the importance of the YpeB C-terminal domain (203-446), specifically residues beyond the first PepSY domain, for stabilization of SleB in the developing spore (104). Interactions of the YpeB C-terminal domains within the dormant spore were further characterized by employing *in vivo* amino acid-specific chemical cross-linking. Guided by homology modeling of the YpeB C-terminal domain to that of the metalloprotease Vibriolysin (193), several amino acid residues were selected as potential interaction sites. Residues were chosen based on the following criteria: predicted to be surface exposed, critical in PepSY domain interactions in Vibriolysin, and/or conserved in *ypeB* orthologs. Each of the selected residues was then mutagenized, substituting the wild type codon with that for cysteine, and YpeB-cysteine alleles were recombined into the chromosome of a *ΔypeB* strain. These alleles also carried a C-terminal hexa-histidine tag for protein purification purposes. This tag has previously been shown to not interfere with YpeB function (104). The functionality of the YpeB-Cys proteins were verified by examination of the abundance of YpeB and SleB in the dormant spores, quantification of OD loss during spore germination, and observation of YpeB proteolysis to stable C-terminal products

during germination. All YpeB-Cys alleles were very similar to the wild type in all of these assays. Specifically, the two alleles utilized for further studies, *ypeBS358C-6His* and *ypeBK437C-6His* were nearly identical to the wild type in these regards (Figure S7). Sulfhydryl specific cross-linking was conducted using the cross-linker APB, which is a heterobifunctional cross-linker with a sulfhydryl specific α-bromo-ketone motif in addition to a non-specific photoactivatable azide, separated by a spacer arm of 9 angstroms. In total, 12 YpeB-Cys allele-carrying strains, corresponding to 12 different amino acid substitutions across the C-terminal PepSY domains (Table 3.1), were created and tested in site-specific cross-linking schemes of dormant spores. Of the 12 alleles tested, those encoding Cys substitutions for residues 358 and 437 revealed higher migrating complexes of roughly ~100 kDa in anti-YpeB western blots of dormant whole spore extracts following APB cross-linking (Figure 3.1). It was theorized that because these higher migrating bands appeared at roughly double the mass of the YpeB monomer (~50 kDa) that these complexes might contain a cross-linked YpeB dimer.

***In vivo* site directed cross-linking of YpeB$_{\Delta 25\text{-}203}$ dormant spores.** Attempting to the further demonstrate the possibility of a YpeB dimer, similar cross-linking experiments were performed using an allele of *ypeB*, *ypeB*$_{\Delta 25\text{-}203}$, that is internally truncated within the N-terminal domain, and that was previously demonstrated to produce a protein that was stably incorporated into the dormant spore (104). Cys residues that were reactive in the previous assay were created in YpeB$_{\Delta 25\text{-}203}$, and the alleles were recombined into both Δ*ypeB* and wild type *B. anthracis* backgrounds. Dormant spores from YpeB$_{\Delta 25\text{-}203}$-Cys strains were then cross-linked with APB and proteins were extracted and visualized via western blot (Figure 3.2). Cross-linked extracts of YpeB$_{\Delta 25\text{-}203}$ K437C in a Δ*ypeB* background feature both the truncated monomer (~30 kDa) and what appears to be a truncated YpeB dimer (~60 kDa). Extracts of YpeB$_{\Delta 25\text{-}203}$ K437C in WT

background suggest the possibility of a $YpeB_{\Delta 25\text{-}203}$-WT YpeB heterodimer (~80 kDa) in addition to complexes previously visualized. We next sought to confirm that this newly visualized band contained the 6x-His-tagged YpeB. Spores encoding $YpeB_{\Delta 25\text{-}203}$ K437C were cross-linked, and 6x-His-tagged proteins in extracts were purified via Ni^{2+} NTA affinity column. Column elutions were visualized with western blotting (Figure 3.3). The higher-migrating band (~60 kDa) was visualized in the cross-linked samples but was not seen in the uncross-linked controls, indicating the potential for multimerization of the YpeB C-terminal domain even in the absence of most of the N-terminal domain.

Analyzing individual YpeB domain contributions to multimerization using bacterial two-hybrid analysis. A bacterial two-hybrid system was implemented to better elucidate contributions of individual YpeB domains to possible multimer formation. Individual YpeB N- ($YpeB^{N}$ 21-202) and C-terminal domains ($YpeB^{C}$ 203-446), full-length YpeB (lacking its signal peptide)($YpeB^{Full}$ 21-446), and the SleB C-terminal catalytic domain ($SleB^{Cat}$ 125-253)(194) were cloned in both pKT25 and pUT18C creating N-terminal fusions to the two domains of adenylate cyclase. Constructs were co-transformed into *E. coli*, which was plated on MacConkey agar supplemented with maltose, where positive domain interactions were visualized by red colony coloration. In agreement with cross-linking results, bacterial two-hybrid assays indicated that $YpeB^{Full}$ self-associated. (Figure 3.4). Additionally, $YpeB^{N}$ also demonstrated self-association while $YpeB^{C}$ did not. However, both $YpeB^{N}$ and $YpeB^{C}$ appear to interact with $YpeB^{Full}$ indicating that each of these domains are involved in dimer or higher multimer structure formation. $YpeB^{C}$ interacted with $YpeB^{Full}$ in only one orientation of the adenylate cyclase domains. This negative result might result from this specific interaction of YpeB domains placing the fusion domains too far apart for a productive interaction. Interestingly, one orientation of the fusion domains also

indicates an interaction between the $YpeB^N$ and $YpeB^C$ domains. Also of note, none of the YpeB constructs tested in the bacterial two-hybrid system appeared to interact with $SleB^{Cat}$, although $SleB^{Cat}$ did appear to associate with itself, suggesting that SleB also exists as a multimer.

DISCUSSION

This study further characterized interactions of YpeB within the dormant spore through *in vivo* chemical cross-linking and the roles of individual domains of YpeB in potential multimer formation using bacterial adenylate cyclase two-hybrid assays. Both *in vivo* crosslinking and two-hybrid analyses indicate that YpeB forms a dimer or higher-order multimer. The $YpeB^N$ domain alone exhibits strong self-association, while the $YpeB^C$ domain alone does not. However, YpeB-Cys substitutions at some positions in the C-terminal domain can be crosslinked to other YpeB molecules, suggesting close approach of C-terminal domains within the dormant spore. The C-terminal domain alone can interact with full-length YpeB, suggesting that either both domains are required for stable interaction with the isolated C-terminal domain, or that multimerization of the full-length protein allows further interaction with the isolated C-terminal domain.

YpeB was not demonstrated to form cross-links to SleB from selected residues within the YpeB C-terminal PepSY domains. This may indicate that the YpeB C-terminal domain, although required for stabilization of SleB (104), is not directly interacting with SleB within the dormant spore. It is also possible that these selected residues are not in the correct orientation to detect an YpeB-SleB interaction. YpeB multimerization may be required for interaction or stabilization of SleB *in vivo.* Both N- and C-terminal YpeB domains have been demonstrated to be required for SleB stabilization (104, 106), however both domains may be required not because of direct

interaction with SleB, but rather these domains are necessary for multimer formation. Previous work demonstrated that the YpeB N-terminal can cause inhibition of SleB activity *in vitro* (106) and that a region beyond the first PepSY domain was required for stable incorporation of both YpeB and SleB into the spore (104). Cross-linking data now demonstrates that residues beyond the first PepSY domain appear to be close enough to one another for multiple copies of YpeB to form a dimer within the dormant spore. Bacterial two-hybrid analysis indicates that both the isolated YpeB N- and C-terminal domains are able to interact with full-length YpeB, thus possibly contributing to a larger multimeric structure, and N-terminal YpeB appears to strongly associate with itself, suggesting it plays a primary role in multimerization.

The structure of the YpeB C-terminal PepSY domains of *B. megaterium* has been solved (195). Authors of the structure suggested a possible binding pocket within a channel traversing the YpeB C-terminal domain, outlined by positive charges of four lysine residues (K345, K347, K361 and K366) (195). $YpeB^{S358C}$, one of the residues demonstrated to be reactive in our cross-linking experiments lies directly within this potential binding-pocket. $YpeB^{K437C}$, the other reactive residue, lies just beneath the channel but is still surface exposed. It is not immediately obvious how multiple C-terminal domains of YpeB may interact relative to this pocket.

Previous work identified conserved amino acid residues in YpeB PepSY domains required for YpeB, and subsequent SleB, stabilization in dormant spores (104). In context of the structure of the YpeB PepSY domains, these amino acids were predicted to contribute to stabilization of the structure through intra-molecular interactions (195). YpeB structure could be a major factor in maintaining stability of any larger multimer in which it could be involved and as such even

minor disruption of its structure may ultimately lead to degradation during spore formation (104).

Although YpeB cross-linked to SleB was not detected, the list of residues tested was by no means exhaustive and it is entirely possible that the two proteins do interact, especially via the YpeB N-terminal domain (106). YpeB may also interact with other proteins such as HtrC, which has been previously demonstrated to specifically cleave YpeB during spore germination (107). Interaction between these, and likely other, proteins on the surface of the dormant spore membrane may serve to stabilize the proteins during long-term dormancy, and to play a key role during spore germination.

ACKNOWLEDGEMENTS

We thank Keane Dye for help in constructing mutant alleles, and Florian Schubot, Jordan Mancl, and Kylie Ryan for contributing *E. coli* strains and assisting with protein modeling. Research reported in this publication was supported by the National Institute of Allergy and Infectious Disease of the National Institutes of Health under award R21AI088298.

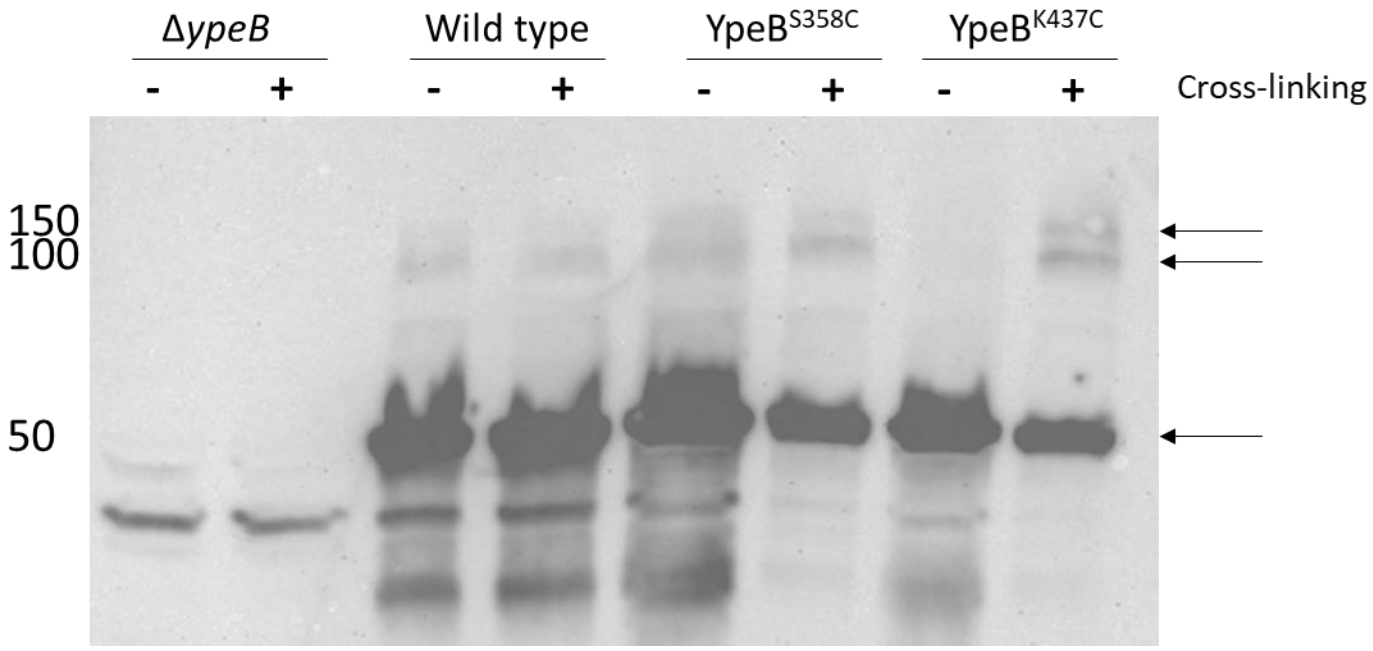

Figure 3.1: YpeB-cysteine cross-linked spores. Ten OD units of decoated dormant spores were incubated with 5 mM APB for 30 min at 37°C in reduced light and then irradiated with UV light for 15 min. Cross-linked spores were lypholized, mechanically broken and proteins were extracted with 1x SLB. Whole spore lysates were then visualized via western blot using YpeB antibodies (104). YpeB monomer is indicated by band at 50 kDa, higher migrating bands are visualized at 100 and 150 kDa in YpeB-cysteine cross-linked sample extracts.

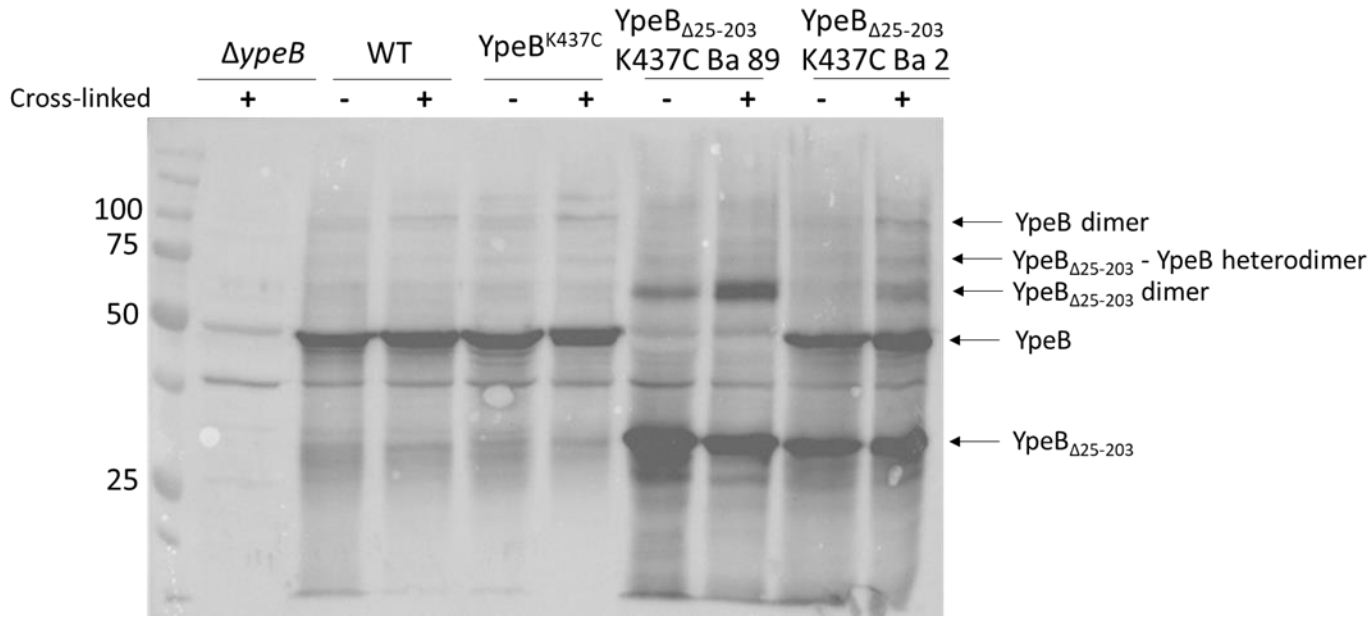

Figure 3.2: YpeB$_{\Delta 25\text{-}203}$-cysteine cross-linked spores. Ten OD units of decoated dormant spores were cross-linked with APB as described previously. Cross-linked spores were lypholized, mechanically broken and proteins were extracted with 1x SLB. Whole spore lysates were then visualized via western blot using anti-YpeB antibodies (104). YpeB monomer is indicated by band at 50 kDa. YpeB$_{\Delta 25\text{-}203}$ monomer is indicated at roughly ~30 kDa. YpeB multimers are visualized in YpeB^{K437C} (lane 5) migrating at 100 and 150 kDa. YpeB$_{\Delta 25\text{-}203}$ multimers are indicated in YpeB$_{\Delta 25\text{-}203}$K437C (lane 7) by band migrating ~60 kDa. YpeB and YpeB$_{\Delta 25\text{-}203}$ heterodimers (lane 9) are visualized by band migrating to ~80 kDa, in addition to multimers identified in previous lanes.

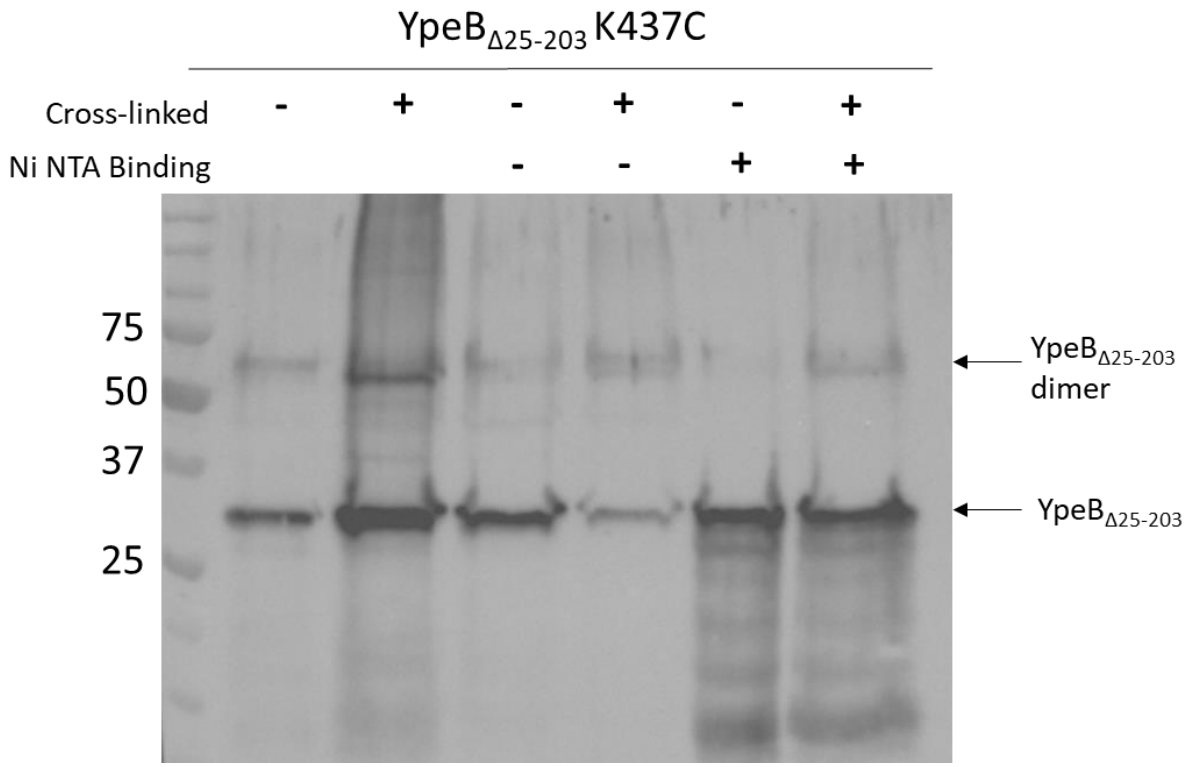

Figure 3.3: Purified YpeB$_{\Delta 25\text{-}203}$ K437C cross-linked complex. Two hundred OD units of decoated dormant spores were cross-linked with APB. Cross-linked spores were lypholized, mechanically broken and proteins were extracted with 8 M urea binding buffer for 120 min. Spore lysates were then passed over a Ni^{2+} NTA column to isolate YpeB$_{\Delta 25\text{-}203}$-His$_6$ in addition to those proteins covalently bound via cross-links. Fractions were visualized via western blot using anti-YpeB antibodies (104). YpeBΔ25-203 K437C monomers and dimers were detected in both the load (lane 2) and elutions (lane 6) of cross-linked spore samples.

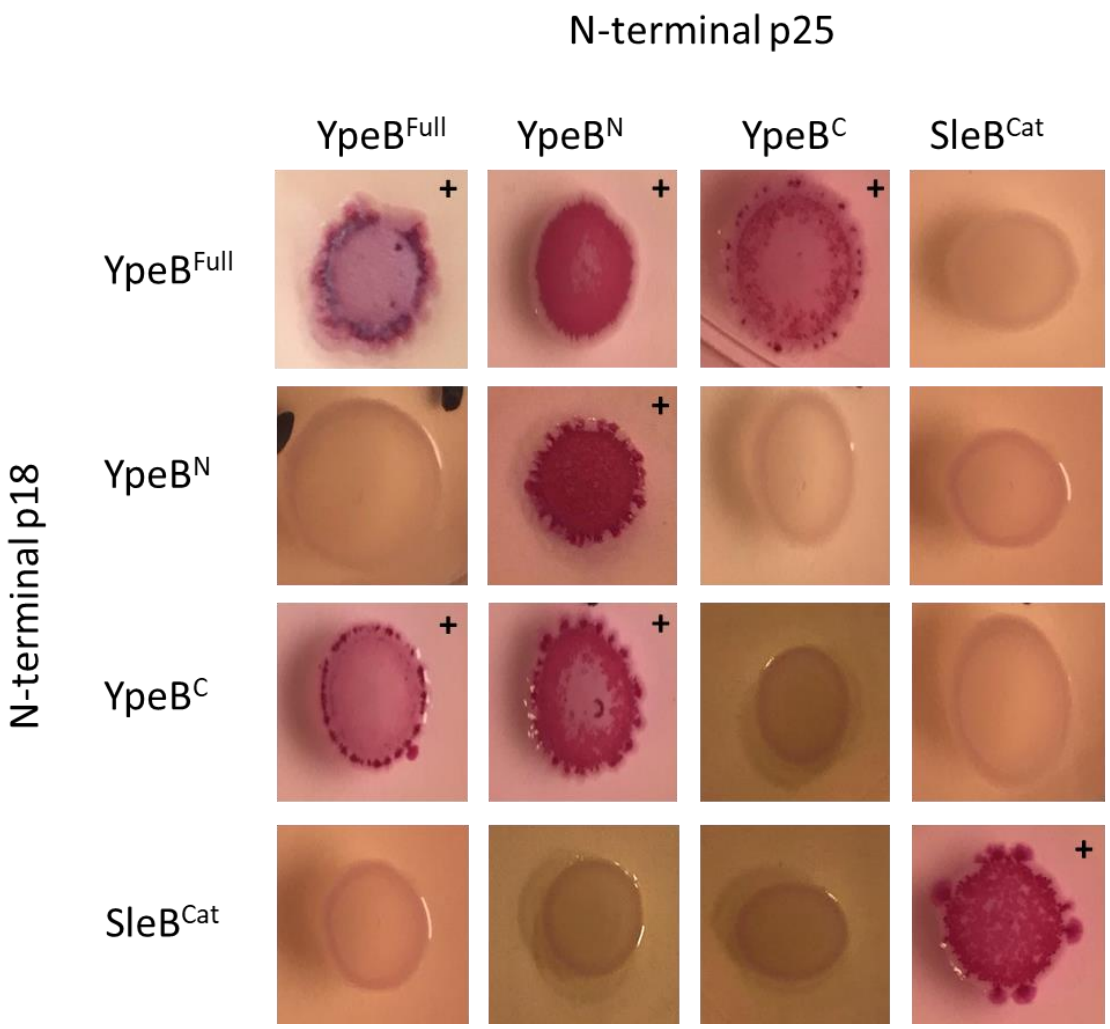

Figure 3.4: Individual YpeB domain contribution to multimer formation. Individual domains of YpeB and SleB were cloned into both pUT18C and pKT25 creating N-terminal fusions to domains of adenylate cyclase. YpeB and SleB domains were then co-transformed and screened against one another for protein-protein interactions. $YpeB^{N}$ demonstrates strong self-association, while both $YpeB^{C}$ and $YpeB^{N}$ appear to interact with $YpeB^{Full}$. No interactions of YpeB domains with $SleB^{Cat}$ were detected but, $SleB^{Cat}$ was indicated to interact with itself.

Table 3.1. Bacterial strains and plasmids

Strain	Genotype	Construction	Source
B. anthracis			
Sterne 34F2	$pXO1^{+}$ $pXO2^{-}$		P. Hanna
DPBa89	Δ*ypeB*	pDPV392 > 34F2	(104)
DPBa127	Δ*ypeB*::pDPV422 ($YpeB_{1-446}$-His_6 Er^R)	pDPV424 > DPBa89	(104)
DPBa204	Δ*ypeB*::pDPV476 ($YpeB^{K437C}$-His_6 Er^R)	pDPV476 > DPBa89	This Study
DPBa205	Δ*ypeB*::pDPV477 ($YpeB^{S358C}$-His_6 Er^R)	pDPV477 > DPBa89	This Study
DPBa210	Δ*ypeB*::pDPV478 ($YpeB^{T328C}$-His_6 Er^R)	pDPV478 > DPBa89	This Study
DPBa211	Δ*ypeB*::pDPV479 ($YpeB^{M282C}$-His_6 Er^R)	pDPV479 > DPBa89	This Study
DPBa212	Δ*ypeB*::pDPV480 ($YpeB^{Y339C}$-His_6 Er^R)	pDPV480 > DPBa89	This Study
DPBa213	Δ*ypeB*::pDPV481 ($YpeB^{E314C}$-His_6 Er^R)	pDPV481 > DPBa89	This Study
DPBa214	Δ*ypeB*::pDPV482 ($YpeB^{V355C}$-His_6 Er^R)	pDPV482 > DPBa89	This Study
DPBa215	Δ*ypeB*::pDPV483 ($YpeB^{V324C}$-His_6 Er^R)	pDPV483 > DPBa89	This Study
DPBa216	Δ*ypeB*::pDPV484 ($YpeB^{T420C}$-His_6 Er^R)	pDPV484 > DPBa89	This Study
DPBa217	Δ*ypeB*::pDPV485 ($YpeB^{A342C}$-His_6 Er^R)	pDPV485 > DPBa89	This Study
DPBa218	Δ*ypeB*::pDPV486 ($YpeB^{V435C}$-His_6 Er^R)	pDPV486 > DPBa89	This Study
DPBa219	Δ*ypeB*::pDPV487 ($YpeB^{Q438C}$-His_6 Er^R)	pDPV487 > DPBa89	This Study
DPBa220	Δ*ypeB*::pDPV488 ($YpeB_{\Delta 25-203}$ K437C-His_6 Er^R)	pDPV488 > DPBa89	This Study
DPBa221	pDPV488 ($YpeB_{\Delta 25-203}$ K437C-His_6 Er^R)	pDPV488 > 34F2	This Study
DPBa222	Δ*ypeB*::pDPV489 ($YpeB_{\Delta 25-203}$ S358C-His_6 Er^R)	pDPV489 > DPBa89	This Study
DPBa223	pDPV489 ($YpeB_{\Delta 25-203}$ S358C-His_6 Er^R)	pDPV489 > 34F2	This Study
E.coli			
DPVE544	BTH101		Euromedex
DPVE545	pKT25-zip + pUT18C-zip	pKT25-zip + pUT18C-zip > BTH101	Euromedex
DPVE546	pKT25 + pUT18C		This Study
DPVE547	p25-$YpeB_{21-446}$ + p18-$YpeB_{21-446}$	pDPV494 + pDPV490 > BTH101	This Study
DPVE548	p25-$YpeB_{21-446}$ + p18-$YpeB_{21-202}$	pDPV494 + pDPV491 > BTH101	This Study
DPVE549	p25-$YpeB_{21-446}$ + p18-$YpeB_{203-446}$	pDPV494 + pDPV492 > BTH101	This Study
DPVE550	p25-$YpeB_{21-446}$ + p18-$SleB_{125-253}$	pDPV494 + pDPV493 > BTH101	This Study
DPVE551	p25-$YpeB_{21-203}$ + p18-$YpeB_{21-446}$	pDPV495 + pDPV490 > BTH101	This Study

DPVE552	p25-YpeB$_{21-202}$ + p18-YpeB$_{21-202}$	pDPV495 + pDPV491 > BTH101	This Study
DPVE553	p25-YpeB$_{21-202}$ + p18-YpeB$_{203-446}$	pDPV495 + pDPV492 > BTH101	This Study
DPVE554	p25-YpeB$_{21-202}$ + p18-SleB$_{125-253}$	pDPV495 + pDPV493 > BTH101	This Study
DPVE555	p25-YpeB$_{203-446}$ + p18-YpeB$_{21-446}$	pDPV496 + pDPV490 > BTH101	This Study
DPVE556	p25-YpeB$_{203-446}$ + p18-YpeB$_{21-202}$	pDPV496 + pDPV491 > BTH101	This Study
DPVE557	p25-YpeB$_{203-446}$ + p18-YpeB$_{203-446}$	pDPV496 + pDPV492 > BTH101	This Study
DPVE558	p25-YpeB$_{203-446}$ + p18-SleB$_{125-253}$	pDPV496 + pDPV493 > BTH101	This Study
DPVE559	p25-SleB$_{125-253}$ + p18-YpeB$_{21-446}$	pDPV497 + pDPV490 > BTH101	This Study
DPVE560	p25-SleB$_{125-253}$ + p18-YpeB$_{21-202}$	pDPV497 + pDPV491 > BTH101	This Study
DPVE561	p25-SleB$_{125-253}$ + p18-YpeB$_{203-446}$	pDPV497 + pDPV492 > BTH101	This Study
DPVE562	p25-SleB$_{125-253}$ + p18-SleB$_{125-253}$	pDPV497 + pDPV493 > BTH101	This Study

Plasmids	**Genotype**	**Construction**	**Source**
pBKJ236	ErR *ori*(Ts)		(191)
pKT25-zip			Euromedex
pUT18C-zip			Euromedex
pKT25			Euromedex
pUT18C			Euromedex
pDPV392	Δ*ypeB*	pBKJ236::Δ*ypeB*	(104)
pDPV424	YpeB$_{1-446}$-His$_6$	pBKJ236::Δ*sleB ypeB*$_{1-446}$-His6	(104)
pDPV448	YpeB$_{\Delta 25-203}$-His$_6$	pBKJ236::Δ*sleB ypeB*$_{\Delta 25-203}$-His$_6$	(104)
pDPV476	YpeB^{K437C}	pBKJ236::Δ*sleB ypeB*^{K437C}-His$_6$	This Study
pDPV477	YpeB^{S358C}	pBKJ236::Δ*sleB ypeB*^{S358C}-His$_6$	This Study
pDPV478	YpeB^{T328C}	pBKJ236::Δ*sleB ypeB*^{T328C}-His$_6$	This Study
pDPV479	YpeB^{M282C}	pBKJ236::Δ*sleB ypeB*^{M282C}-His$_6$	This Study
pDPV480	YpeB^{Y339C}	pBKJ236::Δ*sleB ypeB*^{Y339C}-His$_6$	This Study
pDPV481	YpeB^{E314C}	pBKJ236::Δ*sleB ypeB*^{E314C}-His$_6$	This Study
pDPV482	YpeB^{V355C}	pBKJ236::Δ*sleB ypeB*^{V355C}-His$_6$	This Study
pDPV483	YpeB^{V324C}	pBKJ236::Δ*sleB ypeB*^{V324C}-His$_6$	This Study
pDPV484	YpeB^{T420C}	pBKJ236::Δ*sleB ypeB*^{T420C}-His$_6$	This Study
pDPV485	YpeB^{A342C}	pBKJ236::Δ*sleB ypeB*^{A324C}-His$_6$	This Study
pDPV486	YpeB^{V435C}	pBKJ236::Δ*sleB ypeB*^{V435C}-His$_6$	This Study
pDPV487	YpeB^{Q438C}	pBKJ236::Δ*sleB ypeB*^{Q438C}-His$_6$	This Study

pDPV488	YpeB$_{\Delta 25\text{-}203}$ K437C-His$_6$	pBKJ236::Δ*sleB ypeB*$_{\Delta 25\text{-}203}$ K437C-His$_6$	This Study
pDPV489	YpeB$_{\Delta 25\text{-}203}$ S358C-His$_6$	pBKJ236::Δ*sleB ypeB*$_{\Delta 25\text{-}203}$ S358C-His$_6$	This Study
pDPV490	p18-YpeB$_{21\text{-}446}$	pUT18C:: *ypeB*$_{21\text{-}446}$	This Study
pDPV491	p18-YpeB$_{21\text{-}202}$	pUT18C:: *ypeB*$_{21\text{-}202}$	This Study
pDPV492	p18-YpeB$_{203\text{-}446}$	pUT18C:: *ypeB*$_{203\text{-}446}$	This Study
pDPV493	p18-SleB$_{125\text{-}253}$	pUT18C:: *sleB*$_{125\text{-}253}$	This Study
pDPV494	p25-YpeB$_{21\text{-}446}$	pKT25:: *ypeB*$_{21\text{-}446}$	This Study
pDPV495	p25-YpeB$_{21\text{-}202}$	pKT25:: *ypeB*$_{21\text{-}202}$	This Study
pDPV496	p25-YpeB$_{203\text{-}446}$	pKT25:: *ypeB*$_{203\text{-}446}$	This Study
pDPV497	p25-SleB$_{125\text{-}253}$	pKT25:: *sleB*$_{125\text{-}253}$	This Study

CHAPTER 4

Final Discussion

The utilization and effectiveness of *B. anthracis* as a bioweapon has unfortunately been demonstrated. Accidental release of weaponized spores from a production facility resulted in the deaths of civilians caught unaware in remote Russia. Anthrax spores disseminated through the U.S. postal system in 2001 caused not only illness but had a substantial economic impact as well due to arduous and expensive decontamination efforts. The innate characteristics that allow the spore to remain in a dehydrated dormant state also confer it resistance to most standard bactericidal methods. Therefore there is an acute need to further understanding of the underlying mechanisms of spore germination, specifically initiation and degradation of spore specific constructs, so that these processes could one day be subverted to facilitate easier spore decontamination. Many events of spore germination are still poorly understood, such as signal transfer from germinant receptor to trigger germination, how germination specific-lytic enzymes are activated, or how these enzymes remain inactive within the dormant spore. By furthering our understanding of these key events early in germination we may reveal targets for cleanup methods in which germination is efficiently triggered causing the return to a vegetative growth state, thus facilitating spore killing.

The work presented in this dissertation seeks to identify and characterize proteins that are active within spore germination, more specifically those proteins that contribute to either germination initiation or inhibition of germination specific lytic enzymes. Chapter 2 describes the implementation of a TnSeq workflow to identify additional proteins active within early stages of germination. Spores were produced from a generated transposon insertion library in *B. subtilis* and germinated in a GerA-dependent manner for 45 min suspended in phosphate buffer. By controlling the specific germination conditions rather than screening through plating assays we theorized that our screen would select for mutants with more subtle germination defects that

may likely have been missed in previous germination studies. In total we identified 42 genes with no previously known role in germination, but are required for efficient germination in response to L-valine. Fourteen of these genes were selected for further characterization based on previous work, placing these proteins within the inner spore membrane (109, 110), where the majority of important germination proteins such as germinant receptors and GSLEs exist within the dormant spore. The mechanism for how germination is initiated from germinant sensing by receptors is unknown. Germinant binding by receptors results in a commitment step, characterized by changes to inner membrane permeability and fluidity in addition to an initial release of ions, followed eventually by Ca^{2+} DPA (46). It has been demonstrated that the Ger receptors colocalize with another protein, GerD, to form the germinosome (81). GerD has been theorized as potentially acting in coordination with receptors to receive any signal that germinant binding has occurred (73, 81). Although GerD is suspected to act in this manner it is also possible that another protein may fulfill this role. Deletion strains of several genes identified in TnSeq screening were demonstrated to have reduced germination initiation mediated through all combinations of receptors, indicating that these genes may perhaps be involved in signal transfer from ger receptor to cause initiation of germination. However, it was determined that the reduced initiation phenotype was likely caused by a reduction in the overall abundance of the GerA receptor in these mutant strains. Overexpression of the GerA receptor within deficient mutant strains appeared to restore normal germination thus suggesting receptor abundance was more responsible than a potential breakdown in signaling. One of the mutants tested, *ΔytxG*, did not have its reduced germination initiation phenotype restored by receptor overexpression, this is likely due to abnormal membrane morphologies as reported previously (120), thus possibly causing receptor instability within the membrane or the result of a larger defect.

TnSeq screening implemented in Chapter 2 identified genes which had an effect on the earliest stages of spore germination, initiation and Stage 1. Genes known to have Stage II blockages were slightly enriched in our screen but not to a significant level, thus we may have missed proteins affecting GSLE stabilization or inhibition. Chapter 3 examines one such protein, YpeB. Utilizing an *in vivo* site directed chemical cross-linking approach, we sought to identify proteins which may either be directly interacting or are near enough for interactions with YpeB within the dormant spore. Sites within the C-terminal PepSY domains were selected as targets for our cross-linking assays, as previous work had indicated that regions beyond the first PepSY domain are required for SleB stabilization (104). Residues within PepSY 2 and PepSY 3 were determined to be within the 10 angstrom arm length of the cross-linker of another protein approximately the same size. Further testing, using previously generated stable internal truncation mutants of YpeB (104), indicated that this association was that of a YpeB dimer.

In-vivo cross-linking suggests that residues within the PepSY domains are involved in mediating multimer formation. To further investigate the contributions of individual YpeB domains to multimer formation, we employed the bacterial adenylate cyclase two-hybrid system. YpeB has been previously demonstrated to be required for stabilization of its partner protein SleB within the dormant spore (98, 104). It has also been determined that both domains of YpeB are required for this stabilizing effect, the N-terminal and the C-terminal PepSY domain containing regions (104, 106). Two-hybrid assays indicated that the N-terminal domain of YpeB has a strong self-association, while also being able to interact with full-length YpeB protein. YpeB C-terminal domains did not indicate self-association in this assay but these domains were again capable of interacting with full-length YpeB protein. These results in concert with chemical cross-linking assays suggest that YpeB likely exists as a multimer within the dormant spore. These interactions

may be strongly mediated by self-association of the N-terminal domain while interactions within PepSY 2 and 3 are required for a stabilization of the putative multimer. How this multimer would then interact with SleB or another protein is still unknown. Two Hybrid assays also suggested self-association between SleB catalytic domains, it is possible that the YpeB-SleB interaction is maintained through the formation of a heteromultimeric structure within the dormant spore.

The atomic structure of the YpeB PepSY-containing C-terminal domain of *B. megatarium* has been solved (195). The structure is composed of three tandem repeats of the PepSY domains and has been demonstrated to adopt a conformation unique to PepSY domain-containing proteins (195). Although no specific insights could be drawn as to how YpeB may be interacting with SleB, the authors identified a channel traversing the structure, they purposed may be a binding site for potential interactions. Of the residues tested in chemical cross-linking in Chapter 3, S358C is surface exposed and falls in the middle of this channel, the other reactive residue, K437C, lies exposed on one end of the channel. If interactions with SleB were occurring at this site, our cross-linking should have detected it. However these residues were indicated in putative YpeB multimer formation, it is possible that this channel is involved in YpeB multimer formation and is not directly associated with SleB. It should be mentioned that the authors did not address the possibility of a YpeB multimer as the crystal packing did not suggest multimer formation of the YpeB C-terminal domain (195). Our two-hybrid data suggests that this domain would not have formed a dimer. Our own *in silico* manipulations of the solved C-terminal domain structure did not indicate an obvious structural organization leading to dimer or multimer formation.

Circumstantial evidence for a direct YpeB-SleB interaction is abundant, however no such interaction has been detected. It is possible that this interaction is one of dimers forming unique structures within the spore and as such require the specific conditions of the inner spore

membrane region, not limited to the presence of a membrane alone. Further studies of the YpeB interactions within the dormant spore should focus on the role of the N-terminal domain. This region has no known homology and limited structural modeling indicates this region to be formed of long alpha helices. Obtaining crystals of this domain to solve its structure have proven difficult. This N-terminal domain has been demonstrated to have inhibitory effect on SleB *in vitro* (106) and may be responsible for interacting with SleB rather than the C-terminal PepSY domains which could act in stabilizing a potential interaction or have another role yet to be determined. It is also possible that YpeB does not interact directly with SleB. Early attempts in cross-linking dormant spores were designed with this approach in mind, using an unbiased nonspecific cross-linking approach. This approach may still be worth exploring as we have yet to rule out the possibility of another protein acting in this relationship.

Additional future directions should continue to investigate candidate genes identified in TnSeq screening. Interestingly, many of the genes identified in the TnSeq screen presented in Chapter 2 are not known to be transcribed under the control of sporulation σ factors. How these genes then affect sporulation or germination is an intriguing area of future studies. Several of the genes feature 5' untranslated regions in their mRNA, possibly sites of post-transcriptional regulation which may be indicative of another layer of regulation within sporulation. Several of the genes identified could function within sporulation and mutations' effects during sporulation were ultimately detected as germination defects. We have largely focused on the potential roles in germination, while now it seems likely that these genes specific function in sporulation is required for effective germination. In addition to the 42 genes listed in Chapter 2, there are 206 more genes significantly differentially represented in our screen, as determined by DeSEQ2

statistical testing, that could be items for future investigations for functions in either germination or sporulation.

APPENDIX

Supplementary Materials

Table S1. *B. subtilis* trains used in this study.

Strain	Genotype	Source/Construction
DPVB724	Δ*gerB* Cm^R	FB72 (196)→PS832
DPVB726	Δ*gerA* Sp^R Δ*gerB* Cm^R	FB72 (196)→PS832
DPVB747	Δ*skfE* MLS^R	BKE01950[a]→PS832
DPVB748	Δ*pcrB* MLS^R	BKE06600[a] →PS832
DPVB749	Δ*ygaC* MLS^R	BKE08680[a] →PS832
DPVB750	Δ*sipT* MLS^R	BKE14410[a] →PS832
DPVB751	Δ*ylbC* MLS^R	BKE14960[a] →PS832
DPVB752	Δ*hfq* MLS^R	BKE17340[a] →PS832
DPVB753	Δ*yqhL* MLS^R	BKE24540[a] →PS832
DPVB754	Δ*dnaJ* MLS^R	BKE25460[a] →PS832
DPVB755	Δ*yqeF* MLS^R	BKE25700[a] →PS832
DPVB756	Δ*phoR* MLS^R	BKE29100[a] →PS832
DPVB757	Δ*phoP* MLS^R	BKE29110[a] →PS832
DPVB758	Δ*ytxG* MLS^R	BKE29780[a] →PS832
DPVB759	Δ*ytpA* MLS^R	BKE30510[a] →PS832
DPVB760	Δ*yybT* MLS^R	BKE40510[a] →PS832
DPVB761	*gerA-lacZ* MLS^R	PS767 (131, 132)→PS832
DPVB763	Δ*skfE* MLS^R Δ*gerB* Cm^R	DPVB724→DPVB747
DPVB764	Δ*pcrB* MLS^R Δ*gerB* Cm^R	DPVB724→DPVB748
DPVB765	Δ*ygaC* MLS^R Δ*gerB* Cm^R	DPVB724→DPVB749
DPVB766	Δ*sipT* MLS^R Δ*gerB* Cm^R	DPVB724→DPVB750
DPVB767	Δ*ylbC* MLS^R Δ*gerB* Cm^R	DPVB724→DPVB751
DPVB768	Δ*hfq* MLS^R Δ*gerB* Cm^R	DPVB724→DPVB752
DPVB769	Δ*yqhL* MLS^R Δ*gerB* Cm^R	DPVB724→DPVB753
DPVB770	Δ*dnaJ* MLS^R Δ*gerB* Cm^R	DPVB724→DPVB754
DPVB771	Δ*yqeF* MLS^R Δ*gerB* Cm^R	DPVB724→DPVB755
DPVB772	Δ*phoR* MLS^R Δ*gerB* Cm^R	DPVB724→DPVB756
DPVB773	Δ*phoP* MLS^R Δ*gerB* Cm^R	DPVB724→DPVB757
DPVB774	Δ*ytxG* MLS^R Δ*gerB* Cm^R	DPVB724→DPVB758
DPVB775	Δ*ytpA* MLS^R Δ*gerB* Cm^R	DPVB724→DPVB759
DPVB776	Δ*yybT* MLS^R Δ*gerB* Cm^R	DPVB724→DPVB760
DPVB805	Δ*skfE*	Cre expression for deletion of MLSR
DPVB806	Δ*pcrB*	Cre expression for deletion of MLSR
DPVB807	Δ*ygaC*	Cre expression for deletion of MLSR
DPVB808	Δ*sipT*	Cre expression for deletion of MLSR
DPVB809	Δ*ylbC*	Cre expression for deletion of MLSR
DPVB810	Δ*hfq*	Cre expression for deletion of MLSR
DPVB811	Δ*yqhL*	Cre expression for deletion of MLSR
DPVB812	Δ*dnaJ*	Cre expression for deletion of MLSR
DPVB813	Δ*yqeF*	Cre expression for deletion of MLSR
DPVB814	Δ*phoR*	Cre expression for deletion of MLSR
DPVB815	Δ*phoP*	Cre expression for deletion of MLSR
DPVB816	Δ*ytxG*	Cre expression for deletion of MLSR
DPVB817	Δ*ytpA*	Cre expression for deletion of MLSR
DPVB818	Δ*yybT*	Cre expression for deletion of MLSR
DPVB819	Δ*skfE gerA-lacZ* MLS^R	DPVB761→DPVB805
DPVB820	Δ*pcrB gerA-lacZ* MLS^R	DPVB761→DPVB806
DPVB821	Δ*ygaC gerA-lacZ* MLS^R	DPVB761→DPVB807

DPVB822	Δ*sipT gerA-lacZ* MLS^R	DPVB761→DPVB808
DPVB823	Δ*ylbC gerA-lacZ* MLS^R	DPVB761→DPVB809
DPVB824	Δ*hfq gerA-lacZ* MLS^R	DPVB761→DPVB810
DPVB825	Δ*yqhL gerA-lacZ* MLS^R	DPVB761→DPVB811
DPVB826	Δ*dnaJ gerA-lacZ* MLS^R	DPVB761→DPVB812
DPVB827	Δ*yqeF gerA-lacZ* MLS^R	DPVB761→DPVB813
DPVB828	Δ*phoR gerA-lacZ* MLS^R	DPVB761→DPVB814
DPVB829	Δ*phoP gerA-lacZ* MLS^R	DPVB761→DPVB815
DPVB830	Δ*ytxG gerA-lacZ* MLS^R	DPVB761→DPVB816
DPVB831	Δ*ytpA gerA-lacZ* MLS^R	DPVB761→DPVB817
DPVB832	Δ*yybT gerA-lacZ* MLS^R	DPVB761→DPVB818
DPVB833	*PsspD::gerA* MLSR	PS3476 (133)
DPVB834	Δ*skfE PsspD::gerA* MLS^R	DPVB833→DPVB805
DPVB835	Δ*pcrB PsspD::gerA* MLS^R	DPVB833→DPVB806
DPVB836	Δ*ygaC PsspD::gerA* MLS^R	DPVB833→DPVB807
DPVB837	Δ*sipT PsspD::gerA* MLS^R	DPVB833→DPVB808
DPVB838	Δ*ylbC PsspD::gerA* MLS^R	DPVB833→DPVB809
DPVB839	Δ*hfq PsspD::gerA* MLS^R	DPVB833→DPVB810
DPVB840	Δ*yqhL PsspD::gerA* MLS^R	DPVB833→DPVB811
DPVB841	Δ*dnaJ PsspD::gerA* MLS^R	DPVB833→DPVB812
DPVB842	Δ*yqeF PsspD::gerA* MLS^R	DPVB833→DPVB813
DPVB843	Δ*phoR PsspD::gerA* MLS^R	DPVB833→DPVB814
DPVB844	Δ*phoP PsspD::gerA* MLS^R	DPVB833→DPVB815
DPVB845	Δ*ytxG PsspD::gerA* MLS^R	DPVB833→DPVB816
DPVB846	Δ*ytpA PsspD::gerA* MLS^R	DPVB833→DPVB817
DPVB847	Δ*yybT PsspD::gerA* MLS^R	DPVB833→DPVB818

[a] Strain obtained from the Bacillus Genetic Stock Center

Table S2. Spore germination in response to diverse germinants following overexpression of *gerA*.

Genotype	% OD Loss at 60 min with 1X AGFK		% OD Loss at 40 min with 2xYT	
	without *sspDp-gerA*	with *sspDp-gerA*	without *sspDp-gerA*	with *sspDp-gerA*
Wild type	13 ± 4	4 ± 1.3*	34 ± 2	34 ± 1
dnaJ	6 ± 3*	1 ± 2*	23 ± 0*	29 ± 2
hfq	9 ± 5	5 ± 1*	33 ± 1	33 ± 2
pcrB	5 ± 1*	0 ± 1*	31 ± 0	36 ± 3
phoP	8 ± 3	1 ± 1*	33 ± 0	30 ± 1
phoR	5 ± 4*	1 ± 1*	32 ± 3	36 ± 4
sipT	6 ± 6*	0 ± 1*	30 ± 6	33 ± 1
skfE	4 ± 5*	3 ± 1*	32 ± 4	35 ± 0
ygaC	10 ± 1*	1 ± 4*	31 ± 3	32 ± 5
ylbC	5 ± 4*	0 ± 1*	16 ± 2*	31 ± 0
yqeF	5 ± 2*	4 ± 2*	33 ± 5	28 ± 3
yqhL	16 ± 5	0 ± 1*	34 ± 4	30 ± 1
ytpA	18 ± 2	13 ± 1	30 ± 1	33 ± 1
ytxG	7 ± 5	0 ± 2*	26 ± 2	29 ± 8
yybT	17 ± 2	0 ± 0*	29 ± 1	36 ± 4

[a] Values are averages and standard deviations of assays on three replicate spore preparations. OD_{600} of purified spore suspension monitored at the indicated time after addition of 1X AGFK or 2xYT while shaking at 37°. * indicates a significant difference from the wild type without P*sspD-gerA* (T-test, $p<0.05$).

Table S3. Long-term germination efficiency of *B. subtilis* mutant strains[a]

Strain	Colonies after 24 hr (cfu/mL/OD)	New colonies after 48 hr (cfu/mL/OD)
Wild type	$3.5x10^8$	0
skfE	$9.2x10^7$	$1.0x10^6$
yqeF	$1.7x10^8$	0
pcrB	$1.7x10^8$	$6.0x10^6$
ytpA	$1.8x10^8$	0
ygaC	$4.0x10^8$	$1.0x10^7$
yqhL	$2.5x10^8$	0
yybT	$2.8x10^8$	$1.0x10^7$
hfq	$3.2x10^8$	0
phoR	$3.5x10^8$	0
phoP	$3.7x10^8$	0
sipT	$1.4x10^8$	$4.0x10^6$
dnaJ	$9.6x10^8$	0
ytxG	$1.2x10^8$	0
ylbC	$1.4x10^8$	$7.0x10^6$

[a] Values are from a single determination for each strain. Purified spores were serially diluted, plated on 2xSG medium, and incubated at 37°C.

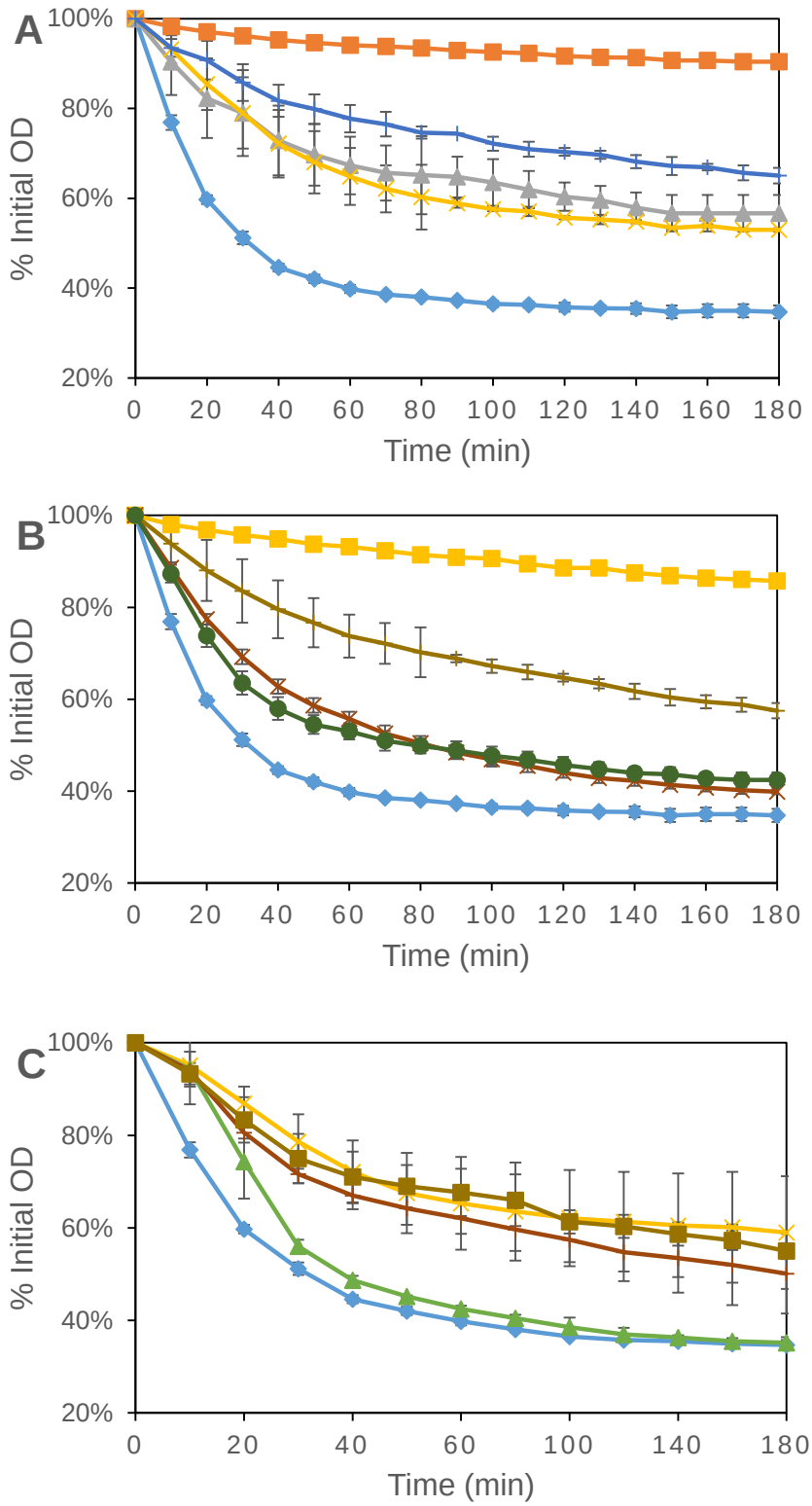
A
100%
80%
60%
40%
20%
% Initial OD
0
20
40
60
80
100
120
140
160
180
Time (min)
B
100%
80%
60%
40%
20%
% Initial OD
0
20
40
60
80
100
120
140
160
180
Time (min)
C
100%
80%
60%
40%
20%
% Initial OD
0
20
40
60
100
140
180
Time (min)

Fig S1. Germination rates of *B. subtilis* strains. Purified spores of *B. subtilis* wild type and mutant strains were heat activated, stimulated to germinate by addition of 10 mM L-Val, and shaken at 37°C, during which the OD_{600} was monitored. Values are averages of three assays and error bars are standard deviations. Each assay was performed on three replicate spore preparations. A) Wild type ♦, *ytxG* **X,** *yqhL* ▲**,** *ygaC* **+**, *dnaJ* ■ B) Wild type ♦, *phoR* **X,** *hfq* **+**, *sipT* ■, *yybT* ● C) Wild type ♦, *sfkE* **X,** *pcrB* ▲**,** *yqeF* **+**, *ytpA* ■.

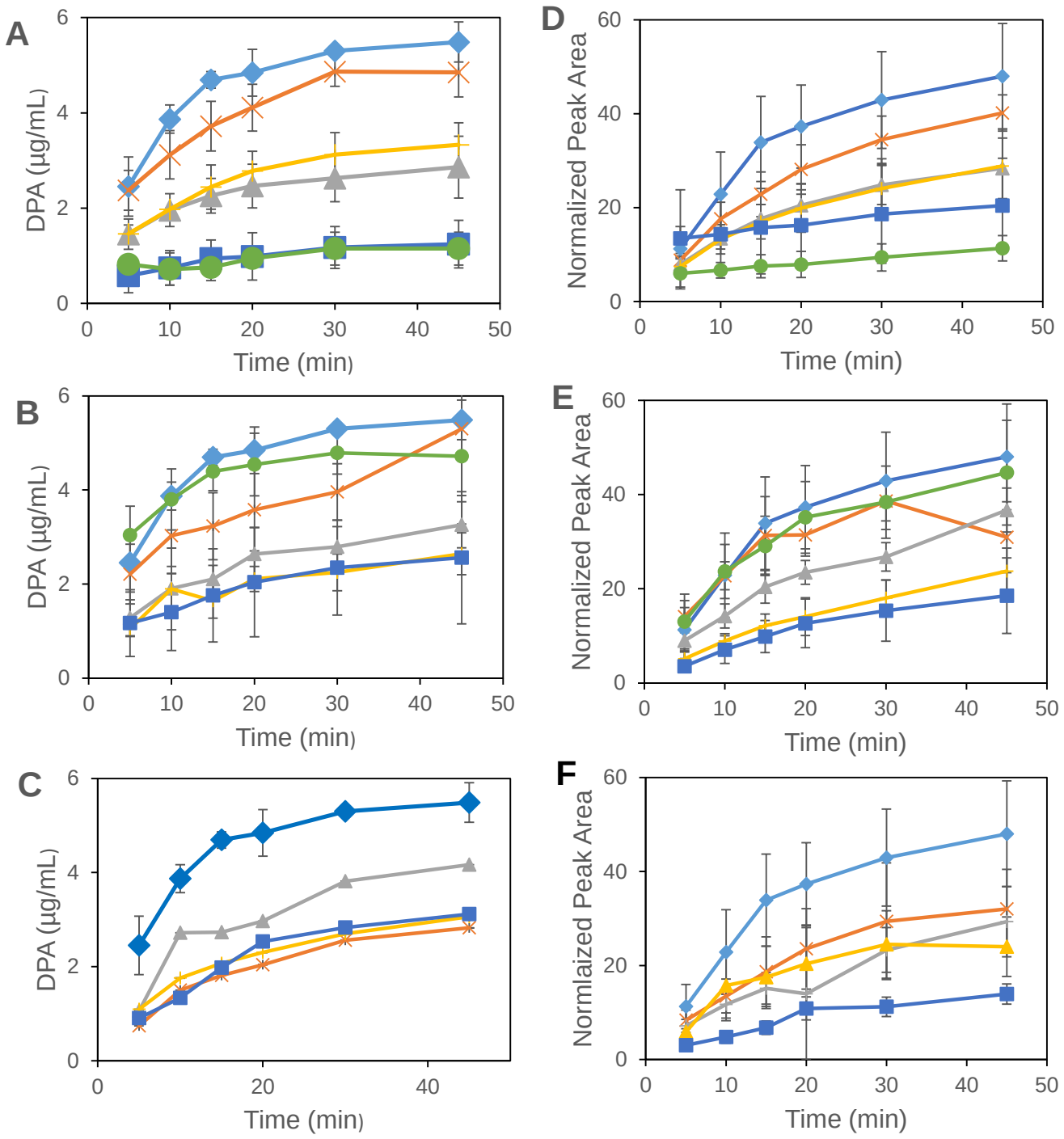

Fig S2. Release of DPA and NAM by *B. subtilis* strains. Purified spores were heat activated, stimulated to germinate by addition of 10 mM L-Val, and shaken at 37°C. Samples were taken at designated intervals, centrifuged, and the supernatant was saved for later analysis. Values are averages of three assays for DPA (panels A-C) and NAM (panels D-F), and error bars are standard

deviations. Each assay was performed on three replicate spore preparations. Panels A and D: Wild type ♦, *ytxG* **X,** *yqhL* ▲**,** *ygaC* **+**, *dnaJ* ■, *ylbC* ●. Panels B and E: Wild type ♦, *phoR* **X,** *phoP* ▲**,** *hfq* **+**, *sipT* ■, *yybT* ●. Panels C and F: Wild type ♦, *sfkE* **X,** *pcrB* ▲**,** *yqeF* **+**, *ytpA* ■. For DPA release: *dnaJ* and *ylbC* strains are significantly different from the wild type at all time points; *yqhL, ygaC, sipT, hfq,* and *phoP* strains are significantly different from 10 min onwards; and *yybT, ytxG,* and *phoR* strains are not significantly different from the wild type at any time point. For NAM release: *sipT* , *ylbC*, and *ytpA* strains are significantly different from the wild type from 20 min onwards. Some other strains exhibited reduced NAM release, but this was not found to be statistically significant due to high variability between replicates.

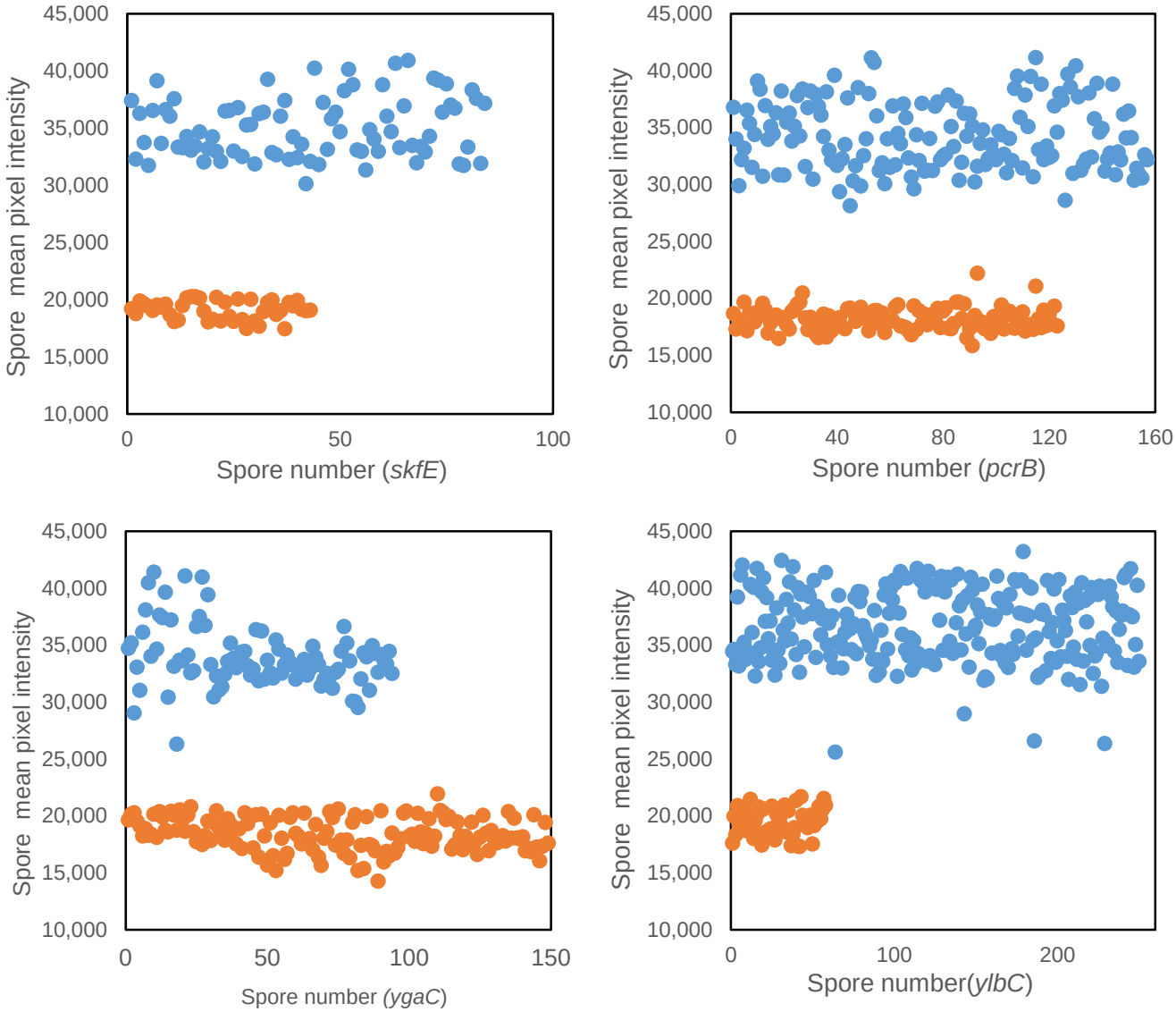
45,000
40,000
35,000
30,000
25,000
20,000
15,000
10,000
Spore mean pixel intensity
0
50
100
Spore number (skfE)
0
40
80
120
160
Spore number (pcrB)
0
50
100
150
Spore number (ygaC)
0
100
200
Spore number(ylbC)

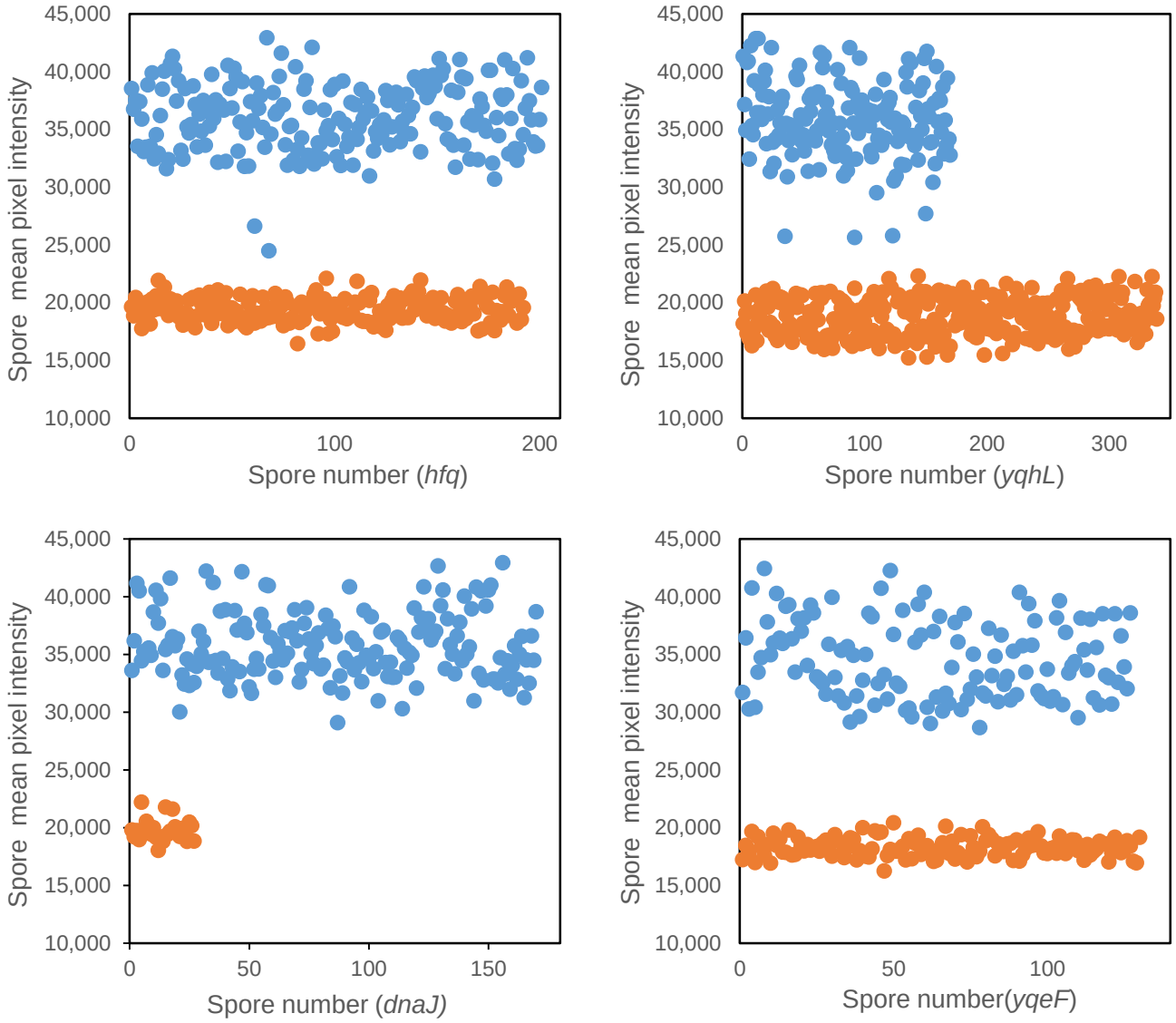
45,000
40,000
35,000
30,000
25,000
20,000
15,000
10,000
Spore mean pixel intensity
0
100
200
Spore number (*hfq*)
45,000
40,000
35,000
30,000
25,000
20,000
15,000
10,000
Spore mean pixel intensity
0
100
200
300
Spore number (*yqhL*)
45,000
40,000
35,000
30,000
25,000
20,000
15,000
10,000
Spore mean pixel intensity
0
50
100
150
Spore number (*dnaJ)*
45,000
40,000
35,000
30,000
25,000
20,000
15,000
10,000
Spore mean pixel intensity
0
50
100
Spore number(*yqeF*)

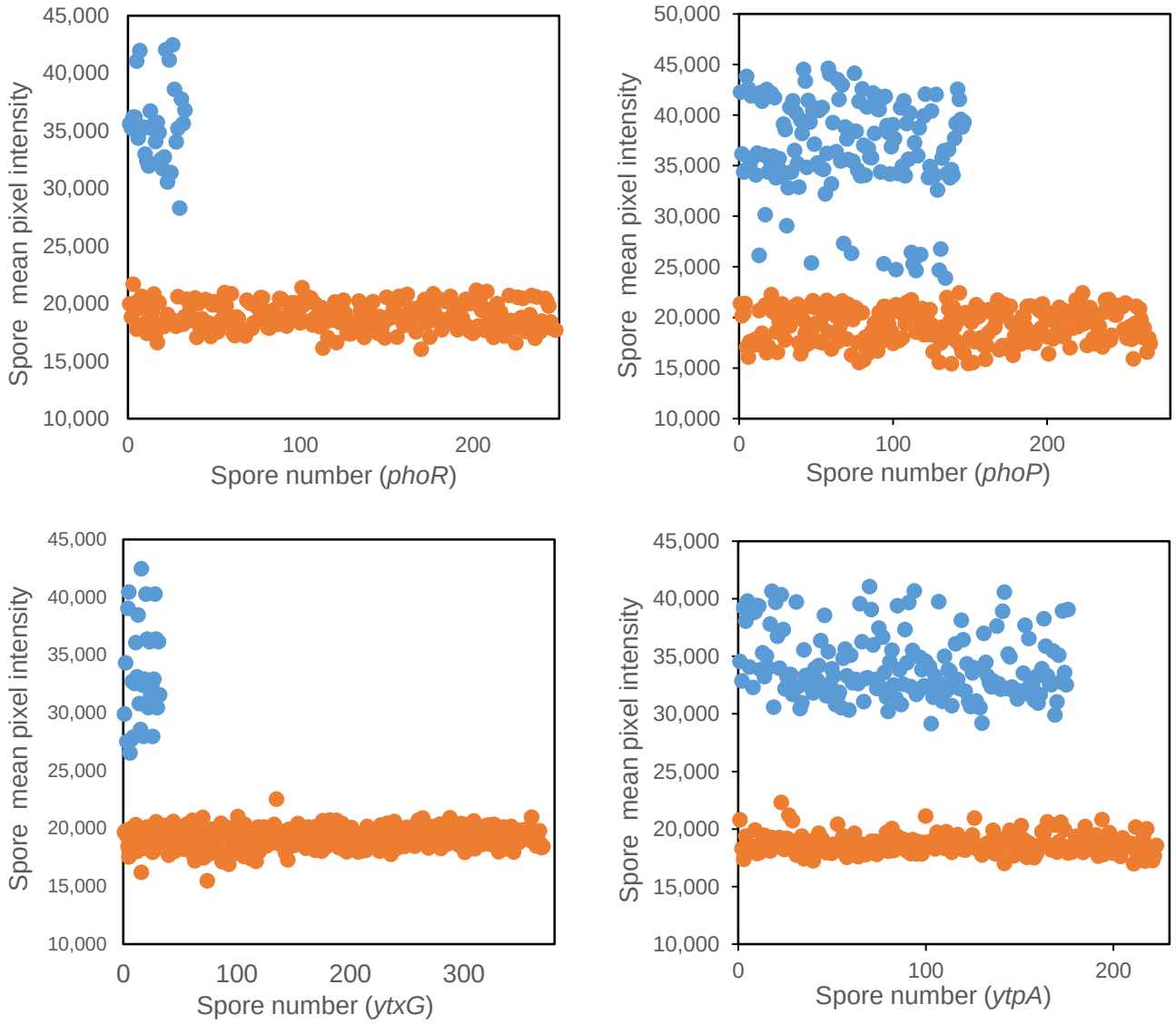
45,000
40,000
35,000
30,000
25,000
20,000
15,000
10,000
Spore mean pixel intensity
0
100
200
Spore number (*phoR*)
50,000
45,000
40,000
35,000
30,000
25,000
20,000
15,000
10,000
Spore mean pixel intensity
0
100
200
Spore number (*phoP*)
45,000
40,000
35,000
30,000
25,000
20,000
15,000
10,000
Spore mean pixel intensity
0
100
200
300
Spore number (*ytxG*)
45,000
40,000
35,000
30,000
25,000
20,000
15,000
10,000
Spore mean pixel intensity
0
100
200
Spore number (*ytpA*)

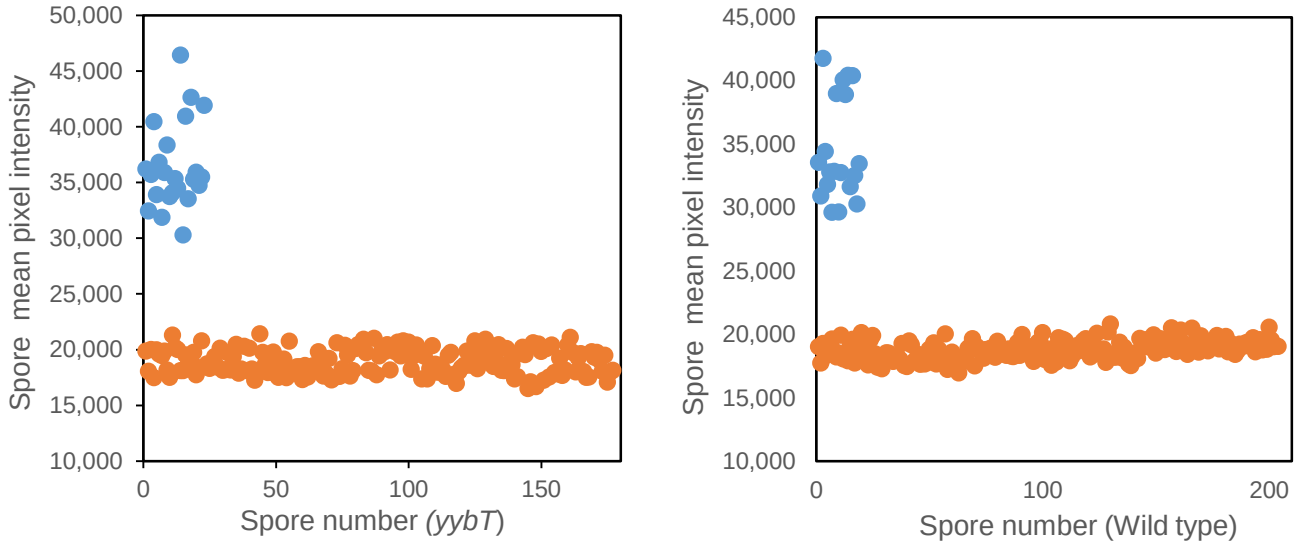

Fig S3. Phase contrast microscopy image pixel intensities during spore germination. Spores were subjected to germination conditions, 10 mM L-Valine at 37°C, for 1 hour. For each strain, pixel intensities were averaged for each spore detected in three images, including a total of at least 127-509 spores. Blue dots indicate spores classified as phase bright, which had similar intensities as spores in the initial dormant population, and orange dots indicate spores classified as phase-dark, in order to determine population percentages in Table 3. Phase bright and phase dark spores are plotted independently on the X-axes.

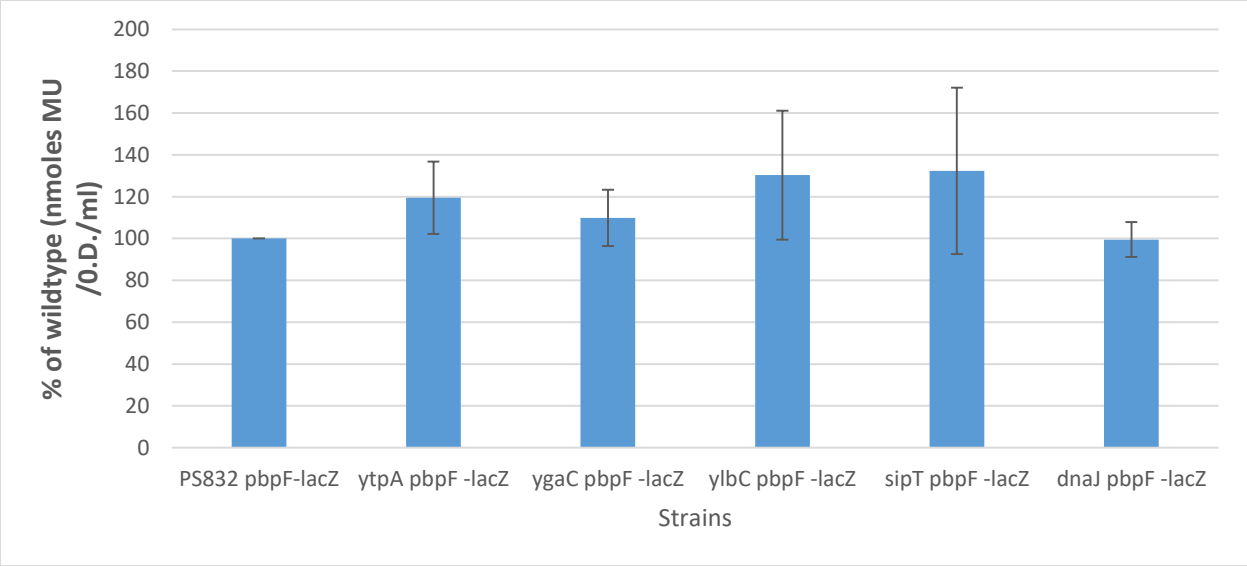

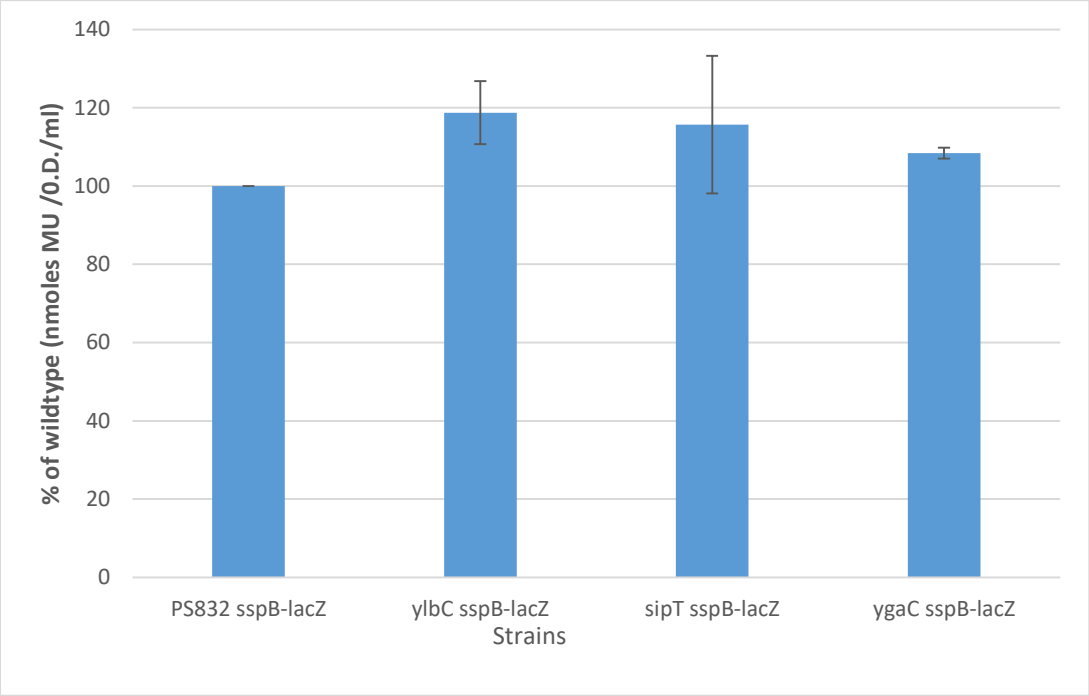

Fig S4. Expression of σ^G-dependent genes in *B. subtilis* mutant strains.

Purified spore carrying *lacZ* transcriptional fusions were decoated and lysed, and extracts were assayed for β-galactosidase. Values are expressed as a percentage of that detected in the wild type strain containing the same *lacZ* fusion. Values are averages of assays on three (A, *pbpF-lacZ*) or two (B, *sspB-lacZ*) replicate spore preparations and error bars are standard deviations.

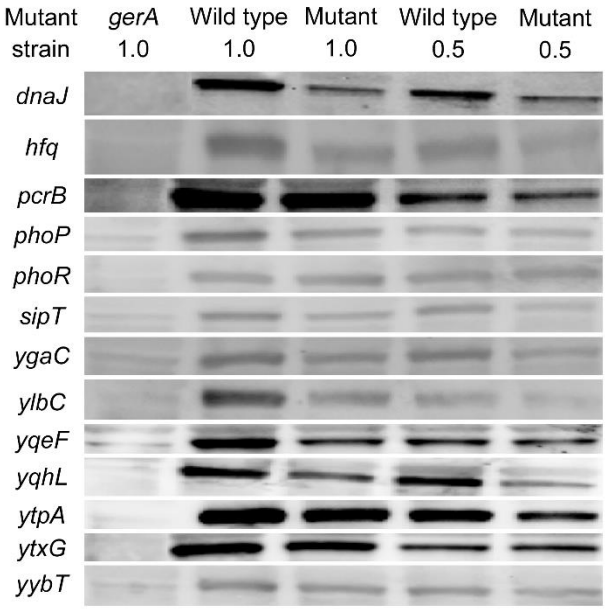

Fig S5. GerAC is reduced in the spores of several *B. subtilis* mutant strains. Equal quantities of spore suspensions were decoated and broken, and proteins were extracted, serially diluted, run on SDS-PAGE, and transferred to PVDF membrane as described previously (84). The membrane was probed with anti-GerAC antibodies (87). Strain genotype (All strains were also Δ*gerB*.) and sample dilution is indicated above each lane or on the left of each panel.

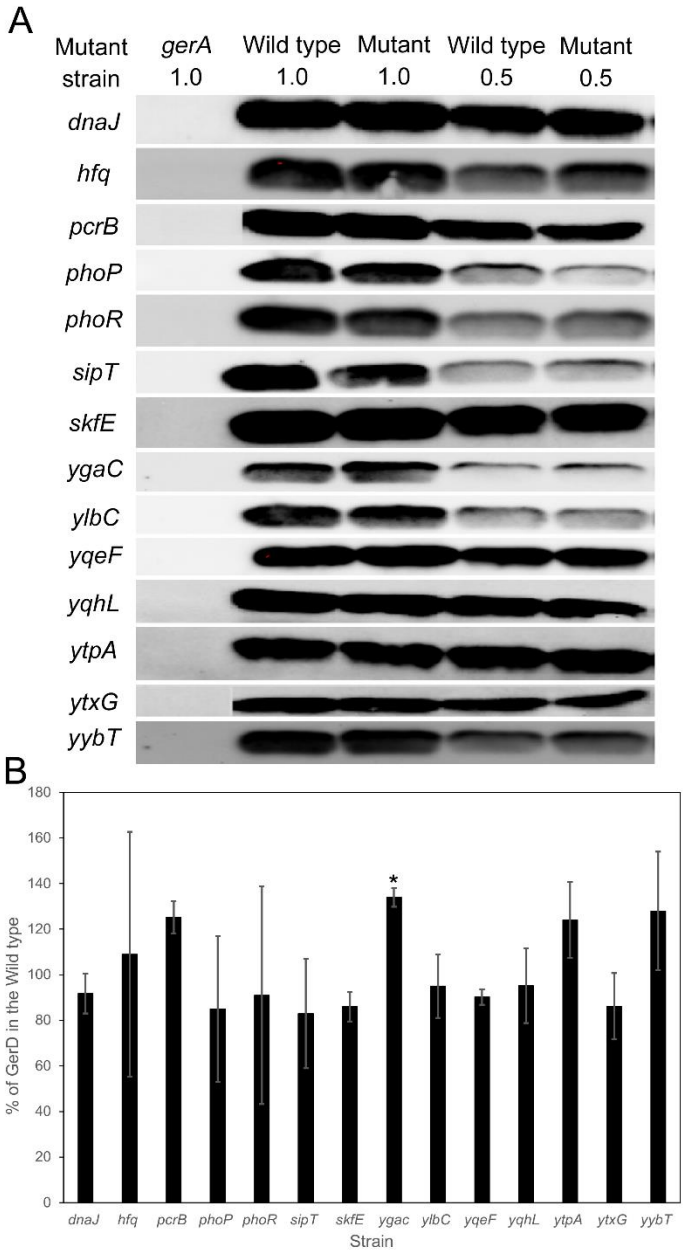

Figure S6: GerD is not reduced in the spores of *B. subtilis* germination mutants. Equal quantities of spore suspensions were decoated and broken, and proteins were extracted, serially diluted, run on SDS-PAGE, and transferred to PVDF membrane as described previously (84). The membrane was probed with anti-GerD antibodies (87) (Panel A). Strain genotype (All strains were also Δ*gerB*.) and sample dilution is indicated above each lane or on the left of each

panel. Protein load and transfer to membrane in each lane was normalized as described in Materials and Methods, and the amount of GerD detected in each strain was compared to that found in the wild type (Panel B). Values are averages of two biological replicates and error bars indicate standard deviations. * indicates a significant difference from the wild type ($p \leq 0.05$).

A

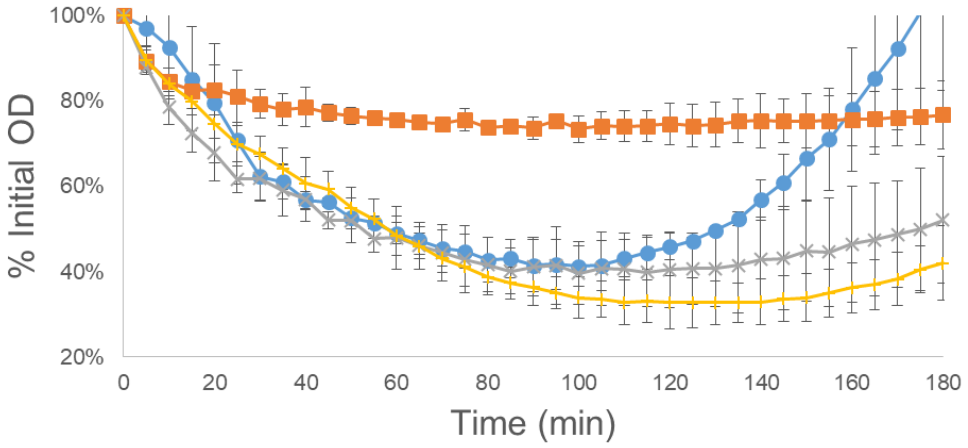
100%
80%
60%
40%
20%
% Initial OD
0
20
40
60
80
100
120
140
160
180
Time (min)

B

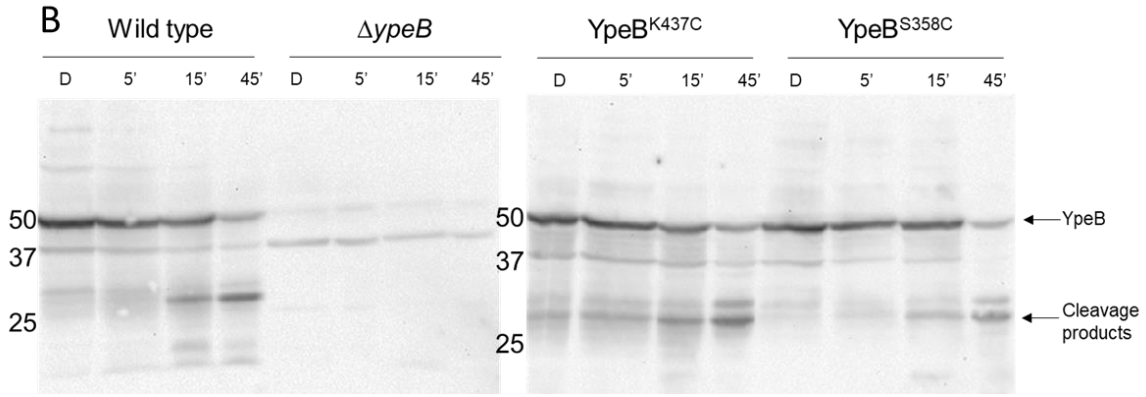
Wild type
ΔypeB
YpeBK437C
YpeBS358C
D
5'
15'
45'
50
37
25
YpeB
Cleavage products

C

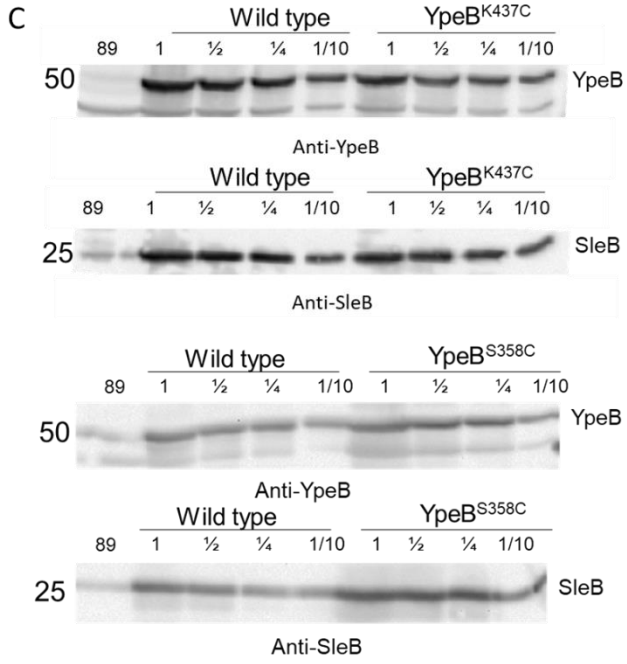
Wild type
YpeBK437C
YpeBS358C
89
1
½
¼
1/10
50
25
YpeB
SleB
Anti-YpeB
Anti-SleB

Figure S7. YpeB-cysteine mutant strain functional screens. A. Germination rates of Wild type (●), Δ*ypeB* (■), YpeB^{K437C} (**+**), and YpeB^{S358C} (**X**) were determined by monitoring OD_{600} change over time following addition of rich media. **B.** Visualization of YpeB proteolytic processing through out germination. Dormant spores were submit to germination inducing conditions, aliquots were taken at specified time points and flash frozen for later analysis via western blot. **C.** 10 OD of dormant spores encoding YpeB-cysteine alleles and controls were lypholized, mechanically broken, and extracts were visualized via western blot detected for both YpeB and SleB abundance and stability within mutant strains.

Table S4. Primer Sequences

Plasmid Constructed	Primer Name	Sequence 5' to 3'
pDPV478	693	ATGATAATGTTGGAGTATTTTGCTATGTAGTAAATGTGAATGG
	694	CCATTCACATTTACTACATAGCAAAATACTCCAACATTATCAT
pDPV480	697	ATGTGAATGGCGTACGAATTTGTCCTGAAGCAATTCAAATGAA
	698	TTCATTTGAATTGCTTCAGGACAAATTGGTACGCCATTCACAT
pDPV476, pDPV488	699	GAGCAGAAGAAAAAGTGAAGTGCATGCAGGCTGTTGAAAAAAT
	700	ATTTTTTCAACAGCCTGCATGCACTTCACTTTTTCTTCTGCTC
pDPV479	701	GCGGATATCCAATTTGGGTTTGCAATAATCGAGAAATTAAAGA
	702	TCTTTAATTTCTCGATTATTGCAAACCCAAATTGGATATCCGC
pDPV481	703	GGACCATAAGTTTAATAATATGTGCCTTTATGATAGCTCACAATATG
	704	TATTGTGAGCTATCATAAAGGCACATATTATTAAACTTATGGTCC
pDPV483	705	TGATAGCTCACAATATGATAATTGTGGAGTATTTACGTATGTAGT
	706	ACTACATACGTAAATACTCCACAATTATCATATTGTGAGCTATCA
pDPV487	707	CAGAAGAAAAAGTGAAGAAATGTCAGGCTGTTGAAAAAATTTA
	708	TAAATTTTTTCAACAGCCTGACATTTCTTCACTTTTTCTTCTG
pDPV485	709	AAGCAATTCAAATGAAAATTTGTTTAGATGACGGTTCTATCGT
	710	ACGATAGAACCGTCATCTAAACAAATTTTCATTTGAATTGCTT
pDPV482	711	CTTTAGATGACGGTTCTATCTGTGGATTCTCCGCAAAAGAATA
	712	TATTCTTTTGCGGAGAATCCACAGATAGAACCGTCATCTAAAG
pDPV477, pDPV489	713	ACGGTTCTATCGTTGGATTCTGCGCAAAAGAATAATTAGCGTC
	714	GACGCTAAATATTCTTTTGCACGGAATCCAACGATAGAACCGT
pDPV484	717	TAGGTACGTTAGGGAAAGATTGTTACCAAATCTTCATTAATGC
	718	GCATTAATGAAGATTTGGTAACAATCTTTCCCTAACGTACCTA
pDPV486	719	ATAGCGGAGCAGAAGAAAAATGTAAGAAAATGCAGGCTGTT
	720	TCAACAGCCTGCATTTTCTTACATTTTTCTTCTGCTCCGCTAT
pDPV490, pDPV494	764	TCTAGAGGATCCCGGCTATAAAGAGCATCAAGAGAAGAAT
	765	CTTAGGTACCCGTTAATCATAAATTTTTTCAACAGCCTA
pDPV491, pDPV495	766	CGGGCTGCAGGGGGCTATAAAGAGCATCAAGAGAAGAAT
	767	CCGGGGATCCTCTAATGTAAAGGTAGGTCCGAAGTTTGT
pDPV492, pDPV496	768	TCTAGAGGATCCCAGTGCACAAAAAAATAAAAAAGGTGGA
	769	TCTTAGAATTCTTTAATCATAAATTTTTTCAACAGCCTG
pDPV493, pDPV497	770	CGCCACTGCAGGTCTCAAAATAAAGGGACAAATGTT
	771	CGATGAATTCGATTATTTACAGAAAATATGTTTCCCGAT

References

1. Mock M, Fouet A. 2001. Anthrax. Annu Rev Microbiol 55:647-71.
2. Baillie LW. 2006. Past, imminent and future human medical countermeasures for anthrax. J Appl Microbiol 101:594-606.
3. Spencer RC. 2003. *Bacillus anthracis*. J Clin Pathol 56:182-7.
4. Berger T, Kassirer M, Aran AA. 2014. Injectional anthrax - new presentation of an old disease. Euro Surveill 19.
5. Turnbull PC. 1991. Anthrax vaccines: past, present and future. Vaccine 9:533-9.
6. Lincoln RE, Hodges DR, Klein F, Mahlandt BG, Jones WI, Jr., Haines BW, Rhian MA, Walker JS. 1965. Role of the lymphatics in the pathogenesis of anthrax. J Infect Dis 115:481-94.
7. Shafa F, Moberly BJ, Gerhardt P. 1966. Cytological features of anthrax spores phagocytized *in vitro* by rabbit alveolar macrophages. J Infect Dis 116:401-13.
8. Guidi-Rontani C, Pereira Y, Ruffie S, Sirard JC, Weber-Levy M, Mock M. 1999. Identification and characterization of a germination operon on the virulence plasmid pXO1 of *Bacillus anthracis*. Mol Microbiol 33:407-14.
9. Fisher N, Hanna P. 2005. Characterization of *Bacillus anthracis* germinant receptors *in vitro*. J Bacteriol 187:8055-62.
10. Guidi-Rontani C, Weber-Levy M, Labruyere E, Mock M. 1999. Germination of *Bacillus anthracis* spores within alveolar macrophages. Mol Microbiol 31:9-17.
11. Beall FA, Taylor MJ, Thorne CB. 1962. Rapid lethal effect in rats of a third component found upon fractionating the toxin of *Bacillus anthracis*. J Bacteriol 83:1274-80.
12. Stanley JL, Smith H. 1961. Purification of factor I and recognition of a third factor of the anthrax toxin. J Gen Microbiol 26:49-63.
13. Petosa C, Collier RJ, Klimpel KR, Leppla SH, Liddington RC. 1997. Crystal structure of the anthrax toxin protective antigen. Nature 385:833-8.
14. Gordon VM, Klimpel KR, Arora N, Henderson MA, Leppla SH. 1995. Proteolytic activation of bacterial toxins by eukaryotic cells is performed by furin and by additional cellular proteases. Infect Immun 63:82-7.
15. Beauregard KE, Collier RJ, Swanson JA. 2000. Proteolytic activation of receptor-bound anthrax protective antigen on macrophages promotes its internalization. Cell Microbiol 2:251-8.
16. Wesche J, Elliott JL, Falnes PO, Olsnes S, Collier RJ. 1998. Characterization of membrane translocation by anthrax protective antigen. Biochemistry 37:15737-46.
17. Liu S, Moayeri M, Leppla SH. 2014. Anthrax lethal and edema toxins in anthrax pathogenesis. Trends Microbiol 22:317-25.
18. Wade BH, Wright GG, Hewlett EL, Leppla SH, Mandell GL. 1985. Anthrax toxin components stimulate chemotaxis of human polymorphonuclear neutrophils. Proc Soc Exp Biol Med 179:159-62.
19. Vitale G, Pellizzari R, Recchi C, Napolitani G, Mock M, Montecucco C. 1999. Anthrax lethal factor cleaves the N-terminus of MAPKKS and induces tyrosine/threonine phosphorylation of MAPKS in cultured macrophages. J Appl Microbiol 87:288.
20. Uchida I, Hornung JM, Thorne CB, Klimpel KR, Leppla SH. 1993. Cloning and characterization of a gene whose product is a trans-activator of anthrax toxin synthesis. J Bacteriol 175:5329-38.
21. Makino S, Uchida I, Terakado N, Sasakawa C, Yoshikawa M. 1989. Molecular characterization and protein analysis of the cap region, which is essential for encapsulation in *Bacillus anthracis*. J Bacteriol 171:722-30.
22. Zwartouw HT, Smith H. 1956. Polyglutamic acid from *Bacillus anthracis* grown *in vivo*; structure and aggressin activity. Biochem J 63:437-42.

23. Goodman JW, Nitecki DE. 1967. Studies on the relation of a prior immune response to immunogenicity. Immunology 13:577-83.
24. Turnbull PC, Leppla SH, Broster MG, Quinn CP, Melling J. 1988. Antibodies to anthrax toxin in humans and guinea pigs and their relevance to protective immunity. Med Microbiol Immunol 177:293-303.
25. Abramova FA, Grinberg LM, Yampolskaya OV, Walker DH. 1993. Pathology of inhalational anthrax in 42 cases from the Sverdlovsk outbreak of 1979. Proc Natl Acad Sci U S A 90:2291-4.
26. Justice USDo. 2010. Amerithrax Investigative Summary. Justice USDo,
27. Hendricks KA, Wright ME, Shadomy SV, Bradley JS, Morrow MG, Pavia AT, Rubinstein E, Holty JE, Messonnier NE, Smith TL, Pesik N, Treadwell TA, Bower WA. 2014. Centers for disease control and prevention expert panel meetings on prevention and treatment of anthrax in adults. Emerg Infect Dis 20.
28. Beatty ME, Ashford DA, Griffin PM, Tauxe RV, Sobel J. 2003. Gastrointestinal anthrax: review of the literature. Arch Intern Med 163:2527-31.
29. Barakat LA, Quentzel HL, Jernigan JA, Kirschke DL, Griffith K, Spear SM, Kelley K, Barden D, Mayo D, Stephens DS, Popovic T, Marston C, Zaki SR, Guarner J, Shieh WJ, Carver HW, 2nd, Meyer RF, Swerdlow DL, Mast EE, Hadler JL. 2002. Fatal inhalational anthrax in a 94-year-old Connecticut woman. Jama 287:863-8.
30. Holty JE, Bravata DM, Liu H, Olshen RA, McDonald KM, Owens DK. 2006. Systematic review: a century of inhalational anthrax cases from 1900 to 2005. Ann Intern Med 144:270-80.
31. Louie A, Vanscoy BD, Heine HS, 3rd, Liu W, Abshire T, Holman K, Kulawy R, Brown DL, Drusano GL. 2012. Differential effects of linezolid and ciprofloxacin on toxin production by *Bacillus anthracis* in an *in vitro* pharmacodynamic system. Antimicrob Agents Chemother 56:513-7.
32. Durmaz R, Doganay M, Sahin M, Percin D, Karahocagil MK, Kayabas U, Otlu B, Karagoz A, Buyuk F, Celebi O, Ozturk Z, Ertek M. 2012. Molecular epidemiology of the *Bacillus anthracis* isolates collected throughout Turkey from 1983 to 2011. Eur J Clin Microbiol Infect Dis 31:2783-90.
33. Brook I, Elliott TB, Pryor HI, 2nd, Sautter TE, Gnade BT, Thakar JH, Knudson GB. 2001. *In vitro* resistance of *Bacillus anthracis* Sterne to doxycycline, macrolides and quinolones. Int J Antimicrob Agents 18:559-62.
34. Friedlander AM, Welkos SL, Pitt ML, Ezzell JW, Worsham PL, Rose KJ, Ivins BE, Lowe JR, Howe GB, Mikesell P, et al. 1993. Postexposure prophylaxis against experimental inhalation anthrax. J Infect Dis 167:1239-43.
35. Wright JG, Quinn CP, Shadomy S, Messonnier N. 2010. Use of anthrax vaccine in the United States: recommendations of the Advisory Committee on Immunization Practices (ACIP), 2009. MMWR Recomm Rep 59:1-30.
36. Barnard JP, Friedlander AM. 1999. Vaccination against anthrax with attenuated recombinant strains of *Bacillus anthracis* that produce protective antigen. Infect Immun 67:562-7.
37. Turnbull PC. 2000. Current status of immunization against anthrax: old vaccines may be here to stay for a while. Curr Opin Infect Dis 13:113-120.
38. Cohen S, Mendelson I, Altboum Z, Kobiler D, Elhanany E, Bino T, Leitner M, Inbar I, Rosenberg H, Gozes Y, Barak R, Fisher M, Kronman C, Velan B, Shafferman A. 2000. Attenuated nontoxinogenic and nonencapsulated recombinant *Bacillus anthracis* spore vaccines protect against anthrax. Infect Immun 68:4549-58.
39. Spizizen J. 1958. Transformation of Biochemically Deficient Strains of *Bacillus subtilis* by Deoxyribonucleate. Proc Natl Acad Sci U S A 44:1072-8.
40. Cui W, Han L, Suo F, Liu Z, Zhou L, Zhou Z. 2018. Exploitation of *Bacillus subtilis* as a robust workhorse for production of heterologous proteins and beyond. World J Microbiol Biotechnol 34:145.

41. Liu L, Liu Y, Shin HD, Chen RR, Wang NS, Li J, Du G, Chen J. 2013. Developing *Bacillus* spp. as a cell factory for production of microbial enzymes and industrially important biochemicals in the context of systems and synthetic biology. Appl Microbiol Biotechnol 97:6113-27.
42. Schallmey M, Singh A, Ward OP. 2004. Developments in the use of *Bacillus* species for industrial production. Can J Microbiol 50:1-17.
43. Abdel-Mawgoud AM, Aboulwafa MM, Hassouna NA. 2008. Optimization of surfactin production by *Bacillus subtilis* isolate BS5. Appl Biochem Biotechnol 150:305-25.
44. Shi S, Chen T, Zhang Z, Chen X, Zhao X. 2009. Transcriptome analysis guided metabolic engineering of *Bacillus subtilis* for riboflavin production. Metab Eng 11:243-52.
45. Korenblum E, der Weid I, Santos AL, Rosado AS, Sebastian GV, Coutinho CM, Magalhaes FC, Paiva MM, Seldin L. 2005. Production of antimicrobial substances by *Bacillus subtilis* LFE-1, B. firmus HO-1 and *B. licheniformis* T6-5 isolated from an oil reservoir in Brazil. J Appl Microbiol 98:667-75.
46. Setlow P. 2003. Spore germination. Curr Opin Microbiol 6:550-6.
47. Setlow P. 2006. Spores of *Bacillus subtilis*: their resistance to and killing by radiation, heat and chemicals. J Appl Microbiol 101:514-25.
48. Gould GW. 2006. History of science--spores. J Appl Microbiol 101:507-13.
49. Setlow P. 1995. Mechanisms for the prevention of damage to DNA in spores of *Bacillus* species. Annu Rev Microbiol 49:29-54.
50. Driks A. 2009. The *Bacillus anthracis* spore. Mol Aspects Med 30:368-73.
51. Stragier P, Losick R. 1996. Molecular genetics of sporulation in *Bacillus subtilis*. Annu Rev Genet 30:297-41.
52. Losick R, Youngman P, Piggot PJ. 1986. Genetics of endospore formation in *Bacillus subtilis*. Annu Rev Genet 20:625-69.
53. Giorno R, Bozue J, Cote C, Wenzel T, Moody KS, Mallozzi M, Ryan M, Wang R, Zielke R, Maddock JR, Friedlander A, Welkos S, Driks A. 2007. Morphogenesis of the *Bacillus anthracis* spore. J Bacteriol 189:691-705.
54. Liu H, Bergman NH, Thomason B, Shallom S, Hazen A, Crossno J, Rasko DA, Ravel J, Read TD, Peterson SN, Yates J, 3rd, Hanna PC. 2004. Formation and composition of the *Bacillus anthracis* endospore. J Bacteriol 186:164-78.
55. Setlow P. 2007. I will survive: DNA protection in bacterial spores. Trends Microbiol 15:172-80.
56. Cowan AE, Olivastro EM, Koppel DE, Loshon CA, Setlow B, Setlow P. 2004. Lipids in the inner membrane of dormant spores of *Bacillus* species are largely immobile. Proc Natl Acad Sci U S A 101:7733-8.
57. Makino S, Moriyama R. 2002. Hydrolysis of cortex peptidoglycan during bacterial spore germination. Med Sci Monit 8:Ra119-27.
58. Atrih A, Zollner P, Allmaier G, Foster SJ. 1996. Structural analysis of *Bacillus subtilis* 168 endospore peptidoglycan and its role during differentiation. J Bacteriol 178:6173-83.
59. Popham DL, Helin J, Costello CE, Setlow P. 1996. Analysis of the peptidoglycan structure of *Bacillus subtilis* endospores. J Bacteriol 178:6451-8.
60. Warth AD, Strominger JL. 1969. Structure of the peptidoglycan of bacterial spores: Occurrence of the lactam of muramic acid. Proc Natl Acad Sci U S A 64:528-35.
61. Meador-Parton J, Popham DL. 2000. Structural analysis of *Bacillus subtilis* spore peptidoglycan during sporulation. J Bacteriol 182:4491-9.
62. Popham DL. 2002. Specialized peptidoglycan of the bacterial endospore: the inner wall of the lockbox. Cell Mol Life Sci 59:426-33.
63. Piggot PJ, Hilbert DW. 2004. Sporulation of *Bacillus subtilis*. Curr Opin Microbiol 7:579-86.

64. Nicholson WL, Munakata N, Horneck G, Melosh HJ, Setlow P. 2000. Resistance of *Bacillus* endospores to extreme terrestrial and extraterrestrial environments. Microbiol Mol Biol Rev 64:548-72.
65. Driks A. 1999. *Bacillus subtilis* spore coat. Microbiol Mol Biol Rev 63:1-20.
66. Henriques AO, Moran CP, Jr. 2007. Structure, assembly, and function of the spore surface layers. Annu Rev Microbiol 61:555-88.
67. Chesnokova ON, McPherson SA, Steichen CT, Turnbough CL, Jr. 2009. The spore-specific alanine racemase of *Bacillus anthracis* and its role in suppressing germination during spore development. J Bacteriol 191:1303-10.
68. McKenney PT, Driks A, Eichenberger P. 2013. The *Bacillus subtilis* endospore: assembly and functions of the multilayered coat. Nat Rev Microbiol 11:33-44.
69. Vreeland RH, Rosenzweig WD, Powers DW. 2000. Isolation of a 250 million-year-old halotolerant bacterium from a primary salt crystal. Nature 407:897-900.
70. Moir A, Corfe BM, Behravan J. 2002. Spore germination. Cell Mol Life Sci 59:403-9.
71. Behravan J, Chirakkal H, Masson A, Moir A. 2000. Mutations in the *gerP* locus of *Bacillus subtilis* and *Bacillus cereus* affect access of germinants to their targets in spores. J Bacteriol 182:1987-94.
72. Yi X, Setlow P. 2010. Studies of the commitment step in the germination of spores of *Bacillus* species. J Bacteriol 192:3424-33.
73. Vepachedu VR, Setlow P. 2007. Analysis of interactions between nutrient germinant receptors and SpoVA proteins of *Bacillus subtilis* spores. FEMS Microbiol Lett 274:42-7.
74. Setlow B, Peng L, Loshon CA, Li YQ, Christie G, Setlow P. 2009. Characterization of the germination of *Bacillus megaterium* spores lacking enzymes that degrade the spore cortex. J Appl Microbiol 107:318-28.
75. Giebel JD, Carr KA, Anderson EC, Hanna PC. 2009. The germination-specific lytic enzymes SleB, CwlJ1, and CwlJ2 each contribute to *Bacillus anthracis* spore germination and virulence. J Bacteriol 191:5569-76.
76. Heffron JD, Lambert EA, Sherry N, Popham DL. 2010. Contributions of four cortex lytic enzymes to germination of *Bacillus anthracis* spores. J Bacteriol 192:763-70.
77. Ross C, Abel-Santos E. 2010. The Ger receptor family from sporulating bacteria. Curr Issues Mol Biol 12:147-58.
78. Setlow P. 2013. Summer meeting 201--when the sleepers wake: the germination of spores of *Bacillus* species. J Appl Microbiol 115:1251-68.
79. Ramirez-Guadiana FH, Meeske AJ, Wang X, Rodrigues CDA, Rudner DZ. 2017. The *Bacillus subtilis* germinant receptor GerA triggers premature germination in response to morphological defects during sporulation. Mol Microbiol 105:689-704.
80. Pelczar PL, Igarashi T, Setlow B, Setlow P. 2007. Role of GerD in germination of *Bacillus subtilis* spores. J Bacteriol 189:1090-8.
81. Li Y, Jin K, Ghosh S, Devarakonda P, Carlson K, Davis A, Stewart KA, Cammett E, Pelczar Rossi P, Setlow B, Lu M, Setlow P, Hao B. 2014. Structural and functional analysis of the GerD spore germination protein of *Bacillus* species. J Mol Biol 426:1995-2008.
82. Christie G, Lowe CR. 2007. Role of chromosomal and plasmid-borne receptor homologues in the response of *Bacillus megaterium* QM B1551 spores to germinants. J Bacteriol 189:4375-83.
83. Li Y, Setlow B, Setlow P, Hao B. 2010. Crystal structure of the GerBC component of a *Bacillus subtilis* spore germinant receptor. J Mol Biol 402:8-16.
84. Stewart KA, Setlow P. 2013. Numbers of individual nutrient germinant receptors and other germination proteins in spores of *Bacillus subtilis*. J Bacteriol 195:3575-82.

85. Griffiths KK, Zhang J, Cowan AE, Yu J, Setlow P. 2011. Germination proteins in the inner membrane of dormant *Bacillus subtilis* spores colocalize in a discrete cluster. Mol Microbiol 81:1061-77.
86. Traag BA, Ramirez-Peralta A, Wang Erickson AF, Setlow P, Losick R. 2013. A novel RNA polymerase-binding protein controlling genes involved in spore germination in *Bacillus subtilis*. Mol Microbiol 89:113-22.
87. Ramirez-Peralta A, Zhang P, Li YQ, Setlow P. 2012. Effects of sporulation conditions on the germination and germination protein levels of *Bacillus subtilis* spores. Appl Environ Microbiol 78:2689-97.
88. Zhang P, Garner W, Yi X, Yu J, Li YQ, Setlow P. 2010. Factors affecting variability in time between addition of nutrient germinants and rapid dipicolinic acid release during germination of spores of *Bacillus* species. J Bacteriol 192:3608-19.
89. Zhang P, Liang J, Yi X, Setlow P, Li YQ. 2014. Monitoring of commitment, blocking, and continuation of nutrient germination of individual *Bacillus subtilis* spores. J Bacteriol 196:2443-54.
90. Atrih A, Foster SJ. 2001. *In vivo* roles of the germination-specific lytic enzymes of *Bacillus subtilis* 168. Microbiology 147:2925-32.
91. Foster SJ, Johnstone K. 1987. Purification and properties of a germination-specific cortex-lytic enzyme from spores of *Bacillus megaterium* KM. Biochem J 242:573-9.
92. Heffron JD, Orsburn B, Popham DL. 2009. Roles of germination-specific lytic enzymes CwlJ and SleB in *Bacillus anthracis*. J Bacteriol 191:2237-47.
93. Lambert EA, Popham DL. 2008. The *Bacillus anthracis* SleL (YaaH) protein is an N-acetylglucosaminidase involved in spore cortex depolymerization. J Bacteriol 190:7601-7.
94. Ishikawa S, Yamane K, Sekiguchi J. 1998. Regulation and characterization of a newly deduced cell wall hydrolase gene (*cwlJ*) which affects germination of *Bacillus subtilis* spores. J Bacteriol 180:1375-80.
95. Bagyan I, Setlow P. 2002. Localization of the cortex lytic enzyme CwlJ in spores of *Bacillus subtilis*. J Bacteriol 184:1219-24.
96. Chirakkal H, O'Rourke M, Atrih A, Foster SJ, Moir A. 2002. Analysis of spore cortex lytic enzymes and related proteins in *Bacillus subtilis* endospore germination. Microbiology 148:2383-92.
97. Ragkousi K, Eichenberger P, van Ooij C, Setlow P. 2003. Identification of a new gene essential for germination of *Bacillus subtilis* spores with Ca2+-dipicolinate. J Bacteriol 185:2315-29.
98. Boland FM, Atrih A, Chirakkal H, Foster SJ, Moir A. 2000. Complete spore-cortex hydrolysis during germination of *Bacillus subtilis* 168 requires SleB and YpeB. Microbiology 146 (Pt 1):57-64.
99. Moriyama R, Fukuoka H, Miyata S, Kudoh S, Hattori A, Kozuka S, Yasuda Y, Tochikubo K, Makino S. 1999. Expression of a germination-specific amidase, SleB, of Bacilli in the forespore compartment of sporulating cells and its localization on the exterior side of the cortex in dormant spores. J Bacteriol 181:2373-8.
100. Kuwana R, Kasahara Y, Fujibayashi M, Takamatsu H, Ogasawara N, Watabe K. 2002. Proteomics characterization of novel spore proteins of *Bacillus subtilis*. Microbiology 148:3971-82.
101. Heffron JD, Sherry N, Popham DL. 2011. *In vitro* studies of peptidoglycan binding and hydrolysis by the *Bacillus anthracis* germination-specific lytic enzyme SleB. J Bacteriol 193:125-31.
102. Yeats C, Rawlings ND, Bateman A. 2004. The PepSY domain: a regulator of peptidase activity in the microbial environment? Trends Biochem Sci 29:169-72.
103. Gao X, Wang J, Yu DQ, Bian F, Xie BB, Chen XL, Zhou BC, Lai LH, Wang ZX, Wu JW, Zhang YZ. 2010. Structural basis for the autoprocessing of zinc metalloproteases in the thermolysin family. Proc Natl Acad Sci U S A 107:17569-74.

104. Bernhards CB, Popham DL. 2014. Role of YpeB in cortex hydrolysis during germination of *Bacillus anthracis* spores. J Bacteriol 196:3399-409.
105. Panzer S, Losick R, Sun D, Setlow P. 1989. Evidence for an additional temporal class of gene expression in the forespore compartment of sporulating *Bacillus subtilis*. J Bacteriol 171:561-4.
106. Li Y, Butzin XY, Davis A, Setlow B, Korza G, Ustok FI, Christie G, Setlow P, Hao B. 2013. Activity and regulation of various forms of CwlJ, SleB, and YpeB proteins in degrading cortex peptidoglycan of spores of *Bacillus* species in vitro and during spore germination. J Bacteriol 195:2530-40.
107. Bernhards CB, Chen Y, Toutkoushian H, Popham DL. 2015. HtrC is involved in proteolysis of YpeB during germination of *Bacillus anthracis* and *Bacillus subtilis* spores. J Bacteriol 197:326-36.
108. Fabret C, Hoch JA. 1998. A two-component signal transduction system essential for growth of *Bacillus subtilis*: implications for anti-infective therapy. J Bacteriol 180:6375-83.
109. Chen Y, Barat B, Ray WK, Helm RF, Melville SB, Popham DL. 2019. Membrane proteomes and ion transporters in *Bacillus anthracis* and *Bacillus subtilis* dormant and germinating spores. J Bacteriol 201.
110. Zheng L, Abhyankar W, Ouwerling N, Dekker HL, van Veen H, van der Wel NN, Roseboom W, de Koning LJ, Brul S, de Koster CG. 2016. *Bacillus subtilis* spore inner membrane proteome. J Proteome Res 15:585-94.
111. Sinz A. 2010. Investigation of protein-protein interactions in living cells by chemical crosslinking and mass spectrometry. Anal Bioanal Chem 397:3433-40.
112. Vasilescu J, Guo X, Kast J. 2004. Identification of protein-protein interactions using *in vivo* cross-linking and mass spectrometry. Proteomics 4:3845-54.
113. Guerrero C, Tagwerker C, Kaiser P, Huang L. 2006. An integrated mass spectrometry-based proteomic approach: quantitative analysis of tandem affinity-purified *in vivo* cross-linked protein complexes (QTAX) to decipher the 26 S proteasome-interacting network. Mol Cell Proteomics 5:366-78.
114. Sutherland BW, Toews J, Kast J. 2008. Utility of formaldehyde cross-linking and mass spectrometry in the study of protein-protein interactions. J Mass Spectrom 43:699-715.
115. Zhou YB, Gerchman SE, Ramakrishnan V, Travers A, Muyldermans S. 1998. Position and orientation of the globular domain of linker histone H5 on the nucleosome. Nature 395:402-5.
116. Chen JL, Nolan JM, Harris ME, Pace NR. 1998. Comparative photocross-linking analysis of the tertiary structures of *Escherichia coli* and *Bacillus subtilis* RNase P RNAs. Embo j 17:1515-25.
117. Pinard R, Heckman JE, Burke JM. 1999. Alignment of the two domains of the hairpin ribozyme-substrate complex defined by interdomain photoaffinity crosslinking. J Mol Biol 287:239-51.
118. van Opijnen T, Bodi KL, Camilli A. 2009. Tn-seq: high-throughput parallel sequencing for fitness and genetic interaction studies in microorganisms. Nat Methods 6:767-72.
119. Johnson CM, Grossman AD. 2014. Identification of host genes that affect acquisition of an integrative and conjugative element in *Bacillus subtilis*. Mol Microbiol 93:1284-301.
120. Meeske AJ, Rodrigues CD, Brady J, Lim HC, Bernhardt TG, Rudner DZ. 2016. High-throughput genetic screens identify a large and diverse collection of new sporulation genes in *Bacillus subtilis*. PLoS Biol 14:e1002341.
121. Kwon YM, Ricke SC, Mandal RK. 2016. Transposon sequencing: methods and expanding applications. Appl Microbiol Biotechnol 100:31-43.
122. Moir A. 2006. How do spores germinate? J Appl Microbiol 101:526-530.
123. Setlow P. 2003. Spore germination. Curr Opin Microbiol 6:550-556.
124. Mallozzi M, Viswanathan VK, Vedantam G. 2010. Spore-forming *Bacilli* and *Clostridia* in human disease. Future Microbiology 5:1109-1123.

125. Setlow P, Johnson EA. 2007. Spores and Their Significance. Food Microbiology: Fundamentals and Frontiers, Third Edition:35-67.
126. Cowan AE, Olivastro EM, Koppel DE, Loshon CA, Setlow B, Setlow P. 2004. Lipids in the inner membrane of dormant spores of *Bacillus* species are largely immobile. Proc Natl Acad Sci USA 101:7733-7738.
127. Koshikawa T, Beaman TC, Pankratz HS, Nakashio S, Corner TR, Gerhardt P. 1984. Resistance, germination, and permeability correlates of *Bacillus megaterium* spores successively divested of integument layers. J Bacteriol 159:624-32.
128. Igarashi T, Setlow P. 2005. Interaction between individual protein components of the GerA and GerB nutrient receptors that trigger germination of *Bacillus subtilis* spores. J Bacteriol 187:2513-2518.
129. Popham DL, Bernhards CB. 2015. Spore Peptidoglycan, p In Press. *In* Driks A, Eichenberger P (ed), The Bacterial Spore: From Molecules to Systems. ASM Press, Washington, D.C.
130. Koo BM, Kritikos G, Farelli JD, Todor H, Tong K, Kimsey H, Wapinski I, Galardini M, Cabal A, Peters JM, Hachmann AB, Rudner DZ, Allen KN, Typas A, Gross CA. 2017. Construction and Analysis of Two Genome-Scale Deletion Libraries for *Bacillus subtilis*. Cell Syst 4:291-305 e7.
131. Feavers IM, Foulkes J, Setlow B, Sun D, Nicholson W, Setlow P, Moir A. 1990. The regulation of transcription of the *gerA* spore germination operon of *Bacillus subtilis*. Molec Microbiol 4:275-282.
132. Zuberi AR, Moir A, Feavers IM. 1987. The nucleotide sequence and gene organization of the *gerA* spore germination operon of *Bacillus subtilis* 168. Gene 51:1-11.
133. Cabrera-Martinez RM, Tovar-Rojo F, Vepachedu VR, Setlow P. 2003. Effects of overexpression of nutrient receptors on germination of spores of *Bacillus subtilis*. J Bacteriol 185:2457-64.
134. Leighton TJ, Doi RH. 1971. The stability of messenger ribonucleic acid during sporulation in *Bacillus subtilis*. J Biol Chem 254:3189-3195.
135. Kearse M, Moir R, Wilson A, Stones-Havas S, Cheung M, Sturrock S, Buxton S, Cooper A, Markowitz S, Duran C, Thierer T, Ashton B, Meintjes P, Drummond A. 2012. Geneious Basic: an integrated and extendable desktop software platform for the organization and analysis of sequence data. Bioinformatics 28:1647-9.
136. Smith JL, Goldberg JM, Grossman AD. 2014. Complete Genome Sequences of *Bacillus subtilis subsp. subtilis* Laboratory Strains JH642 (AG174) and AG1839. Genome Announc 2.
137. Love MI, Huber W, Anders S. 2014. Moderated estimation of fold change and dispersion for RNA-seq data with DESeq2. Genome Biol 15:550.
138. Nicholson WL, Setlow P. 1990. Sporulation, germination, and outgrowth., p 391-450. *In* Harwood CR, Cutting SM (ed), Molecular biological methods for *Bacillus*. John Wiley & Sons Ltd., Chichester, England.
139. Dowd MM, Orsburn B, Popham DL. 2008. Cortex peptidoglycan lytic activity in germinating *Bacillus anthracis* spores. J Bacteriol 190:4541-8.
140. Schindelin J, Arganda-Carreras I, Frise E, Kaynig V, Longair M, Pietzsch T, Preibisch S, Rueden C, Saalfeld S, Schmid B, Tinevez JY, White DJ, Hartenstein V, Eliceiri K, Tomancak P, Cardona A. 2012. Fiji: an open-source platform for biological-image analysis. Nat Methods 9:676-82.
141. Hall M, Frank E, Holmes G, Pfahringer B, Reutemann P, Witten IH. 2009. The WEKA data mining software: an update. ACM SIGKDD Explorations Newsletter 11:10-18.
142. Ghosh S, Scotland M, Setlow P. 2012. Levels of germination proteins in dormant and superdormant spores of *Bacillus subtilis*. J Bacteriol 194:2221-7.
143. Ramirez-Peralta A, Stewart KA, Thomas SK, Setlow B, Chen Z, Li YQ, Setlow P. 2012. Effects of the SpoVT regulatory protein on the germination and germination protein levels of spores of *Bacillus subtilis*. J Bacteriol 194:3417-25.

144. Setlow B, Melly E, Setlow P. 2001. Properties of spores of *Bacillus subtilis* blocked at an intermediate stage in spore germination. J Bacteriol 183:4894-4899.
145. Robinson DG, Chen W, Storey JD, Gresham D. 2014. Design and analysis of Bar-seq experiments. G3 (Bethesda) 4:11-8.
146. Straus D, Walter W, Gross CA. 1990. DnaK, DnaJ, and GrpE heat shock proteins negatively regulate heat shock gene expression by controlling the synthesis and stability of sigma^{32}. Genes & Dev 4:2202-2209.
147. Kavita K, de Mets F, Gottesman S. 2018. New aspects of RNA-based regulation by Hfq and its partner sRNAs. Curr Opin Microbiol 42:53-61.
148. Zhu B, Stulke J. 2018. SubtiWiki in 2018: from genes and proteins to functional network annotation of the model organism Bacillus subtilis. Nucleic Acids Res 46:D743-d748.
149. Wang ST, Setlow B, Conlon EM, Lyon JL, Imamura D, Sato T, Setlow P, Losick R, Eichenberger P. 2006. The forespore line of gene expression in *Bacillus subtilis*. J Mol Biol 358:16-37.
150. Marchler-Bauer A, Bo Y, Han L, He J, Lanczycki CJ, Lu S, Chitsaz F, Derbyshire MK, Geer RC, Gonzales NR, Gwadz M, Hurwitz DI, Lu F, Marchler GH, Song JS, Thanki N, Wang Z, Yamashita RA, Zhang D, Zheng C, Geer LY, Bryant SH. 2017. CDD/SPARCLE: functional classification of proteins via subfamily domain architectures. Nucleic Acids Res 45:D200-D203.
151. Zhou R, Cusumano C, Sui D, Garavito RM, Kroos L. 2009. Intramembrane proteolytic cleavage of a membrane-tethered transcription factor by a metalloprotease depends on ATP. Proc Natl Acad Sci U S A 106:16174-9.
152. Steil L, Serrano M, Henriques AO, Volker U. 2005. Genome-wide analysis of temporally regulated and compartment-specific gene expression in sporulating cells of *Bacillus subtilis*. Microbiol 151:399-420.
153. Korza G, Camilleri E, Green J, Robinson J, Nagler K, Moeller R, Caimano MJ, Setlow P. 2019. Analysis of the messenger RNAs in spores of *Bacillus subtilis*. J Bacteriol doi:10.1128/JB.00007-19.
154. Gundlach J, Mehne FM, Herzberg C, Kampf J, Valerius O, Kaever V, Stulke J. 2015. An essential poison: synthesis and degradation of cyclic di-AMP in *Bacillus subtilis*. J Bacteriol 197:3265-74.
155. Gundlach J, Rath H, Herzberg C, Mader U, Stulke J. 2016. Second messenger signaling in *Bacillus subtilis*: accumulation of cyclic di-AMP inhibits biofilm formation. Front Microbiol 7:804.
156. Luo Y, Helmann JD. 2012. Analysis of the role of *Bacillus subtilis* sigma(M) in beta-lactam resistance reveals an essential role for c-di-AMP in peptidoglycan homeostasis. Mol Microbiol 83:623-39.
157. Gandara C, Alonso JC. 2015. DisA and c-di-AMP act at the intersection between DNA-damage response and stress homeostasis in exponentially growing *Bacillus subtilis* cells. DNA Repair (Amst) 27:1-8.
158. Tjalsma H, Bolhuis A, Jongbloed JD, Bron S, van Dijl JM. 2000. Signal peptide-dependent protein transport in *Bacillus subtilis*: a genome-based survey of the secretome. Microbiol Mol Biol Rev 64:515-47.
159. Eiamphungporn W, Helmann JD. 2008. The *Bacillus subtilis* sigma(M) regulon and its contribution to cell envelope stress responses. Mol Microbiol 67:830-48.
160. Tamehiro N, Okamoto-Hosoya Y, Okamoto S, Ubukata M, Hamada M, Naganawa H, Ochi K. 2002. Bacilysocin, a novel phospholipid antibiotic produced by *Bacillus subtilis* 168. Antimicrob Agents Chemother 46:315-20.
161. Guldan H, Matysik FM, Bocola M, Sterner R, Babinger P. 2011. Functional assignment of an enzyme that catalyzes the synthesis of an archaea-type ether lipid in bacteria. Angew Chem Int Ed Engl 50:8188-91.

162. Bagyan I, Hobot J, Cutting S. 1996. A compartmentalized regulator of developmental gene expression in *Bacillus subtilis*. J Bacteriol 178:4500-7.
163. Popham DL, Meador-Parton J, Costello CE, Setlow P. 1999. Spore peptidoglycan structure in a *cwlD dacB* double mutant of *Bacillus subtilis*. J Bacteriol 181:6205-6209.
164. Sekiguchi J, Akeo K, Yamamoto H, Khasanov FK, Alonso JC, Kuroda A. 1995. Nucleotide sequence and regulation of a new putative cell wall hydrolase gene, *cwlD*, which effects germination in *Bacillus subtilis*. J Bacteriol 177:5582-5589.
165. Wetzstein M, Volker U, Dedio J, Lobau S, Zuber U, Schiesswohl M, Herget C, Hecker M, Schumann W. 1992. Cloning, sequencing, and molecular analysis of the *dnaK* locus from *Bacillus subtilis*. J Bacteriol 174:3300-10.
166. Dambach M, Irnov I, Winkler WC. 2013. Association of RNAs with *Bacillus subtilis* Hfq. PLoS One 8:e55156.
167. Au N, Kuester-Schoeck E, Mandava V, Bothwell LE, Canny SP, Chachu K, Colavito SA, Fuller SN, Groban ES, Hensley LA, O'Brien TC, Shah A, Tierney JT, Tomm LL, O'Gara TM, Goranov AI, Grossman AD, Lovett CM. 2005. Genetic composition of the *Bacillus subtilis* SOS system. J Bacteriol 187:7655-66.
168. Puri-Taneja A, Paul S, Chen Y, Hulett FM. 2006. CcpA causes repression of the *phoPR* promoter through a novel transcription start site, P(A6). J Bacteriol 188:1266-78.
169. Kaushal B, Paul S, Hulett FM. 2010. Direct regulation of *Bacillus subtilis phoPR* transcription by transition state regulator ScoC. J Bacteriol 192:3103-13.
170. Tjalsma H, Bolhuis A, van Roosmalen ML, Wiegert T, Schumann W, Broekhuizen CP, Quax WJ, Venema G, Bron S, van Dijl JM. 1998. Functional analysis of the secretory precursor processing machinery of *Bacillus subtilis*: identification of a eubacterial homolog of archaeal and eukaryotic signal peptidases. Genes Dev 12:2318-31.
171. Allenby NE, Watts CA, Homuth G, Pragai Z, Wipat A, Ward AC, Harwood CR. 2006. Phosphate starvation induces the sporulation killing factor of *Bacillus subtilis*. J Bacteriol 188:5299-303.
172. Molle V, Fujita M, Jensen ST, Eichenberger P, Gonzalez-Pastor JE, Liu JS, Losick R. 2003. The Spo0A regulon of *Bacillus subtilis*. Mol Microbiol 50:1683-701.
173. Strauch MA, Bobay BG, Cavanagh J, Yao F, Wilson A, Le Breton Y. 2007. Abh and AbrB control of *Bacillus subtilis* antimicrobial gene expression. J Bacteriol 189:7720-32.
174. DeLoughery A, Lalanne JB, Losick R, Li GW. 2018. Maturation of polycistronic mRNAs by the endoribonuclease RNase Y and its associated Y-complex in *Bacillus subtilis*. Proc Natl Acad Sci U S A 115:E5585-E5594.
175. Petersohn A, Brigulla M, Haas S, Hoheisel JD, Volker U, Hecker M. 2001. Global analysis of the general stress response of *Bacillus subtilis*. J Bacteriol 183:5617-31.
176. Rao F, See RY, Zhang D, Toh DC, Ji Q, Liang ZX. 2010. YybT is a signaling protein that contains a cyclic dinucleotide phosphodiesterase domain and a GGDEF domain with ATPase activity. J Biol Chem 285:473-82.
177. Luo Y, Helmann JD. 2012. A sigmaD-dependent antisense transcript modulates expression of the cyclic-di-AMP hydrolase GdpP in *Bacillus subtilis*. Microbiology 158:2732-41.
178. Chen Y, Fukuoka S, Makino S. 2000. A novel spore peptidoglycan hydrolase of *Bacillus cereus*: biochemical characterization and nucleotide sequence of the corresponding gene, *sleL*. J Bacteriol 182:1499-1506.
179. Lambert EA, Sherry N, Popham DL. 2012. *In vitro* and *in vivo* analyses of the *Bacillus anthracis* spore cortex lytic protein SleL. Microbiology 158:1359-1368.
180. Makino S, Moriyama R. 2002. Hydrolysis of cortex peptidoglycan during bacterial spore germination. Med Sci Monit 8:RA119-127.

181. Popham DL, Helin J, Costello CE, Setlow P. 1996. Muramic lactam in peptidoglycan of *Bacillus subtilis* spores is required for spore outgrowth but not for spore dehydration or heat resistance. Proc Natl Acad Sci U S A 93:15405-10.
182. Meador-Parton J, Popham DL. 2000. Structural analysis of *Bacillus subtilis* spore peptidoglycan during sporulation. J Bacteriol 182:4491-4499.
183. Warth AD, Strominger JL. 1969. Structure of the peptidoglycan of bacterial spores: occurrence of the lactam of muramic acid. Proc Natl Acad Sci USA 64:528-535.
184. Popham DL, Bernhards CB. 2015. Spore Peptidoglycan. Microbiol Spectr 3.
185. Boland FM, Atrih A, Chirakkal H, Foster SJ, Moir A. 2000. Complete spore-cortex hydrolysis during germination of *Bacillus subtilis* 168 requires SleB and YpeB. Microbiology 146:57-64.
186. Moriyama R, Kudoh S, Miyata S, Nonobe S, Hattori A, Makino S. 1996. A germination-specific spore cortex-lytic enzyme from *Bacillus cereus* spores: Cloning and sequencing of the gene and molecular characterization of the enzyme. J Bacteriol 178:5330-2.
187. Hu K, Yang H, Liu G, Tan H. 2007. Cloning and identification of a gene encoding spore cortex-lytic enzyme in *Bacillus thuringiensis*. Curr Microbiol 54:292-5.
188. Moriyama R, Hattori A, Miyata S, Kudoh S, Makino S. 1996. A gene (*sleB*) encoding a spore cortex-lytic enzyme from *Bacillus subtilis* and response of the enzyme to L-alanine-mediated germination. J Bacteriol 178:6059-6063.
189. Ho SN, Hunt HD, Horton RM, Pullen JK, Pease LR. 1989. Site-directed mutagenesis by overlap extension using the polymerase chain reaction. Gene 77:51-9.
190. van den Ent F, Lowe J. 2006. RF cloning: a restriction-free method for inserting target genes into plasmids. J Biochem Biophys Methods 67:67-74.
191. Janes BK, Stibitz S. 2006. Routine markerless gene replacement in *Bacillus anthracis*. Infect Immun 74:1949-1953.
192. Kim HU, Goepfert JM. 1974. A sporulation medium for *Bacillus anthracis*. J Appl Bacteriol 37:265-267.
193. Gao X, Wang J, Yu DQ, Bian F, Xie BB, Chen XL, Zhou BC, Lai LH, Wang ZX, Wu JW, Zhang YZ. 2010. Structural basis for the autoprocessing of zinc metalloproteases in the thermolysin family. Proceedings of the National Academy of Sciences of the United States of America 107:17569-74.
194. Jing X, Robinson HR, Heffron JD, Popham DL, Schubot FD. 2012. The catalytic domain of the germination-specific lytic transglycosylase SleB from *Bacillus anthracis* displays a unique active site topology. Proteins 80:2469-75.
195. Ustok FI, Chirgadze DY, Christie G. 2015. Crystal structure of the PepSY-containing domain of the YpeB protein involved in germination of *Bacillus* spores. Proteins 83:1914-21.
196. Paidhungat M, Setlow B, Driks A, Setlow P. 2000. Characterization of spores of *Bacillus subtilis* which lack dipicolinic acid. J Bacteriol 182:5505-5512.